MEASUREMENT OF RELATIVE CROSS SECTIONS FOR SIMULTANEOUS IONIZATION AND EXCITATION OF THE HELIUM 4^2s AND 4^2p STATES

by John F. Sutton

Goddard Space Flight Center
Greenbelt, Md. 20771

NATIONAL AERONAUTICS AND SPACE ADMINISTRATION • WASHINGTON, D. C. • JUNE 1972

1. Report No.	2. Government Accession No.	3. Recipient's Catalog No.
NASA TR R-378		

4. Title and Subtitle
Measurement of Relative Cross Sections for Simultaneous Ionization and Excitation of the Helium 4^2s and 4^2p States

5. Report Date
June 1972

6. Performing Organization Code

7. Author(s)
John F. Sutton

8. Performing Organization Report No.
G-1046

9. Performing Organization Name and Address
Goddard Space Flight Center
Greenbelt, Maryland 20771

10. Work Unit No.

11. Contract or Grant No.

12. Sponsoring Agency Name and Address
National Aeronautics and Space Administration
Washington, D.C. 20546

13. Type of Report and Period Covered
Technical Report

14. Sponsoring Agency Code

15. Supplementary Notes

16. Abstract

The relative cross sections for simultaneous ionization and excitation of helium by 200-eV electrons into the 4^2p and 4^2s states have been measured via a fast delayed-coincidence technique. Results are in poor agreement with Born approximation calculations for simultaneous ionization and excitation of helium, but show good agreement with the relative cross sections for single-electron excitation of helium and hydrogen.

An application of the results of the measurement to the development of ultraviolet intensity standard is suggested. This technique involves the use of known branching ratios, a visible-light flux reference, and the measured relative cross sections.

17. Key Words (Selected by Author(s))	18. Distribution Statement
Helium Ions Cross Sections Simultaneous Ionization and Excitation Electron Bombardment	Unclassified—Unlimited

19. Security Classif. (of this report)	20. Security Classif. (of this page)	21. No. of Pages	22. Price*
Unclassified	Unclassified	96	$3.00

*For sale by the National Technical Information Service, Springfield, Virginia 22151.

CONTENTS

MEASUREMENT OF RELATIVE CROSS SECTIONS FOR SIMULTANEOUS IONIZATION AND EXCITATION OF THE HELIUM 4^2s AND 4^2p STATES

by

John F. Sutton
Goddard Space Flight Center

1.0 INTRODUCTION

This research is concerned with the measurement of the relative cross sections for simultaneous ionization and excitation of helium into the $n = 4$ levels by electron impact. These energy levels are nearly degenerate. One may determine the relative populations by either (a) interferometry (Larson and Stanley, 1967) or (b) lifetime separation. Method (a) involves the separation and detection of weak radiations that differ in wavelength by only about 1Å, which requires rather sophisticated interferometric techniques. Because the lifetimes of the degenerate $n = 4$ levels of He^+ have sufficient time separation for analysis, method (b) was deemed the more promising approach and was chosen for the present study.

The results of the measurement will be compared with theoretical predictions. The results also are useful for the development of an absolute ultraviolet intensity standard at 1215Å, as discussed in Section 3.4, and, in addition, may be useful in certain types of Lamb shift measurements, those in which the relative populations of the degenerate levels are important.

2.0 LIFETIMES AND RELATIVE POPULATIONS IN He^+

2.1 Natural Lifetimes

In the absence of other perturbing influences, an excited atom will spontaneously decay because of the interaction between the atom and the zero-point electromagnetic radiation field. The results of a rigorous mathematical treatment involving quantization of the radiation field and the use of time-dependent perturbation theory (e.g., Heitler, 1944) can be simply stated in terms of the Einstein transition probabilities (Einstein, 1917).

Assume that an atom has an excited level j and several lower levels k. The Einstein coefficient A_{jk} is defined as the probability of spontaneous transition, accompanied by photoemission, from level j to level k. The total decay probability is therefore

$$A_j = \sum_k A_{jk} \, . \tag{1}$$

For a dipole transition,

$$A_{jk} = \text{constant} \times \nu_{jk}^3 \ \langle P \rangle_{jk}^2 \ , \tag{2}$$

where ν_{jk} is the emission frequency and $\langle P \rangle_{jk}$ is the dipole-moment expectation value. The value $\langle P \rangle$ can be readily calculated for one-electron atoms through the use of the well-known hydrogenic wave functions. The resulting values of A_{jk} have been tabulated (Wiese et al., 1966).

If n_j atoms have been excited to level j, the decay rate is given by

$$\dot{n}_j = -n_j A_j \ ;$$

hence,

$$n_j(t) = n_j(0) e^{-A_j t} \ . \tag{3}$$

One can define a mean lifetime

$$\tau_j \equiv \frac{1}{n_j(0)} \int_0^{n_j(0)} t \, dn_j(t)$$

$$= A_j \int_0^{\infty} t e^{-A_j t} \, dt$$

$$= A_j^{-1} \ . \tag{4}$$

Thus, the coefficient A is the decay constant for spontaneous decay. The number of photons per second of radiation with frequency ν_{jk} would then be

$$\phi_{jk}(t) = n_j(t) A_{jk}$$

$$= A_j n_j(0) e^{-A_j t} \ .$$

2.2 Relative Populations of Excited States of He^+

When a beam of electrons is directed into a volume of neutral helium gas, a small percentage of the helium atoms will become simultaneously ionized and excited. These atoms will decay according to the hydrogen-like decay scheme illustrated in Figure 1. The rate of population of level j (neglecting cascades from higher states) is

$$\dot{n}_{j\,\text{pop}} = \chi Q_{0j} \ , \tag{5}$$

where

$Q_{0j} \equiv$ cross section for simultaneous ionization and excitation to level j from the ground state

and

$$\chi \equiv \frac{I \rho l'}{e} \ ,$$

in which I is the beam current, ρ is the gas density, l' is the effective electron path length, and e is the charge of an electron.

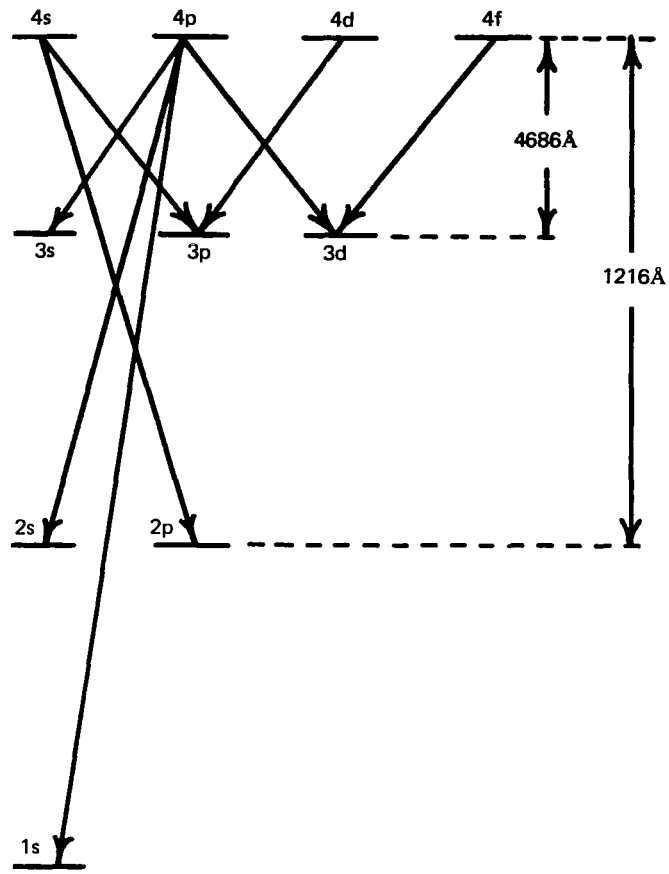

Figure 1—Partial energy-level diagram for helium II, showing hydrogen-like degenerate levels.

As discussed in Section 2.1, the depopulation rate is

$$\begin{aligned} \dot{n}_{j\,\text{depop}} &= -n_j A_j \\ &= -n_j \sum_k A_{jk} \\ &= -\frac{n_j}{\tau_j} \,. \end{aligned}$$

Therefore, the total rate during the time the beam is on would be

$$\begin{aligned} \dot{n}_{j\,\text{total}} &= \dot{n}_{j\,\text{pop}} + \dot{n}_{j\,\text{depop}} \\ &= \chi Q_{0j} - n_j A_j \end{aligned} \tag{6}$$

The solution to Equation 6 is

$$n_j(t) = \chi \frac{Q_{0j}}{A_j} \gamma_j \,, \tag{7}$$

where

$$\gamma_j \equiv 1 - e^{-A_j t} \,.$$

The rate of photon emission due to the $j - k$ transition would then be

$$\phi_{jk}(t) = n_j(t) A_{jk}$$

$$= \chi Q_{0j} \frac{A_{jk}}{A_j} \gamma_j \,. \tag{8}$$

Hence, the populations of the excited states of He^+ are pumped by an electron beam and decay with natural lifetimes of a few nanoseconds in a manner completely analogous to the charging and discharging of capacitors in a set of RC circuits. In the present investigation of He^+, the natural lifetimes of interest, obtained from the Einstein A coefficients tabulated by the National Bureau of Standards (Weise et al., 1966) for H and scaled according to Z^4, are

$$\tau_{4p} = 0.769 \text{ ns},$$

$$\tau_{4d} = 2.26 \text{ ns},$$

$$\tau_{4f} = 4.53 \text{ ns},$$

and

$$\tau_{4s} = 14.16 \text{ ns}.$$

These times, analogous to RC time constants, indicate that in order for all of the states of interest to be excited to saturation, the electron pulse duration should be approximately $3\tau_{4s}$ or 42.48 ns. Because of the difficulty of analyzing the resulting composite decay curve, however, it was deemed advisable to employ a much shorter pulse (1 to 2 ns) to accentuate the faster components relative to the slower ones. The effect of this shorter pulse duration is discussed in Section 6.0.

2.3 Cascades

If only first-order cascades are considered, the contribution to the population of the jth (e.g., 4s) level due to cascades from the higher kth (e.g., 5p) level is given by $n_k A_{kj}$; i.e.,

$$n_j^*(t) = \chi Q_{0j} - n_j A_j + n_k A_{kj} \,, \tag{9}$$

where

$$n_k(t) = \frac{\chi Q_{0k} \gamma_k}{A_k} \,. \tag{10}$$

The solution to Equation 9, with $n_k(t)$ as in Equation 10, is

$$n_j^*(t) = \frac{C_1 + C_2}{A_j} \frac{C_1}{A_j - A_k} \gamma_j(\gamma_k - \gamma_j) , \tag{11}$$

where

$$C_1 \equiv \frac{\chi Q_{0k} A_{kj}}{A_k}$$

and

$$C_2 \equiv \chi Q_{0j} .$$

Note that the cascade causes a second exponential decay to appear in the depopulation rate of level j. To find the relative importance of these exponentials, one can compare the coefficients as follows:

$$\frac{n_j^* - n_j}{n_j} = \frac{Q_{0k} A_j A_{kj} [\gamma_k - \gamma_j]}{Q_{0j} A_k (A_j - A_k) \gamma_j} .$$

This ratio, expressed in percent, has the following values:

0.22 percent, for k = 5p and j = 4s,

and

0.73 percent, for k = 5p and j = 4d.

These errors are small compared to the effects of the random noise in the data and may therefore be neglected.

3.0 PREVIOUS STUDIES

3.1 General Theory

The theoretical calculations of Dalgarno and McDowell (1956), Lee and Lin (1965), and Anderson, Lee, and Lin (1967) are based on a Born approximation treatment of the electron-atom collision. Dalgarno and McDowell begin their treatment by expressing the differential scattering cross section in the form

$$I_\kappa \, d\kappa \, d\Omega \, d\Omega' = \frac{k_f}{k_i} |N|^2 \, d\kappa \, d\Omega \, d\Omega' \frac{a_0^2}{2\pi} ,$$

where atomic units are used, k_i and k_f are the wave vectors of the incident and scattered electrons, respectively, and

$$N \equiv \iiint V(\mathbf{r}_0, \mathbf{r}_1, \mathbf{r}_2) \psi_i(\mathbf{r}_1, \mathbf{r}_2) \psi_f^*(\mathbf{r}_1, \mathbf{r}_2) e^{i(\mathbf{k}_i - \mathbf{k}_f) \cdot \mathbf{r}_0} \, dr_0 \, dr_1 \, dr_2 ,$$

(where $\mathbf{k}$ is the momentum of the ejected electron)

in which

$$V \equiv 2\left\{\frac{1}{|\mathbf{r}_0 - \mathbf{r}_1|} + \frac{1}{|\mathbf{r}_0 - \mathbf{r}_2|} - \frac{2}{|\mathbf{r}_0|}\right\} .$$

For the initial wave function $\psi_i(\mathbf{r}_1, \mathbf{r}_2)$, Dalgarno and McDowell choose a product of two hydrogenic wave functions with effective charge Z:

$$\psi_i(\mathbf{r}_1, \mathbf{r}_2) = \phi(\mathbf{r}_1, Z)\phi(\mathbf{r}_2, Z) ,$$

where the spin part of the wave function is neglected because exchange effects are unimportant in this approximation. For the final-state wave function, they choose

$$\psi_f(\mathbf{r}_1, \mathbf{r}_2) = \frac{1}{\sqrt{2}}[\phi_{nl}(\mathbf{r}_1)\xi_\kappa(\mathbf{r}_2) + \phi_{nl}(\mathbf{r}_2)\xi_\kappa(\mathbf{r}_1)] ,$$

in which ϕ_{nl} is the wave function of the nl state of He^+, normalized to unity, with nuclear charge $Z' = 2$, and ξ_κ is a wave function of an ionized (unbound) electron, normalized according to

$$\xi_\kappa(r) \sim \frac{\kappa}{(2\pi)^{3/2}} \exp\left\{-i\kappa[Z + \beta\kappa^{-2} \ln \kappa(r - Z)]\right\} .$$

Lee and Lin (1965) and Anderson, Lee, and Lin (1967) use the same procedure except for the approximation of the final wave function, which they give as the continuum wave function in a Coulomb field of charge Z'' (after Sommerfeld, 1931), where Z'' is effectively a somewhat arbitrary parameter in the calculation.

3.2 Theoretical Calculations of Cross Sections of He^+

Dalgarno and McDowell (1956), using the Born approximation, calculated cross sections for the processes

$$e + \mathrm{He} \rightarrow e + \mathrm{He}^+ (nl) + e$$

and

$$\mathrm{H}^+ + \mathrm{He} \rightarrow \mathrm{H}^+ + \mathrm{He}^+ (nl) + e ,$$

for

$$nl = 2\mathrm{p}, 3\mathrm{p}, 4\mathrm{p}, 3\mathrm{d}, \text{ and } 4\mathrm{d} .$$

Due to a large degree of arbitrariness in the choice of the initial and final wave functions, errors of the order of a factor of five were predicted. However, Dalgarno and McDowell pointed out that simultaneous ionization and excitation of helium should occur with about the same efficiency as double excitation and that the rate of population of the excited states of He^+ should be approximately 1/200th the rate at which single excitation populates excited states of He^+.

Lee and Lin (1965) extended the Born approximation calculation of Dalgarno and McDowell to include the 4s state. By using the 4p and 4d calculation of Dalgarno and McDowell as a guide for

choosing a value of effective nuclear charge, their calculations were extended to include the 4f state. The results of their calculations indicated that about 90 percent of the total $4 \rightarrow 3$ emission originates in the $4s \rightarrow 3p$ transition. This is due to the fact that the 4s state can cascade to 3p and 2p (with an intensity ratio of 3:4), whereas the majority of the atoms in 4p cascade to 1s, leaving only a small fraction of the 4p population for the $4p \rightarrow 3s$ and $4p \rightarrow 3d$ transitions. If a cascade correction of 10 percent for the calculation of Lee and Lin is assumed, the theoretical value obtained by Lee and Lin for the total cross section agrees with the experimental results of St. John and Lin (1964 and 1967) (described in the next section) to within 15 percent. The factor-of-5 errors mentioned by Dalgarno and McDowell in the calculation of cross sections for the 4p and 4d states do not apply to the 4s state, which contributed the majority of the 4686Å radiation.

Anderson, Lee, and Lin (1967) extended the Born approximation calculations of Dalgarno and McDowell and of Lee and Lin to compute the direct ionization-excitation cross sections of the ns, np, and nd states (where $n = 5$, 6, and 7), from which the theoretical excitation cross sections of the $5 \rightarrow 3$, $6 \rightarrow 3$, and $7 \rightarrow 3$ transitions were calculated. In each case, the $ns \rightarrow 3p$ transitions were found to account for about 90 percent of the total radiation of the $n \rightarrow 3$ transitions. Agreement to within factors of 2 to 3.5 times the measured values was claimed. Cascade contributions to the observed intensities of the three lines were estimated to be less than 5 percent. Table 1 is a summary of the calculations and measurements of Lee and Lin and of Anderson, Lee, and Lin.

3.3 Experimental Results of Cross-Section Measurements of He^+

Hughes and Weaver (Hughes and Weaver, 1963; Weaver and Hughes, 1967) measured the absolute cross sections for the excitation of the He^+ 4686Å line as a function of energy from threshold to 500 eV (Figure 2). Their apparatus consisted of a brass chamber filled to about 10 μm pressure with natural helium, the electron gun from a type 3API cathode-ray tube (CRT), and a deep Faraday cup for collecting the electrons. The 4686Å line was isolated via a spectrometer, and a maximum-level cross section $\sigma_{max}(4 \rightarrow 3)$ of 10.2×10^{-21} cm^2, at approximately 200 eV, was measured. The absolute calibration was obtained by measuring simultaneously the excitation functions of the He II line and an adjacent known He I 4713Å line (Stewart and Gabuthuler, 1959) and by normalizing to the latter. It should be noted, however, that the absolute cross section of the 4713Å line is still uncertain to approximately ±20 percent.

St. John and Lin (1964 and 1967) also measured the absolute cross section for the collision process that yields the $n = 4 \rightarrow n = 3$ transitions in He^+. The apparatus used was different from that of Hughes and Weaver in that a flat plate positively biased to 45 V was used to collect the beam electrons, rather than a deep Faraday cup. In addition, the use of a mechanical light-chopper wheel operating at a rate of 140 pps made it possible to use a lock-in amplifier in the data-reduction signal path. An analog computer was employed to calculate automatically the ratio of the light yield to the electron-beam current. The output of the computer was displayed on an oscilloscope and photographed.

St. John and Lin estimated that the peak of the total cross section for the $n = 4 \rightarrow n = 3$ transition is 9.8×10^{-21} cm^2. Because the branching ratios for the various members of the observed transitions are different, the separate cross sections for the direct excitation-ionization process to the various members of the $n = 4$ states could not be determined. The curve obtained agreed qualitatively

Table 1—Calculated and experimental values of cross sections (in 10^{-21} cm^2) of He^+ for excitation-ionization by electron impact (Lee and Lin, 1965; Anderson, Lee, and Lin, 1967).

Cross Section	Value of Cross Section (in 10^{-21} cm^2)				
	200 eV	270 eV	340 eV	405 eV	450 eV
$Q(He^+, 4s)$	8.1	8.2	7.6	6.9	6.6
$Q(He^+, 4p)$	2.9	3.1	2.9	2.8	2.7
$Q(He^+, 4d)$	0.68	0.69	0.66	0.62	0.57
$Q(He^+, 4 \rightarrow 3)$*	3.7	3.8	3.5	3.2	3.0
$Q(He^+, 4 \rightarrow 3)$**	9.8	9.1	7.9	7.0	6.5
$Q(He^+, 5s)$	3.8	3.8	3.5	3.2	3.0
$Q(He^+, 5p)$	1.4	1.4	1.4	1.3	1.3
$Q(He^+, 5d)$	0.36	0.36	0.34	0.32	0.30
$Q(He^+, 5 \rightarrow 3)$*	1.4	1.4	1.3	1.2	1.1
$Q(He^+, 5 \rightarrow 3)$**	2.6	2.8	2.4	—	—
$Q(He^+, 6s)$	2.1	2.1	1.9	1.8	1.7
$Q(He^+, 6p)$	0.78	0.80	0.77	0.74	0.71
$Q(He^+, 6d)$	0.13	0.12	0.10	0.09	0.08
$Q(He^+, 6 \rightarrow 3)$*	0.63	0.63	0.59	0.54	0.51
$Q(He^+, 6 \rightarrow 3)$**	1.9	1.8	1.7	—	—
$Q(He^+, 7s)$	1.3	1.3	1.2	1.1	1.0
$Q(He^+, 7p)$	0.48	0.49	0.48	0.45	0.44
$Q(He^+, 7d)$	0.08	0.49	0.48	0.45	0.44
$Q(He^+, 7 \rightarrow 3)$*	0.08	0.08	0.07	0.06	0.05
$Q(He^+, 7 \rightarrow 3)$**	0.35	0.35	0.31	0.29	0.27

*Theoretical.
**Experimental.

in shape with that of Hughes and Weaver: There was a single, broad maximum at approximately 150 eV, whereas Hughes and Weaver had a maximum at approximately 200 eV (Figure 2); there was a peak value of 9.8×10^{-21} cm^2, compared with the 10.2×10^{-21}-cm^2 peak of Hughes and Weaver (showing agreement to within 4 percent). The single, smooth, broad maximum indicated a lack of secondary processes such as step-wise excitation and transfer of excitation. In addition, the excitation-ionization function was independent of pressure from 3.7 to 22 μm.

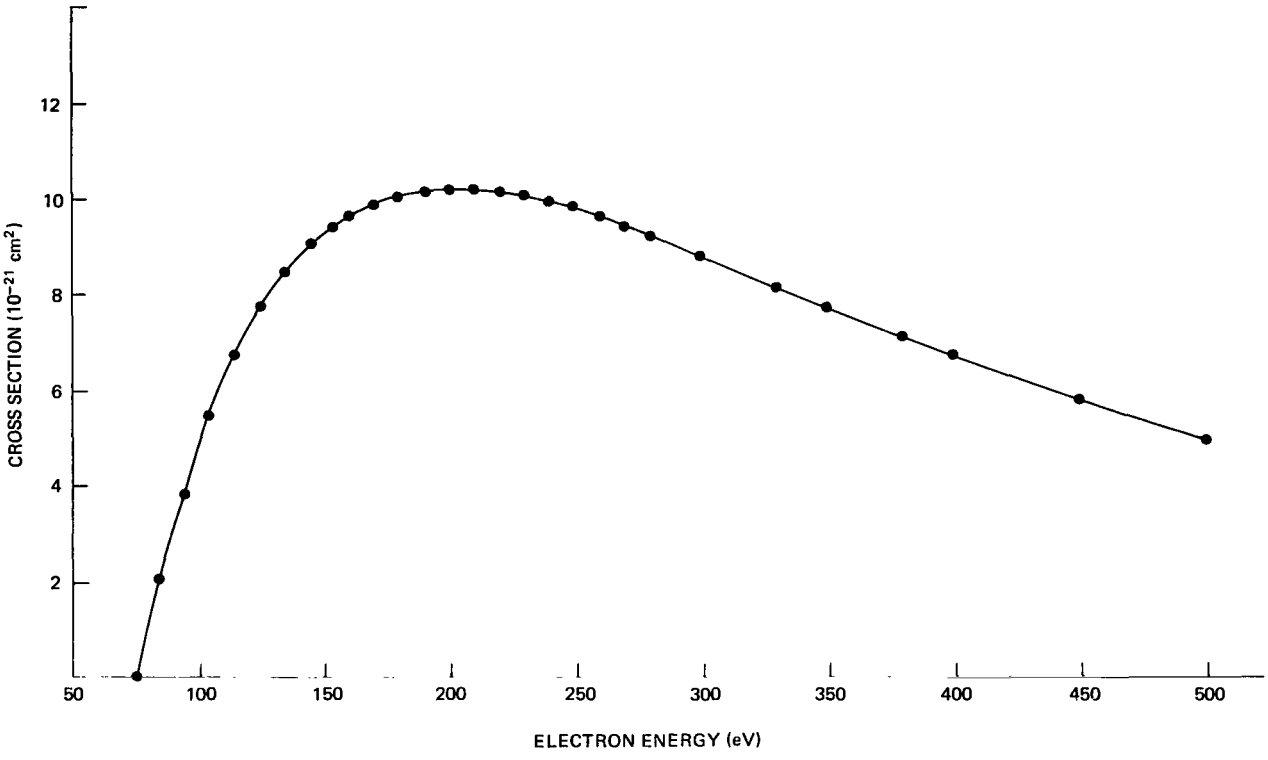

Figure 2–Total cross section for $n = 4 \rightarrow n = 3$ vs. electron energy (Hughes and Weaver, 1963; Weaver and Hughes, 1967).

3.4 Scope of the Investigation

As is evident from the previous sections, although theoretical calculations of the relative cross sections of the excited states of singly ionized helium have been made, the experimental situation remains unsatisfactory. It is the purpose of this investigation to make a measurement of the cross sections of the 4^2s and 4^2p levels to verify the theoretical calculations discussed previously.

Of primary practical importance is the use of the measured relative cross sections in an ultraviolet intensity calibration source. As is shown in Figure 1, the $4 \rightarrow 3$, 4686Å transition is accompanied by a $4 \rightarrow 2$ transition which has the same wavelength as the important Lyman-α transition in hydrogen (1216Å). With the relative cross sections and transition probabilities known, it is possible to calculate the relative light fluxes at the two wavelengths emitted by a chamber filled with helium and excited by an electron beam. Thus, by comparing the visible radiation to that from a standard lamp, the helium gas becomes a transfer standard for the vacuum ultraviolet at 1216Å.

4.0 EXPERIMENTAL TECHNIQUE

4.1 Decay Analysis Technique

There exists a technique (Pendleton, 1964) for observing and analyzing atomic decays which employs a modified sampling cathode-ray oscilloscope (CRO). Pulses in synchronism with the pulse

modulation of an electron beam are used to trigger the sampling CRO. The pulsed electron beam excites atomic decays in a gas. A photomultiplier tube (PMT), in conjunction with a high-gain preamplifier, is used to provide light intensity information (proportional to the populations of the excited states in the gas) to the vertical-axis input. The sampling CRO functions in the normal manner, with the exception that because of the extremely noisy nature of the PMT signal, the averaging time of the instrument must be greatly augmented (e.g., by a factor of 10^4). The increased averaging time necessitates a very slow time sweep, with the attendant problems of zero-shift distortion. The very long averaging times required ruled out this technique for the present investigation.

Another technique, the one employed here, involves the use of a time-to-pulse-height (TPH) converter and a multichannel analyzer (MCA); this is the delayed coincidence technique used to study nuclear decays. As is shown in Figure 3, a pulse generator provides a succession of narrow rectangular pulses to the cathode of a vacuum tube, which serves as an electron gun. The gun is located in a vacuum chamber filled to a pressure of 1 to 100 μm of mercury with the type of gas to be investigated.

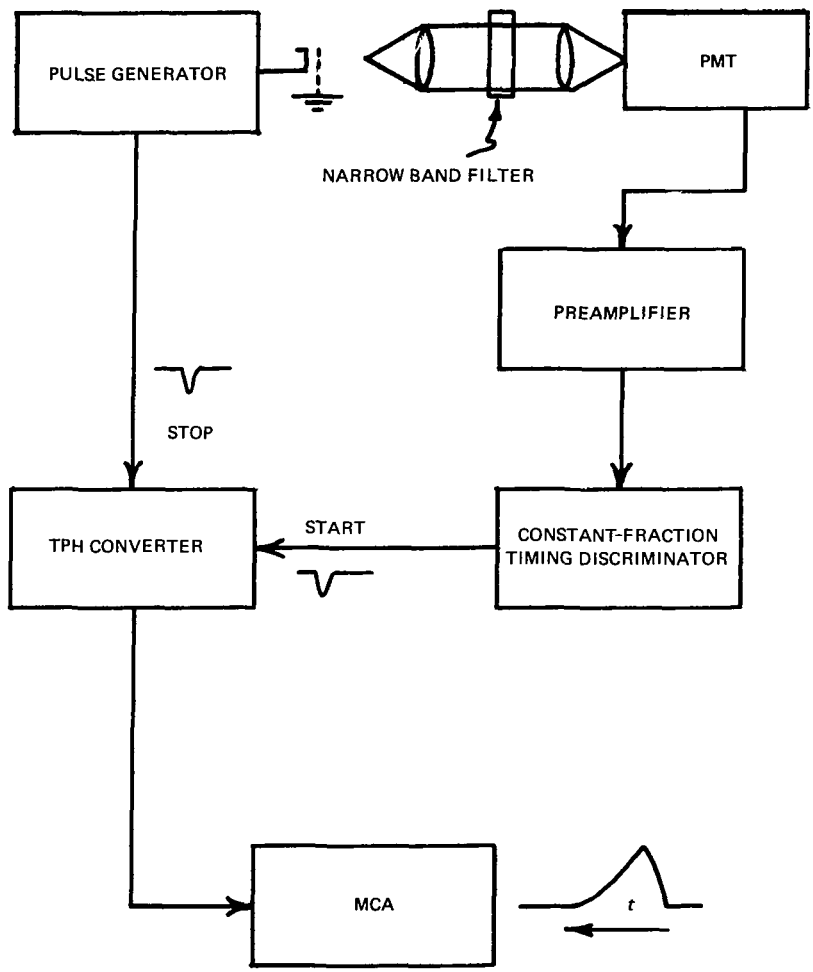

Figure 3—Block diagram of the apparatus.

The light emitted by the atomic decays in the excited gas is detected via a narrow interference filter by a PMT, and synchronizing pulses from the pulse generator are employed to control the TPH converter.

Each time a pulse from the pulse generator turns the electron gun on for a brief interval, electrons flow from the cathode to the collector wall. During this time and for a short time afterwards, determined by the atomic decay times involved, there is a small but finite probability that a decay photon will pass through the lens system of the apparatus and cause the PMT to generate an output pulse. Because of the exponential character of the decay, this probability is greater for shorter time delays than for longer time delays. Thus, more PMT pulses will occur within a small time of the input pulse than will occur later. The TPH converter changes this time information to voltage pulses and stores these pulses, according to amplitude, in channels in the MCA memory bank.

4.2 Apparatus

4.2.1 Excitation System

As is discussed in Section 2.2, the pulse generator employed in this experiment was required to have a narrow (1 to 2 ns) pulse width and, therefore, fast rise and fall times. The pulse generator chosen, the fastest available, had rise and fall times of 0.3 ns and a pulse amplitude of 10 V. Because the probability is $\ll 1$ that a coincident decay photon will be detected by the PMT within 100 ns of the excitation pulse, the pulse generator was also required to have a high repetition rate. The device chosen had a maximum repetition rate of 1 MHz.

The electron-gun assembly consisted of a 7587 Nuvistor,* with the metal shell cut away just above the base. The 7587 Nuvistor was chosen because of the large bandwidth required, i.e., about 10^{10} Hz. Further, the problems of transit-time effects eliminated guns of larger physical dimensions from consideration. The grounded-grid configuration was chosen because it provided a good impedance match to the 50-Ω input cable and because it was less susceptible to distortion resulting from interelectrode capacitances. A modified coupling capacitor provided dc isolation for the input signal line. The CRO monitoring of the input pulse was facilitated by a coaxial signal pickoff, which presented a 5-kΩ dc resistance to ground and therefore served the additional function of preventing charge buildup on the input cable. The first grid was ac grounded by three short leads spot welded to the remaining portion of the metal shell. The tube was inserted into a Nuvistor socket, which was mounted in an ultrahigh-frequency (UHF) connector in such a way as to preserve the cylindrical geometry of the coaxial cable and the tube. A 1/2-in.-diameter hole was bored through an adjacent connector (which served as the shield for the current probe and as the electron collector) to permit the observation of the decay photons. A 1/4-in.-diameter brass disk supported on wires was mounted across the opening to block the light emitted by the hot cathode. The electron-gun circuitry is illustrated in Figure 4, the assembly in Figures 5 and 6, and the modified 7587 in Figure 7.

The input cable itself required careful selection because it was necessary to keep the cable at least 50 ns long to prevent any reflection from causing spurious responses during the conversion time of the TPH converter (100 ns). Such a long cable is subject to "dribble up", a rounding of the corners and

*Registered trademark, RCA.

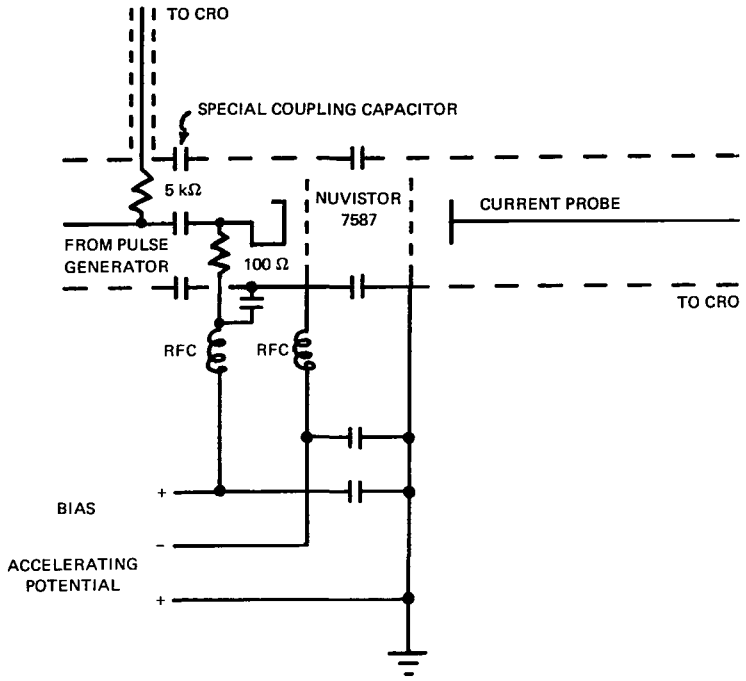

Figure 4—Electron-gun schematic diagram.

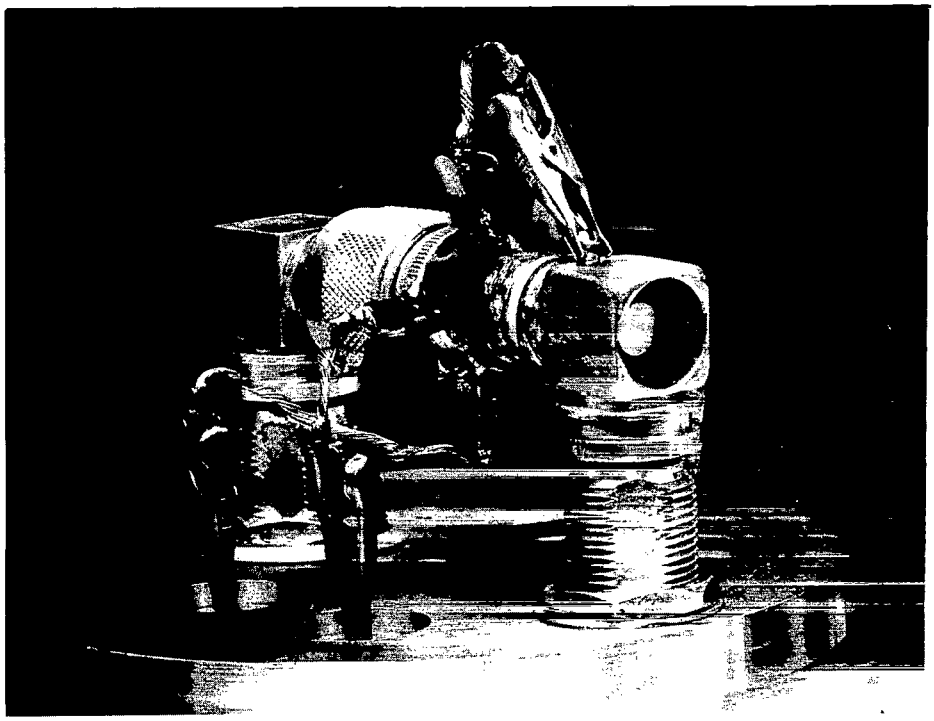

Figure 5—Complete electron-gun assembly.

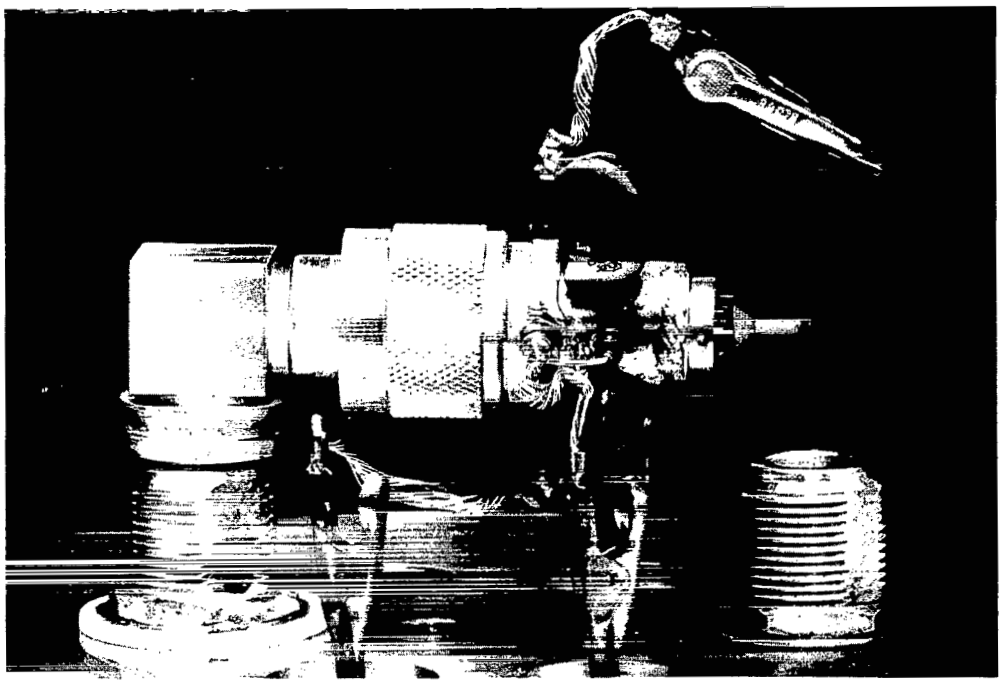

Figure 6—Electron-gun assembly: electron collector removed.

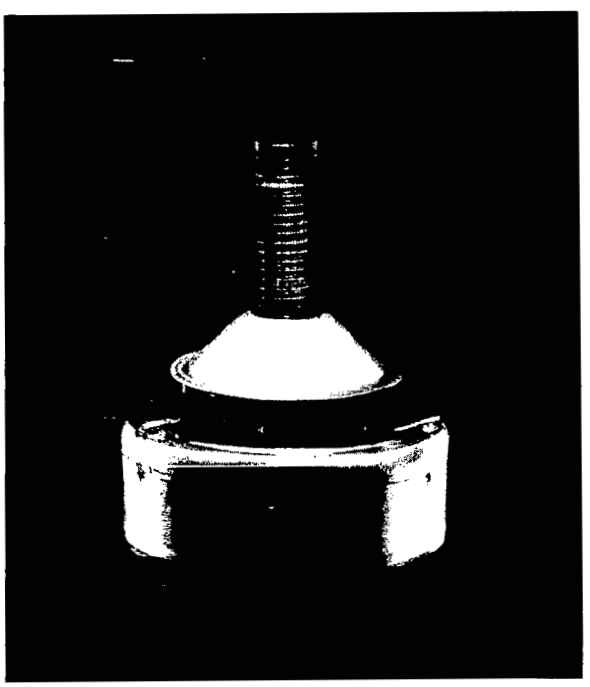

Figure 7—Modified 7587 electron gun.

alteration of the slope of the top of a fast rectangular pulse, caused by dielectric losses. Accordingly, 7/8-in.-diameter air-dielectric cable was chosen; the overall rise time of this cable was less than 0.1 ns.

4.2.2 Detection System

Because of the expected low light intensities, a fast lens system was employed to focus the image of the excitation region via a window in the vacuum chamber wall onto the PMT photocathode. For the same reason, a narrow-band (approximately 10Å) interference filter was used instead of a monochromator for wavelength selection. The filter bandwidth was narrow enough to suppress the nearest strong interfering helium line, that of He I $4^3s \rightarrow 2^3p$, at 4713Å.

The PMT selected had a fast rise time (approximately 2 ns) and a small transit-time spread (approximately 2.5 ns) due to a focused geometry construction. A small capacitor was wired across the output, and an integrating amplifier was used to optimize the shape of the pulse applied to the input of the constant-fraction timing discriminator. The latter was employed to eliminate timing (i.e., "walk") errors due to varying pulse amplitudes. This is accomplished by triggering an output pulse when the input pulse reaches a constant fraction (e.g., 0.2) of its peak value, independent of the magnitude of the peak value.

It was necessary to wire the PMT with the photocathode at a high potential above ground. This eliminated the high-voltage coupling capacitor and the danger of destroying the sampling CRO input diodes with current surges when the PMT high-voltage power supply was turned on or off. Spurious pulses due to high electric-field intensities across the glass envelope of the PMT were eliminated by connecting the mu-metal shield to the cathode potential and by coating the window of the PMT with a transparent conductive compound that is commonly used as an anti-static compound for plastic meter faces. Radiofrequency (RF) shielding was provided by fastening a fine-mesh wire screen across the entrance aperture of one of the lenses.

4.2.3 Vacuum System

The collision chamber was evacuated by a liquid-nitrogen-trapped 4-in. oil diffusion pump, backed by a mechanical forepump. A molecular sieve foreline trap was installed to prevent forepump oil vapor from contaminating the diffusion-pump oil. The chamber could be isolated from the vacuum system by the use valves for operation with helium at high pressure (approximately 20 μm of mercury). Helium pressures were monitored via a Pirani gage, which was calibrated against a tilting McCleod gage. The helium gas was introduced into the chamber through a variable-leak valve. The input line was trapped with a liquid-nitrogen-cooled zeolite trap to preclude accidental contamination of the vacuum system. Another zeolite trap was mounted on the chamber itself to trap impurities that might be present in the system.

An ionization gage was used to ensure that the residual pressure in the system with the high-vacuum system pumping was less than 5×10^{-7} mm of mercury.

5.0 SYSTEM CALIBRATION

5.1 Time-Base Calibration

All of the timing calibrations performed on the electronic portions of the apparatus were referred to standard lengths of coaxial cable. The pulse delay times provided by these cables were known to within 0.1 percent. The TPH-converter and MCA linearity and full-scale calibration were checked by accumulating data in the usual manner (discussed in Section 4.0) and then rerunning the apparatus with no change in the setup other than the insertion of a calibrated length of cable in either the start line or the stop line. The overall system linearity was limited by that of the TPH converter, i.e., about 0.1 percent. The full-scale calibration accuracy was that of the standard cables used.

5.2 System Rise Time

Three separate checks of the system speed were made. First, a Monsanto MV-50 light-emitting diode (LED) was used as a light source in place of the electron gun-excitation chamber combination. The manufacturer quoted a nominal decay time for the MV-50 of 1 ns. The curve obtained with the TPH converter and MCA (Figure 8) has a two-decade pure-exponential decay region, with a slope corresponding to a decay time of 0.8 ns, followed by an irregular curve similar to that obtained by Redfield, Wittke, and Pankove (1970). The rounding evident at the peak is discussed in Section 6.4.1. Because of variability from lot to lot, the manufacturer was unable to quote any accuracy for the LED decay constant; hence, this calibration can be considered nominal only.

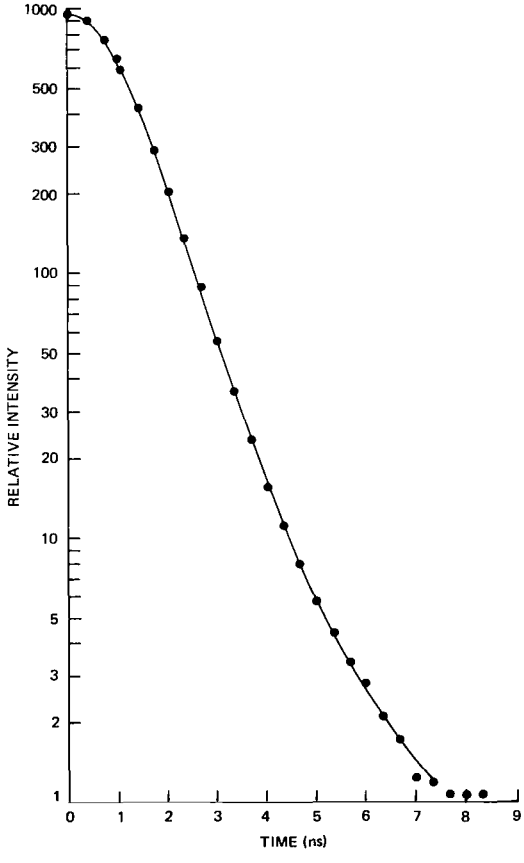

Figure 8—Decay curve for the Monsanto MV-50 LED.

A second rise-time calibration involved the measurement of the decay time of the fast component at 3900Å of a sample of P-15 phosphor. The decay time is known to be less than approximately 4 ns and is probably approximately 1 ns (Kay, 1967). The present measurement indicated a decay time of 1.04 ns.

The third rise-time check was made by consideration of the helium data. During the analysis of the composite decay scheme, successive exponentials are subtracted until the only data remaining must represent the fastest helium component, i.e., that with the 0.769-ns decay time. This remaining portion of the curve must have very nearly the proper slope, as is evidenced by the accuracy of the curve fit. Theoretically, the system rise time should be of the order of 0.12 ns if it is limited by the performance of the TPH converter. The constant-fraction timing

discriminator, because of its insensitivity to pulse amplitude, largely eliminates timing errors from this source. A far more serious problem involving the PMT is discussed in Section 6.0.

5.3 System Linearity

As was described previously, the system timing linearity was checked by the systematic insertion of calibrated lengths of coaxial cable into the start and stop lines of the TPH converter. An amplitude-linearity check was obtained by analysis of the P-15 phosphor data. The 3900Å component is known to consist of a single, pure exponential. The data obtained from the measurement described previously included a fast component which exhibited a uniform exponential decay with no detectable non-linearities. These two linearity checks indicated a system timing linearity of about 2 percent. Amplitude nonlinearity was negligible except for a rounding effect at the peak of the decay curve. This effect is discussed in Section 6.0.

6.0 DATA ANALYSIS

6.1 The Problem

A complex decay curve consisting of a sum of exponentials must be analyzed. From Equation 8, the ratio of the light fluxes for two modes of decay is

$$\frac{\phi_{jk}(t)}{\phi_{lm}(t)} = \frac{n_j(t)A_{jk}}{n_l(t)A_{lm}}$$

$$= \frac{Q_{0j}A_{jk}A_l\gamma_j}{Q_{0l}A_{lm}A_j\gamma_l} \quad . \tag{12}$$

After beam cutoff, the depopulation rate is (neglecting cascades)

$$\dot{n}_j = \dot{n}_j(t)$$

$$= -n_j(t)A_j \ ,$$

or

$$n_j(t) = n_j(0)e^{-A_jt} \ ,$$

where t is time after beam cutoff and $n_j(0)$ is the population of the jth level at beam cutoff. Then,

$$\phi_j = n_jA_j$$

$$= n_j(0)e^{-A_jt}A_j$$

$$= n_j \sum_k \phi_{jk} \ ;$$

thus,

$$\begin{aligned}\phi_{jk} &= n_j A_{jk} \\ &= n_j(0) A_{jk} e^{-A_j t} \ .\end{aligned} \tag{13}$$

In particular, for the He^+ $n = 4$ states

$$\begin{aligned}\phi_{4\to3}(\text{total}) &= \phi_{4s\to3p} + \phi_{4p\to3s} + \phi_{4p\to3d} + \phi_{4d\to3p} + \phi_{4f\to3d} \\ &= [n_{4s}(0) A_{4s\to3p} e^{-t/\tau_{4s}} + n_{4p}(0) e^{-t/\tau_{4p}} (A_{4p\to3s} + A_{4p\to3d}) + n_{4d}(0) A_{4d\to3p} e^{-t/\tau_{4d}} \\ &\qquad + n_{4f}(0) A_{4f\to3d} e^{-t/\tau_{4f}}] \ .\end{aligned} \tag{14}$$

A computer program (discussed in Section 5.0) was developed to analyze the MCA data, beginning at beam cutoff. The computer program solved for the relative magnitudes of the coefficients of the exponentials in Equation 14. These coefficients were then used to solve for the relative cross sections, i.e., from Equation 12,

$$\frac{Q_{0j}}{Q_{0l}} = \frac{\phi_{jk}(T) A_{lm} A_j \gamma_l(T)}{\phi_{lm}(T) A_{jk} A_l \gamma_j(T)} \ , \tag{15}$$

where T is the pulse duration; but from Equation 13,

$$\begin{aligned}\phi_{jk}(T) &= \phi_{jk}(t = 0) \\ &= n_j A_{jk} \\ &= n_j(0) A_{jk} e^{-0/\tau_j} \\ &= n_j(0) A_{jk} \ .\end{aligned}$$

Hence,

$$\frac{\phi_{jk}(T)}{\phi_{lm}(T)} = \frac{n_j(0) A_{jk}}{n_l(0) A_{lm}} \ ,$$

and

$$\frac{Q_{0j}}{Q_{0l}} = \frac{n_j(0) A_j (1 - e^{-T/\tau_l})}{n_l(0) A_l (1 - e^{-T/\tau_j})} \tag{16}$$

The computer program solved for

$$\frac{n_{4p}(0)}{n_{4s}(0)} \frac{A_{4p\to3s} + A_{4p\to3d}}{A_{4s\to3p}} = C_1 \ , \tag{17}$$

$$\frac{n_{4d}(0)}{n_{4s}(0)} \frac{A_{4d\to 3p}}{A_{4s\to 3p}} = C_2 \ , \tag{18}$$

and

$$\frac{n_{4f}(0)}{n_{4s}(0)} \frac{A_{4f\to 3d}}{A_{4s\to 3p}} = C_3 \ , \tag{19}$$

from which one can obtain

$$\frac{Q(\mathrm{He}^+, 4p)}{Q(\mathrm{He}^+, 4s)} = C_1 \frac{A_{4s\to 3p}A_{4p}(1 - e^{-T/\tau_{4s}})}{(A_{4p\to 3s} + A_{4p\to 3d})A_{4s}(1 - e^{-T/\tau_{4p}})} \ , \tag{20}$$

$$\frac{Q(\mathrm{He}^+, 4d)}{Q(\mathrm{He}^+, 4s)} = C_2 \frac{A_{4s\to 3p}A_{4d}(1 - e^{-T/\tau_{4s}})}{A_{4d\to 3p}A_{4s}(1 - e^{-T/\tau_{4d}})} \ , \tag{21}$$

and

$$\frac{Q(\mathrm{He}^+, 4f)}{Q(\mathrm{He}^+, 4s)} = C_3 \frac{A_{4s\to 3p}A_{4f}(1 - e^{-T/\tau_{4s}})}{A_{4f\to 3d}A_{4s}(1 - e^{-T/\tau_{4f}})} \ . \tag{22}$$

6.2 FRANTIC

An attempt was made to analyze the data by means of a fairly elaborate least-squares-fitting digital-computer program similar to FRANTIC (Rogers, 1962). During the course of analyzing a complex decay scheme consisting of a sum of exponential decays, FRANTIC develops a matrix equation $\mathbf{Ax} = \mathbf{b}$, where $\mathbf{A}$ is $m \times n$. It then forms $\mathbf{A}^T$ and $\mathbf{C} \equiv \mathbf{A}^T\mathbf{A}$ and solves $\mathbf{Cx} = \mathbf{d}$, where $\mathbf{C}$ is $m \times m$. This technique requires the calculation of $\mathbf{A}^{-1}$; but, due to the severe scatter in the data, $\mathbf{A}$ becomes singular, and no inverse can be calculated.

A modification of this technique in which the "Q-R decomposition" of $\mathbf{A}$ is formed eliminates the necessity of calculating an inverse. In this technique, matrices $\mathbf{Q}$ and $\mathbf{R}$ are formed such that $\mathbf{A} = \mathbf{QR}$, where $\mathbf{Q}^T = \mathbf{Q}^{-1}$ and $\mathbf{R}$ is upper triangular. Then, $\mathbf{f} = \mathbf{Q}^T\mathbf{b}$ is found and $\mathbf{Rx} = \mathbf{f}$ is solved. This technique seemed to be more stable than the original FRANTIC technique, but because of the scatter in the data, it was unable to produce reasonable results.

6.3 MADCAP

Finally, MADCAP,* a new computer program, was developed. This program closely follows the technique one would employ if faced with the problem of manually analyzing the MCA data, where

*"MADCAP Program for Analysis of Exponential Decay Curves", by J. F. Sutton and A. J. Villasenor (unpublished).

the lifetimes are accurately known. The data are first plotted on semilog paper. Then, the straight portion of the decay curve is fitted to the longest-lived component by subtracting the background. The magnitude of the constant value of the background subtracted is adjusted until a least-squares fit of a straight line with the proper (known) slope is obtained. The magnitude of this first exponential component is calculated, and the entire first exponential is subtracted point by point from the data from which the constant background has previously been subtracted. Similarly, another exponential is fitted to the tail of the remaining data curve, subtracted, and so forth, until all of the exponential decays known to be present in the composite curve have been subtracted out.

MADCAP calculates three indicators of the quality of the analysis: the standard χ^2 value, a cumulative fractional absolute difference (between the calculated curve and the original data), and a set of point-by-point differences between the curves. The standard χ^2 value calculated should be of the order of the number of counts in one channel of the MCA. The cumulative fractional absolute difference,

$$\text{Absolute difference} \equiv \sum_i \frac{1}{y_i}\left[y_i - \left(\sum_j a_j e^{-A_j t}\right)_i\right],$$

gives a useful absolute indication of the quality of the fit. In the case of noisy data, it was found that an absolute difference of 1 percent represented a good fit. An absolute difference of 5 percent could be considered bad. The point-by-point differences give the most reliable indication of the quality of the curve fit. In the case of a very good fit and truly random background noise, these differences will all be of the same order and of randomly changing signs as one progresses along the curve.

MADCAP contains an optional smoothing subroutine that is useful in preliminary analyses of noisy data. Each point is averaged with two, or four, or six, etc., neighboring points, the number being a parameter chosen by the operator.

6.4 Data

Several data runs were taken under various experimental conditions. Runs were made at several pressures and average electron-beam currents to be certain that nonlinear effects due to secondary processes were not severe. Difficulties were experienced in obtaining enough counts in the data curves to ensure adequate statistical confidence. This was the result of a tendency for the oxide-coated cathode of the electron gun to become poisoned when the vacuum system was isolated from the high-vacuum pump. The data from several runs were analyzed carefully with the aid of MADCAP. The run that exhibited the best fit to the theoretical decay times is presented in Appendix A.

The analysis of Appendix A, as well as those following, proceeds as follows. First, that portion of the data from the MCA chosen for analysis is displayed in a table. Next, this is plotted on a three-cycle semilog scale. The constant background, a number obtained from channels of the MCA collected earlier in time than the beginning of the beam pulse, is subtracted, and the result is plotted. The straight portion of the curve is fitted to the longest-lived decay component present, that due to leakage of small amounts of light from the brighter lines of helium through the skirts of the filter. The least-

squares iterative fitting process is then displayed in a table. Next, the computed values of the exponential are compared with those of the data on the straight portion of the experimental curve. After the least-squares fit, the adjusted curve is plotted, the exponential is subtracted from this curve, and the result is listed and plotted. This procedure is continued until all of the remaining exponentials known to be present have been subtracted out. In this case, there are four remaining helium exponentials, making a total of five.

After the last exponential has been plotted, the results of the fitting process are displayed. First, the magnitudes of the computed exponentials are given. Then, the computed values, the experimental values, and the differences are listed. Finally, as described in Section 6.0, the χ^2 and absolute difference values are given.

The data in Appendix A were taken at a 10-μm pressure for 3 1/2 hours with the MCA in the *accumulate* mode, followed by a 3 1/2-hour run in the *subtract* mode with the helium removed in order to subtract the effect of a background consisting of two exponentials. It is believed that this background was developed by excitation of small amounts of CO evolved by the cathode of the electron gun. Several data runs at different pressures indicated that the CO background was independent of helium pressure and could therefore be subtracted in this way.

The analysis of Appendix B is a duplicate of that of Appendix A, with the exception that the analysis was begun at an earlier time (the time of the peak of the data curve). The last two curves in Appendix B are rounded near the vertical axis. The cause of this distortion is discussed in the next section.

6.4.1 Data Curve Distortion

The helium data chosen for study and used in Appendix A are from that portion of the original MCA curve beginning seven channels, or approximately 2 1/3 ns, from the location of the peak. For the first 2 1/3 ns, the original curve exhibits rounding, which indicates that the simplified analysis of Section 6.1 must be modified. It is believed that there are two major causes of the data distortion: a distorted effective current pulse shape, and time jitter in the PMT. Because of transit-time effects, the effective current pulse is believed to be somewhat triangular in shape. The total transit time for 200-eV electrons traveling the 1/4-in. radius of the collision region is 0.7 ns. With a 0.3-ns input-pulse rise time, the rising and falling portions of the effective current pulse would then be approximately 1 ns in duration. The transit-time spread of the PMT is a quasi-Gaussian function with a full width at $1/e$ of 2.5 ns. The convolution effect of this function will be described later.

As was noted above, the simplified analysis of Section 6.1 must be modified to account for the distorted effective input-current pulse shape. The relative magnitudes of the exponentials are known at t_1, the time of the beginning of the digital-computer analysis. There is no excitation of the atomic states between t_2—the time of the end of the input current pulse—and t_1; hence, during the interval, the decays would be pure exponentials, allowing calculation of relative magnitudes of the exponentials at t_2 with digital-computer data obtained for t_1. To find the cross-section ratios, however, it is necessary to know the shapes of the *RC*-like atomic level populations in response to the distorted effective input current pulse shape. These shape functions were found by exciting analog-computer-simulated *RC* circuits with triangular voltage pulses and recording the capacitor voltages as a function of time.

Equation 6 is rewritten:

$$\dot{n}_j(t) + A_j n_j(t) = \left[\frac{I(t)}{e}\right] \rho l' Q_{0j}$$

$$\equiv Q_{0j} S_0 s(t) , \tag{23}$$

where $s(t)$ is the triangular effective current pulse shape function with unit absolute maximum amplitude. The solution is

$$n_j(t) = Q_{0j} S_0 \left[e^{-A_j t} \int_0^t e^{+A_j t} s(t)\, dt \right] . \tag{24}$$

The analogous equation describing the charging of a capacitor in an RC integrator circuit by an applied voltage $E_i(t)$ is

$$\dot{q}(t) + (RC)^{-1} q(t) = \frac{E_i(t)}{R}$$

$$\equiv \frac{E_0 e_i(t)}{R} \tag{25}$$

where $e_i(t) \equiv s(t)$ is the analog-computer simulation of the effective current pulse shape function (unit-absolute-magnitude). The solution to Equation 25 is

$$q(t) = \frac{E_0}{R} \left[e^{-t/RC} \int_0^t e^{+t/RC} e_i(t)\, dt \right] .$$

The analog computer circuit in Figure 9 was employed to generate the RC circuit response functions (capacitor voltages as a function of time) to a triangular voltage pulse (which simulates the effective input current pulse shape) having unit-absolute-maximum-amplitude.

The responses generated by this computer circuit were displayed on an oscilloscope and photographed. They may be represented mathematically by

$$E_c(t) \equiv \frac{q_j(t)}{C_j}$$

$$= (RC)_j^{-1} \left[e^{-t/(RC)_j} \int_0^t e^{+t/(RC)_j} e_i(t)\, dt \right] E_0$$

$$\equiv F_j(t) E_0 . \tag{26}$$

Evidently, Equations 23 and 25 are completely analogous if the following identifications are made:

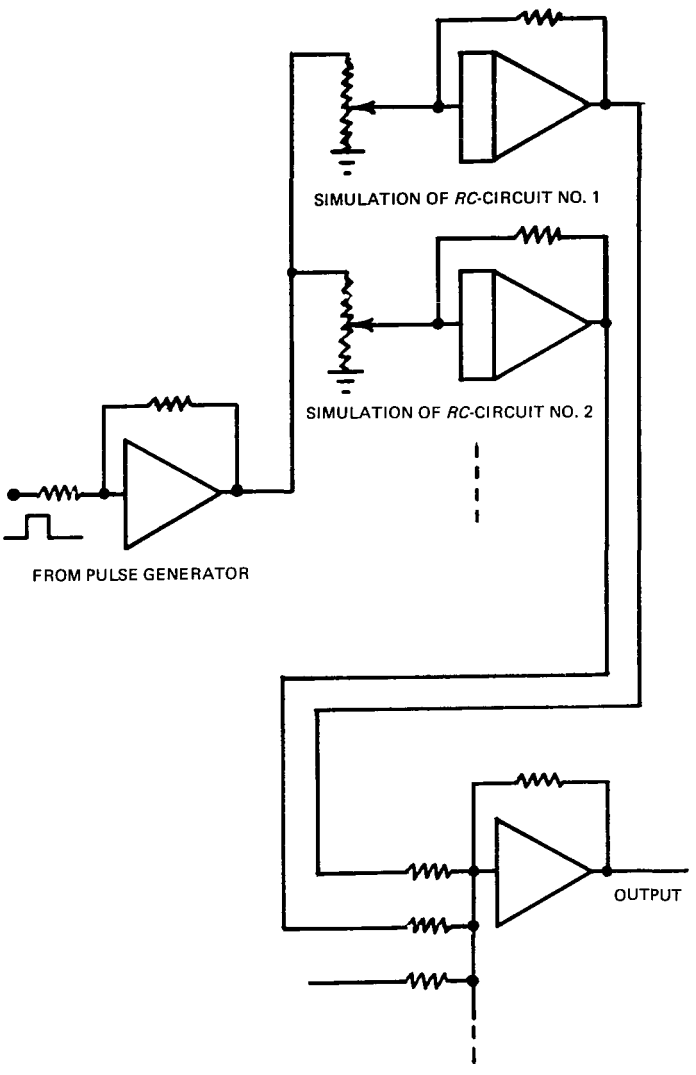

Figure 9—Analog-computer circuit for generation of $F_j(t)$.

$$n_j \equiv q_j \ ,$$

$$A_j \equiv (RC)_j^{-1} \ ,$$

and

$$Q_{0j}S_0 \equiv \frac{E_{0j}}{R_j} \ .$$

The function $F_j(t)$ then represents equally well the response of an atomic system population to $Q_{0j}S_0 s(t)$ in the special case where $Q_{0j}S_0 \equiv 1$, or the capacitor voltage response of an RC integrator to $E_0 e_i(t)/R$ in the special case where $E_0 \equiv 1$. From Equation 24, it follows that

$$n_j(t) = Q_{0j} S_0 F_j(t)(RC)_j \ . \tag{27}$$

Hence, the light flux ratios, analogous to Equation 12, are

$$\frac{\phi_{jk}(t)}{\phi_{lm}(t)} \equiv \frac{n_j(t)A_{jk}}{n_l(t)A_{lm}}$$

$$= \frac{Q_{0j}F_j(t)A_{jk}A_l}{Q_{0l}F_l(t)A_{lm}A_j} \ , \tag{28}$$

in which the identification $A_j = (RC)_j^{-1}$ has been used. Thus, the result analogous to Equation 15 is

$$\frac{Q_{0j}}{Q_{0l}} = \frac{\phi_{jk}(t)F_l(t)A_{lm}A_j}{\phi_{lm}(t)F_j(t)A_{jk}A_l}$$

$$= \frac{n_j(t)A_jF_l(t)}{n_l(t)A_lF_j(t)} \ . \tag{29}$$

Now, for the specific case of He^+, from Equations 17 to 19 of Section 6.1,

$$\frac{n_{4p}(t_1)}{n_{4s}(t_1)} = C_1 \frac{A_{4s\to3p}}{A_{4p\to3s} + A_{4p\to3d}} \ ,$$

$$\frac{n_{4d}(t_1)}{n_{4s}(t_1)} = C_2 \frac{A_{4s\to3p}}{A_{4d\to3p}} \ ,$$

and

$$\frac{n_{4f}(t_1)}{n_{4s}(t_1)} = C_3 \frac{A_{4s\to3p}}{A_{4f\to3d}} \ .$$

Thus, the results analogous to Equations 20 to 22 are

$$\frac{Q(He^+, 4p)}{Q(He^+, 4s)} = C_1 \frac{A_{4s\to3p}F_{4s}(t_2)A_{4p}e^{(A_{4p}-A_{4s})\Delta t}}{(A_{4p\to3s} + A_{4p\to3d})F_{4p}(t_2)A_{4s}} \ , \tag{30}$$

$$\frac{Q(He^+, 4d)}{Q(He^+, 4s)} = C_2 \frac{A_{4s\to3p}F_{4s}(t_2)A_{4d}e^{-A_{4s}\Delta t}}{A_{4d\to3p}F_{4d}(t_2)A_{4s}e^{-A_{4d}\Delta t}} \ , \tag{31}$$

and

$$\frac{Q(He^+, 4f)}{Q(He^+, 4s)} = C_3 \frac{A_{4s\to3p}F_{4s}(t_2)A_{4f}e^{-A_{4s}\Delta t}}{A_{4f\to3d}F_{4f}(t_2)A_{4s}e^{-A_{4f}\Delta t}} \ , \tag{32}$$

where t_2 is the time of the end of the current pulse and t_1 is the time of the digital-computer analysis (Appendix A) (as before, $\Delta t \equiv t_1 - t_2$), and where

$$F_j(t_1) \equiv F_j(t_2) e^{-A_j \Delta t} \quad .$$

Thus, the relative amplitudes of the $F_j(t)$ functions at t_1 are determined from values obtained from photographs of the analog-computer simulation of $F_j(t)$ at t_2.

The interval Δt was determined by doing a graphical convolution of a 2.5-ns-wide Gaussian with triangular pulse-excited RC-integrator signals, where the scaled RC time constants were set equal to the corresponding atomic lifetimes. The amplitudes of the RC responses convoluted separately with the Gaussian resulted in convolution amplitudes at t_1, which corresponded to the results of the digital-computer analysis at t_1. The convolution of the Gaussian with the combined RC responses resulted in a good fit to the original MCA data. The peak of the convolution was found to coincide with the end of the triangular effective input current pulse. The digital-computer analysis begins 2 1/3 ns past the peak of the convolution function (i.e., the peak of the MCA data curve, Figure 10); thus,

$$\Delta t = (t_1 - t_2)$$

$$= 2\ 1/3 \text{ ns.}$$

The values of the ratios of $F_j(t_2)$, taken from the photographs, are

$$\frac{F_{4s}(t_2)}{F_{4p}(t_2)} = 0.173 \ ,$$

$$\frac{F_{4s}(t_2)}{F_{4d}(t_2)} = 0.237 \ ,$$

and

$$\frac{F_{4s}(t_2)}{F_{4f}(t_2)} = 0.390 \ .$$

Entering these values into the equations for the cross sections, with $C_1 = 0.288$, $C_2 = 0.690$, and $C_3 = 2.98$, yields

$$\frac{Q(\text{He}^+, 4\text{p})}{Q(\text{He}^+, 4\text{s})} = 8.34 \ ,$$

$$\frac{Q(\text{He}^+, 4\text{d})}{Q(\text{He}^+, 4\text{s})} = 0.629 \ ,$$

and

$$\frac{Q(\text{He}^+, 4\text{f})}{Q(\text{He}^+, 4\text{s})} = 0.682 \ .$$

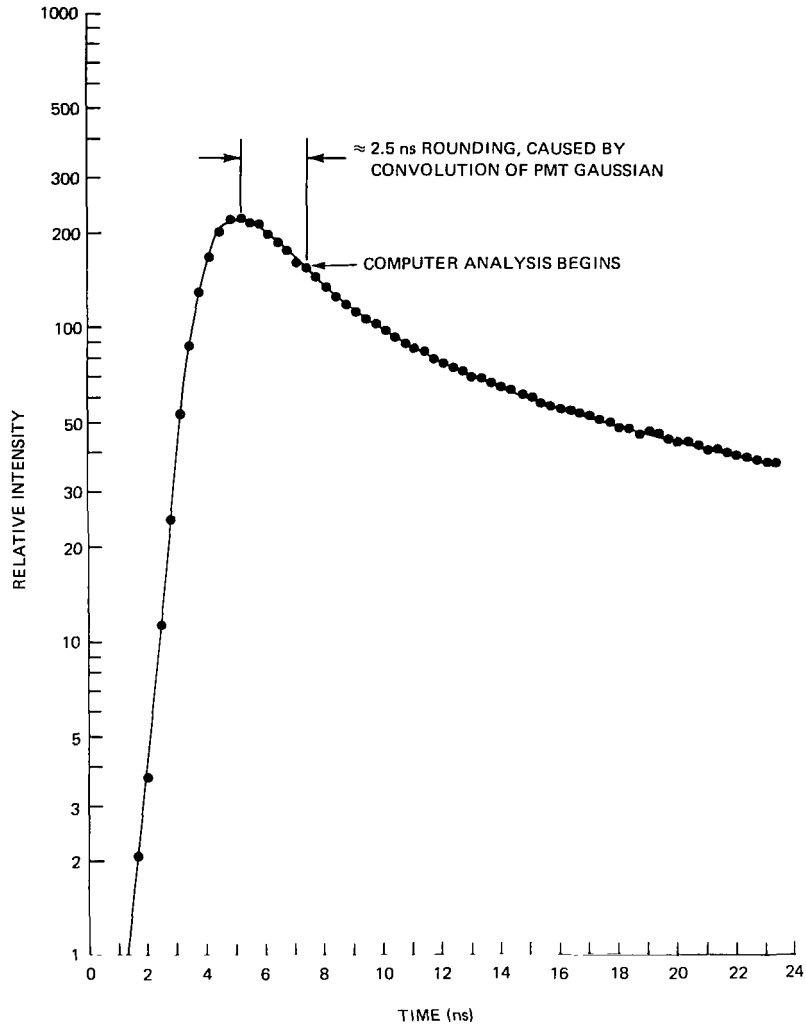

Figure 10—Graph of helium data with constant background removed, illustrating time relationships.

These computed values of the ratios of the cross sections were obtained by using the results of the digital-computer analysis in Appendix A, which included no correction for the transit-time spread of the PMT. If a truncated Gaussian time-scatter function due to system electronics (including the PMT and the discriminator) is assumed, the effect on the data can be obtained by the convolution of the Gaussian with the (assumed) perfect *RC* discharging curves. The convolution can be written as follows:

$$(f_1 * f_2)(t) = \int_0^\infty f_1(\lambda) f_2(t-\lambda)\, d\lambda$$

$$= \int_0^\infty e^{-a\lambda^2} e^{-k(t-\lambda)}\, d\lambda\,, \tag{33}$$

where $k \equiv \tau^{-1}$. Now,

$$\int_0^\infty e^{-(at^2+2bt+c)}\, dt \equiv \frac{1}{2}\left(\frac{\pi}{a}\right)^{1/2} e^{(b^2-ac)/a}\, \mathrm{erfc}\left(\frac{b}{\sqrt{a}}\right), \tag{34}$$

where

$a \equiv$ constant determining the width of the Gaussian,

$b \equiv -1/2\tau$,

and

$c \equiv kt$

$= t/\tau$.

Here, one assumes that the entire convolution of interest will be made far from the origin (i.e., on the tail of a decaying exponential). The result is an exponential decay curve with an adjusted amplitude:

$$(f_1 * f_2)(t) = \left(\frac{T}{4}\right)\sqrt{\pi}\, e^{(T/4\tau)^2}\left[1 - \mathrm{erf}\left(-\frac{T}{4\tau}\right)\right] e^{-t/\tau}\,, \tag{35}$$

where T is the effective width at $1/e$ of the PMT Gaussian.

6.4.2 Determination of Width of PMT Gaussian

The effective width T was determined as follows. The inside surface of the electron collector was coated with an ethyl alcohol suspension of P-15 phosphor and allowed to dry. The apparatus was reassembled and evacuated. Data were obtained with the same gun assembly, optics, PMT, and electronic apparatus used during the helium runs. The data were analyzed beginning at the point where curve rounding is negligible. It was assumed that this curve was effectively convoluted by the PMT Gaussian, and an analog-calculator circuit was constructed to simulate the effect. A time-scaled pulse with 0.3-ns rise times and fall times and a time at full-width, half-maximum of 1.2 ns, simulating as closely as possible the pulse used during the P-15 data run (transit-time effects being negligible because the phosphor was not spread over a large volume as was the helium), was applied to computer realizations of the RC times of the phosphor. The resulting responses were separately convoluted with a simulated Gaussian-shaped pulse, and the amplitudes of the convolutions were adjusted to conform to the computer analysis at the point where rounding began. Next, the RC responses were summed and convoluted with the same Gaussian and compared with the constant background removed. This process was repeated with Gaussian widths adjusted from 1.0 to 4.0 ns. A time $T = 2.5$ ns gave the best match with the data.

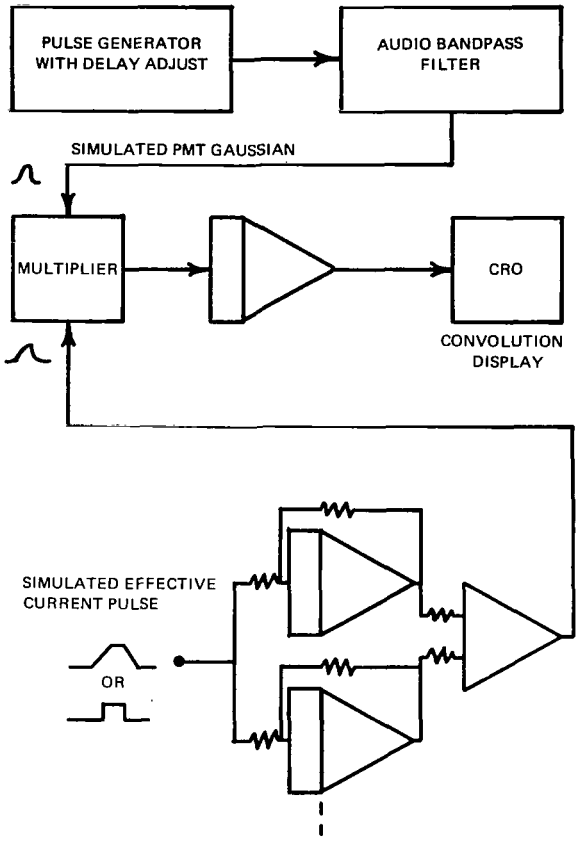

Figure 11—Convolution computer.

Appendix C is the analysis of the P-15 data, starting where rounding begins. Appendix D is the analysis beginning at the peak of the data curve. Figure 11 is a block diagram of the analog convolution computer, and Figure 12 shows the convolutions of Gaussians of 2.0, 2.5, and 3.0 ns with the P-15 phosphor RC responses to a rectangular input pulse. In Figure 13, the data have been replotted on a single set of coordinates. This shows clearly that the experimental data fit the convolution with a 2.5-ns-wide Gaussian.

From Equation 35, the ratios of the convolution correction factors $K(\tau)$ are

$$\frac{K(\tau_1)}{K(\tau_4)} = 1.92 ,$$

$$\frac{K(\tau_1)}{K(\tau_3)} = 1.27 ,$$

and

$$\frac{K(\tau_1)}{K(\tau_2)} = 1.11 ,$$

where

$$K(\tau_i) \equiv \left(\frac{T}{4}\right)\sqrt{\pi}\, e^{(T/4\tau_i)^2}\left[1 - \text{erf}\left(-\frac{T}{4\tau_i}\right)\right] ,$$

and

$\tau_i \equiv$ decay constant of the ith exponential to be convoluted.

The time T is the full width at $1/e$ of the Gaussian.

Because the convolutions generated by the PMT caused the apparent amplitudes of the faster components to be reduced relative to those of the slower ones, the correction factors may be applied directly to the computer-generated constants; i.e.,

$$C_1' = C_1 \times 1.92$$

$$= 0.552,$$

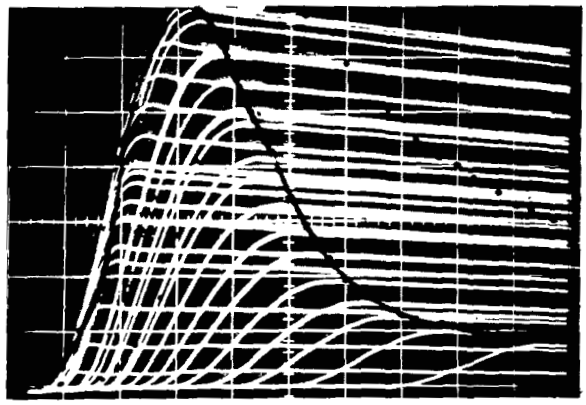

(a) $T = 2.0$ ns.

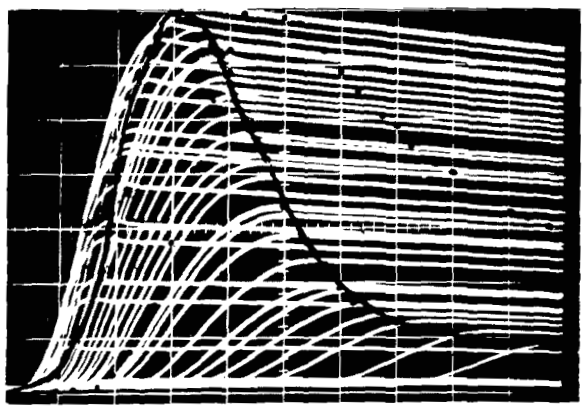

(b) $T = 2.5$ ns.

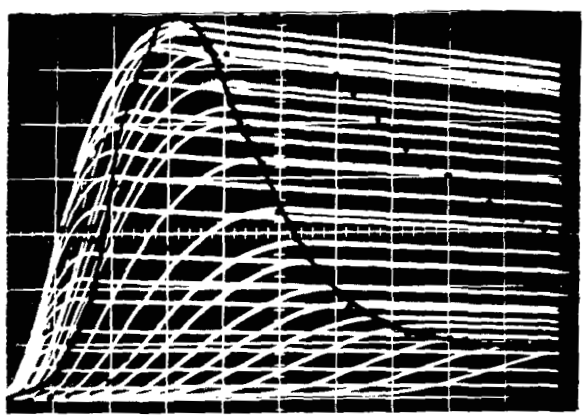

(c) $T = 3.0$ ns.

Figure 12—Analog convolution calculations for P-15 phosphor, compared with data. The vertical units are relative intensity, and the horizontal units are 1 ns per major division. The solid curve is the P-15 phosphor data; the points are the helium data. The peaks of the light curves represent points from the analog calculation.

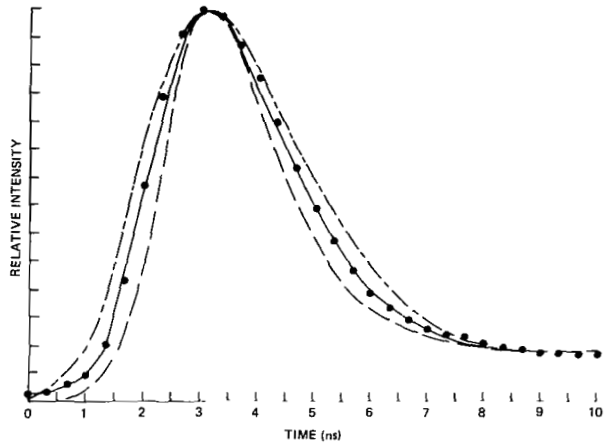

Figure 13—Analog-computer convolution calculations for P-15 phosphor compared with data, showing best fit with Gaussian of width $T = 2.5$ ns. The points are the P-15 phosphor data; the broken curve is the convolution with the Gaussian of width $T = 2.0$ ns; the dot-dash curve is the convolution with the Gaussian of width $T = 3.0$ ns; and the solid curve is the convolution with the the Gaussian of width $T = 2.5$ ns.

$$C_2' = C_2 \times 1.27$$
$$= 0.877,$$

and

$$C_3' = C_3 \times 1.11$$
$$= 3.31 .$$

The cross-section ratios become

$$\frac{Q'(\mathrm{He}^+, 4p)}{Q(\mathrm{He}^+, 4s)} = 16.01 ,$$

$$\frac{Q'(\mathrm{He}^+, 4d)}{Q(\mathrm{He}^+, 4s)} = 0.799 ,$$

and

$$\frac{Q'(\mathrm{He}^+, 4f)}{Q(\mathrm{He}^+, 4s)} = 0.757 .$$

The effective input current pulse and the 2.5-ns Gaussian depicted in Figure 14 were convoluted by the calculator described above. The result is given in Figure 15, where part (a) shows the responses of the *RC* circuits to the triangular input pulse and part (b) compares the calculated convolution with the helium data.

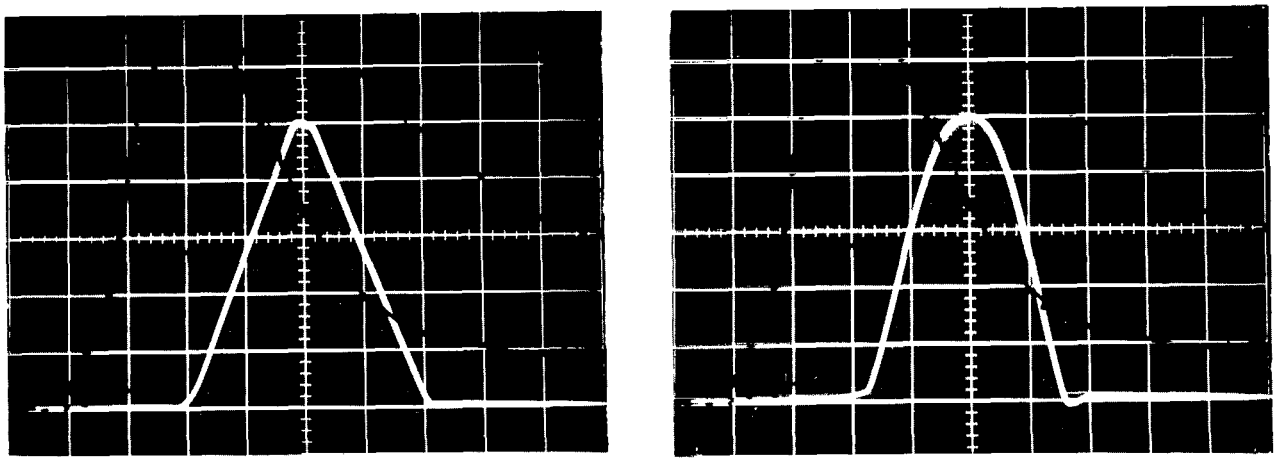

Figure 14—Pulses used in the analog calculations: (a) triangular effective current pulse; (b) Gaussian of width $T = 2.5$ ns. In both cases, the pulses have unit amplitude, and the horizontal units are 0.5 ns per major division.

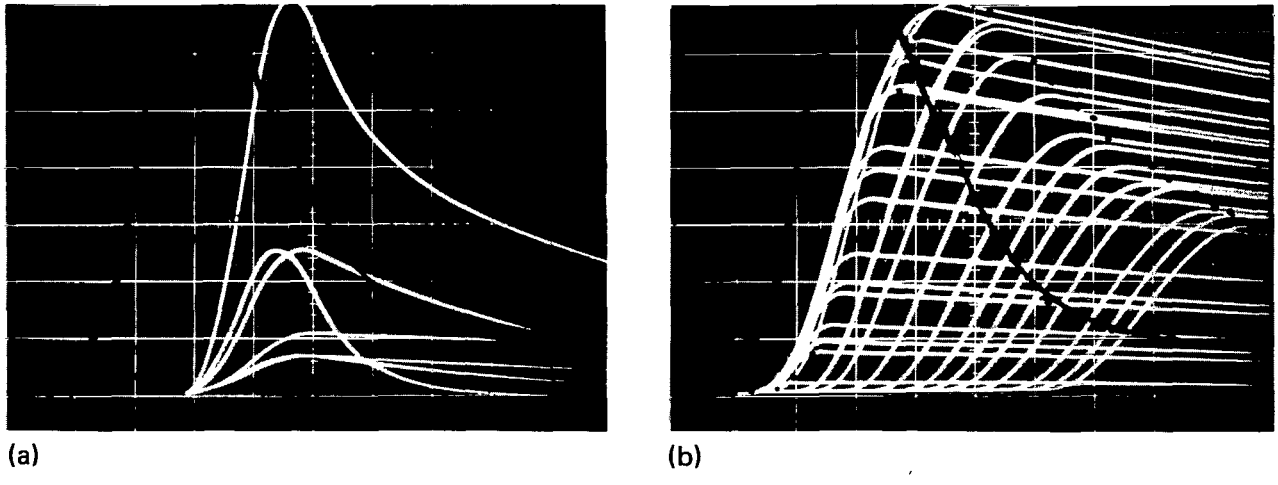

Figure 15—Results of analog-computer simulation for helium: (a) response of *RC* circuits to triangular effective current pulse (top curve is sum of individual *RC* responses); (b) convolution of triangular effective current pulse excited *RC* circuits with 2.5-ns-wide Gaussian (apparent poor fit at peak of curve is due to parallax), where the dark solid curve is the P-15 phosphor data and the dotted curve is the helium data. In both cases, the vertical units are relative amplitude, and the horizontal units are 1 ns per major division.

6.5 Error Analysis

The accuracy of the results is difficult to ascertain. An indication of the order of magnitude of the errors may be obtained by considering the values of the differences between the calculated and the experimental values of the helium data points. Near the ordinate, the differences are about 500 counts (out of a total of 180 000). The worst part of the fit occurs a few nanoseconds later, where differences of about 4000 (out of 120 000) occur. The helium data are compared with theory in Figure 16, where the theoretical curve includes the convolution information from Figure 15 and the magnitudes of the exponentials obtained from Appendix A.

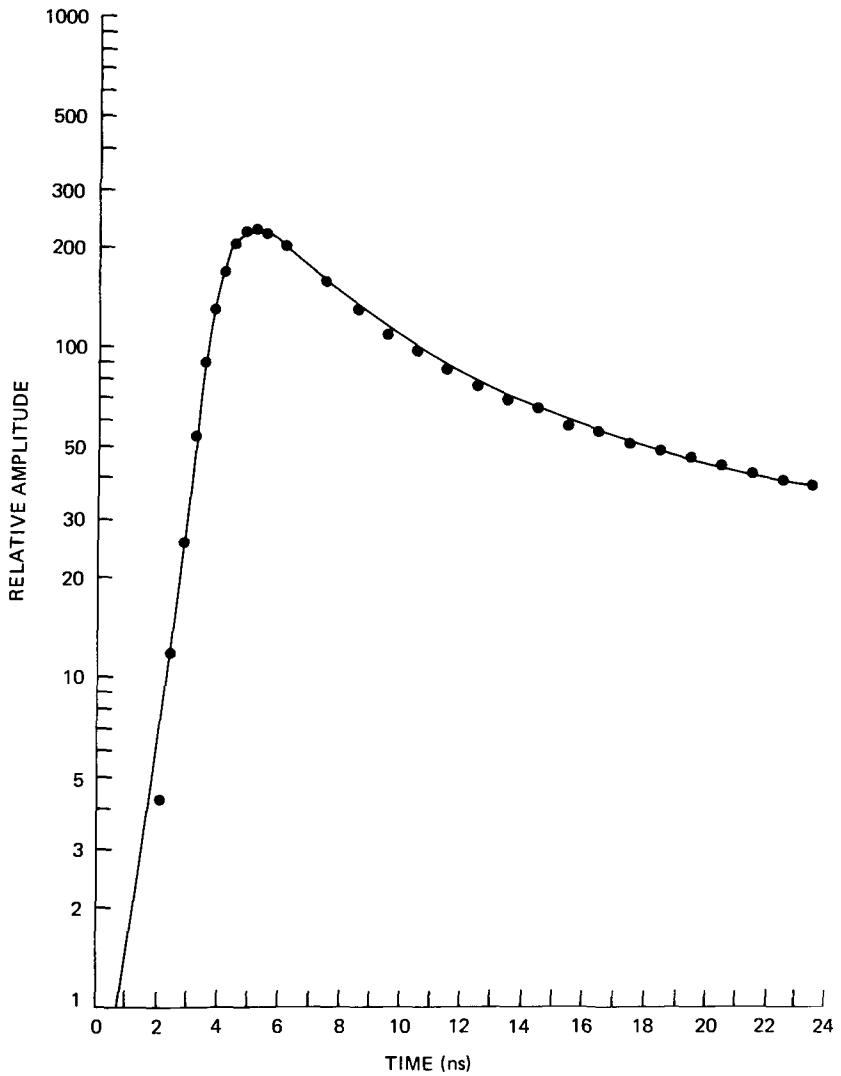

Figure 16—Helium data compared with results of analysis: The points are the helium data (from Appendix A), and the solid curve is the theoretical calculation, including the calculated convolution from time zero to 2.5 ns past peak, and the calculated exponentials thereafter.

Table 2—Variation of results with Gaussian width T.

Cross-Section Ratio	Value		
	T = 2.0 ns	T = 2.5 ns	T = 3.0 ns
$\frac{Q(He^+, 4p)}{Q(He^+, 4s)}$	17	19	21
$\frac{Q(He^+, 4d)}{Q(He^+, 4s)}$	0.81	0.85	0.88
$\frac{Q(He^+, 4f)}{Q(He^+, 4s)}$	0.73	0.78	0.79

The results of varying the values of T are listed in Table 2, where the entries have been adjusted by the factors $\gamma_j(\delta t)/A_j\delta t$ which correct for the bias introduced by the finite channel width (δt = 1/3 ns) of the MCA. Figure 17 illustrates the variation of the convolution correction factors with T. It is estimated that $2.5 < T < 3.0$ ns. Because of this uncertainty in T, the following errors in the cross-section ratios may be expected:

$$\frac{Q(He^+, 4p)}{Q(He^+, 4s)}: \text{ approximately } \pm 10 \text{ percent.}$$

$$\frac{Q(He^+, 4d)}{Q(He^+, 4s)}: \text{ approximately } \pm 5 \text{ percent.}$$

$$\frac{Q(He^+, 4f)}{Q(He^+, 4s)}: \text{ approximately } \pm 2 \text{ percent.}$$

Although the digital-computer program was relatively stable under reasonable perturbations of the control parameters, the fast 4p component exhibited an uncertainty of about 10 percent, with the other components varying about 5 percent. In addition, errors of about 5 percent should be expected from the effects of system nonlinearities. One can then expect the cross-section ratios to be bounded approximately by these errors, giving the final results

$$\frac{Q(He^+, 4p)}{Q(He^+, 4s)} = 19 \text{ (with an estimated } 1\sigma \text{ error of 30 percent)},$$

$$\frac{Q(He^+, 4d)}{Q(He^+, 4s)} = 0.85 \text{ (with an estimated } 1\sigma \text{ error of 20 percent)},$$

and

$$\frac{Q(He^+, 4f)}{Q(He^+, 4s)} = 0.78 \text{ (with an estimated } 1\sigma \text{ error of 10 percent)}.$$

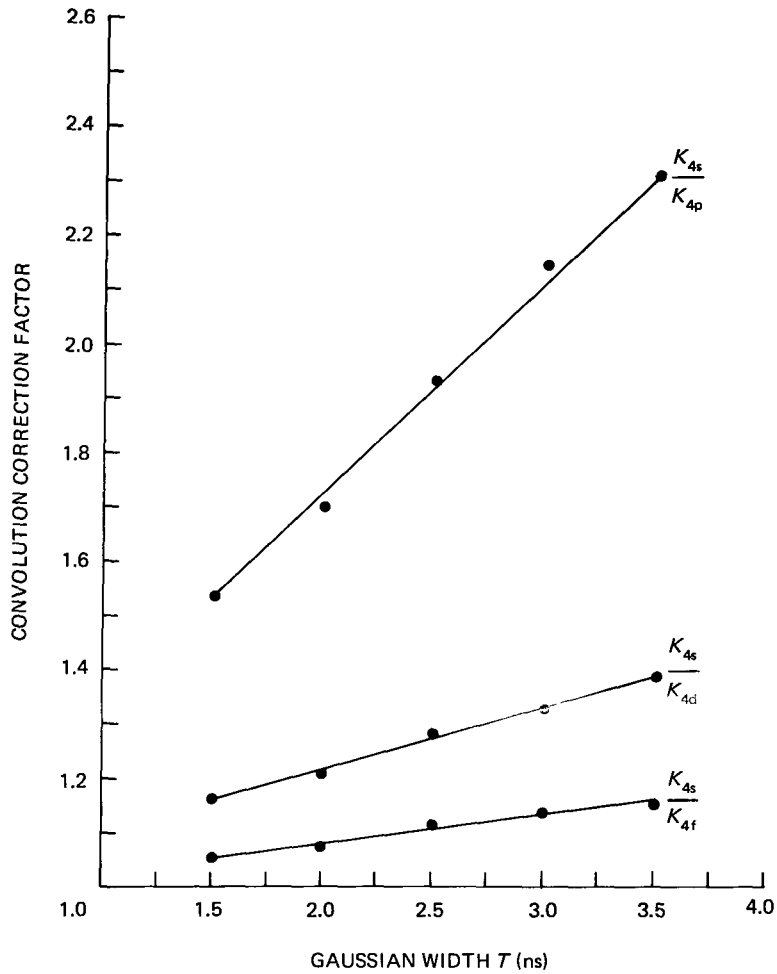

Figure 17—Variation of convolution correction factors with Gaussian width T.

It is conceivable that the noise in the MCA data or an error in the magnitude obtained for Δt might have biased the calculated magnitude of the fast 4p component by as much as a factor of 2 or 3, but it is believed on the basis of the stability mentioned above and on graphical analysis of the data that the listed errors are reasonable estimates.

7.0 RESULTS AND CONCLUSIONS

The author's results and various other experimental and theoretical values are listed in Table 3. There is evidently poor agreement with the Born approximation calculations of Lee and Lin (1967) and Dalgarno and McDowell (1956). However, with the exception of the $Q(He^+, 4p)/Q(He^+, 4f)$ ratio, there seems to be fair agreement with cross-section ratios obtained both theoretically [Ochkur approxima-

Table 3—Comparison of results with other measurements and theoretical predictions.

Simultaneous Ionization and Excitation of Helium (200 eV)			Single-Electron Excitation of Helium (200 eV)			Single-Electron Excitation of Hydrogen (240 eV)	
Ratio	Measured	Theoretical	Ratio	Measured	Theoretical	Ratio	Theoretical
$\frac{Q(He^+, 4p)}{Q(He^+, 4s)}$	19[a]	0.36[b]	$\frac{Q(4^1p)}{Q(4^1s)}$	13.5[c] 22[d]	–	$\frac{Q(4p)}{Q(4s)}$	14.6[e]
$\frac{Q(He^+, 4d)}{Q(He^+, 4s)}$	0.85[a]	0.084[b]	–	–	–	$\frac{Q(4d)}{Q(4s)}$	0.95[e]
$\frac{Q(He^+, 4f)}{Q(He^+, 4s)}$	0.78[a]	–	–	–	–	–	–
$\frac{Q(He^+, 4p)}{Q(He^+, 4d)}$	22[a]	4.27[f]	$\frac{Q(4^1p)}{Q(4^1d)}$	22.4[c] 18[d]	34.4[g]	$\frac{Q(4p)}{Q(4d)}$	15.4[e]
$\frac{Q(He^+, 4p)}{Q(He^+, 4f)}$	24[a]	–	$\frac{Q(4^1p)}{Q(4^1f)}$	–	5000[g]	–	–

[a]Author's measurement.
[b]Anderson et al., 1967.
[c]St. John et al., 1964.
[d]J. G. Showalter, private communication (preliminary data).
[e]Vainshtein, 1965.
[f]Dalgarno and McDowell, 1956.
[g]Ochkur and Bratsev, 1966.

tion (Ochkur and Bratsev, 1965) and Born approximation (Vainshtein, 1965)] and experimentally* (St. John et al., 1964) for single-electron excitation of helium and atomic hydrogen. There is some evidence that the value of 5000 for the $Q(4^1p)/Q(4^1f)$ ratio, obtained theoretically by using the Ochkur approximation, is too large: Anderson, Hughes, and Norton (1969) measured the 4^1f cross section in helium and obtained a value at 100 eV of 1.1×10^{-20} cm^2, which is approximately two orders of magnitude larger than that (3.1×10^{-22} cm^2) obtained theoretically by Ochkur and Bratsev (1965).

The results seem to indicate, therefore, that the simultaneous ionization and excitation process in helium may be thought of primarily as a single-electron excitation process, the ionization of the second electron playing a relatively minor role. This idea corresponds to the "sudden" approximation (Lamb and Skinner, 1950; Mader et al., 1971), in which the second of two contributions to the cross

*J. G. Showalter, private communication (preliminary data).

section is dominant. The first contribution is the ionization cross section times the squared overlap integral between the excited state and the ground state. The other contribution involves the sudden excitation of one atomic electron, followed by ionization of the remaining electron because of the sudden change in the effective nuclear charge.

As is discussed in Section 3.4, the results of this measurement may be applied to the development of an ultraviolet intensity standard. From Equations 6 to 8, one can derive the following expression for the steady-state ($t \to \infty$) ratio of the visible 4686Å light flux to the ultraviolet 1215Å light flux:

$$\frac{\phi_{4\to3}}{\phi_{4\to2}} = \frac{B_{4s\to3p} + \frac{Q(He^+, 4p)}{Q(He^+, 4s)}(B_{4p\to3s} + B_{4p\to3d}) + \frac{Q(He^+, 4d)}{Q(He^+, 4s)}B_{4d\to3p} + \frac{Q(He^+, 4f)}{Q(He^+, 4s)}B_{4f\to3d}}{B_{4s\to2p} + \frac{Q(He^+, 4p)}{Q(He^+, 4s)}B_{4p\to2s} + \frac{Q(He^+, 4d)}{Q(He^+, 4s)}B_{4d\to2p}}.$$

From the measured cross-section ratios from Table 2 and the branching ratios calculated from the data tabulated in the literature (Wiese et al., 1966), the result is

$$\frac{\phi_{4\to3}}{\phi_{4\to2}} = 0.64 \text{ (with an estimated } 1\sigma \text{ error of 5 percent).}$$

Thus, even with measured values of the cross-section ratios uncertain to about 10 to 30 percent, the intensity of the ultraviolet radiation is nevertheless known to within about 5 percent. This is a result of the tendency for the errors to cancel in the above equation. By comparing the visible radiation at 4686Å with that of a standard lamp, one can then effectively standardize the intensity of the 1215Å radiation for use in the calibration of ultraviolet sensors.

The above calculations neglected cascades, which under dc conditions can contribute large differences in the populations $n_j(t)$. By using the calculated cross sections and tabulated A coefficients and values obtained for higher principle quantum numbers by scaling according to n^3, the following adjustments to the n_j were calculated:

$$n'_{4s} = n_{4s} + 40 \text{ percent},$$

$$n'_{4p} = n_{4p} + 1.5 \text{ percent},$$

$$n'_{4d} = n_{4d} + 45 \text{ percent},$$

and

$$n'_{4f} = n_{4f} + 71 \text{ percent}.$$

By using n'_j instead of n_j, one obtains

$$\frac{\phi_{4\to3}}{\phi_{4\to2}} = 0.75 \text{ (within about 5 percent).}$$

ACKNOWLEDGMENTS

The author wishes to thank Dr. R. B. Kay, of American University, for suggesting and guiding this study, in particular for his many helpful discussions of the physical principles involved. The author also gratefully acknowledges the invaluable assistance of A. J. Villasenor, whose expert computer programming made the data analysis possible.

Goddard Space Flight Center
National Aeronautics and Space Administration
Greenbelt, Maryland, July 28, 1971
125-24-10-01-51

REFERENCES

Anderson, R. J., Lee, E. T. P., and Lin, C. C., *Phys. Rev.* 160:20, 1967.

Anderson, R. J., Hughes, R. H., and Norton, T. G., *Phys. Rev.* 181:198, 1969.

Dalgarno, A., and McDowell, M. R. C., in *The Airglow and the Aurorae,* E. B. Armstrong and A. Dalgarno, ed., Pergamon Press, Inc., New York, 1956, p. 340.

Einstein, A., *Phys. Zeits.* 18:121, 1917.

Heitler, W., *The Quantum Theory of Radiation,* Oxford University Press, New York, 1944.

Hughes, R. H., and Weaver, L. D., *Phys. Rev.* 132:710, 1963.

Kay, R. B., doctoral dissertation, *Excitation Transfer in Helium,* University of Arkansas Library, Fayetteville, Arkansas, 1967.

Lamb, W. E., Jr., and Skinner, M., *Phys. Rev.* 78:539, 1950.

Larson, H. P., and Stanley, R. W., *J. Opt. Soc. Amer.* 57:1439, 1967.

Lee, E. T. P., and Lin, C. C., *Phys. Rev.* 138:A301, 1965.

Mader, D. L., Leventhal, M., and Lamb, W. E., Jr., *Phys. Rev.* 3:A1832, 1971.

Ochkur, V. I., and Bratsev, V. F., *Astron. Zh.* 42:1035, 1965 [English translation: *Sov. Astron.—AJ* 9:797, 1966].

Pendleton, W. R., doctoral dissertation, *Radiative Lifetime Measurements in Helium Using a New Sampling Technique,* University of Arkansas Library, Fayetteville, Arkansas, 1964.

Redfield, D., Wittke, J. P., and Pankove, J. I., *Phys. Rev.* 2:B1830, 1970.

Rogers, P. C., "FRANTIC Program for Analysis of Exponential Growth and Decay Curves", Technical Report No. 76, MIT Laboratory for Nuclear Science, Cambridge, Massachusetts, June 1962.

St. John, R. M., and Lin, C. C., *J. Chem. Phys.* 41:195, 1964.

St. John, R. M., Miller, F. L., and Lin, C. C., *Phys. Rev.* 134:A888, 1964.

St. John, R. M., and Lin, C. C., *J. Chem. Phys.* 47:347, 1967.

Sommerfeld, A., *Ann. Physik* II:257, 1931.

Stewart, D. T., and Gabuthuler, E., *Proc. Phys. Soc., London* 74:473, 1959.

Vainshtein, L. A., *Opt. Spektrosk.* 18:947,1965 [English translation: *Opt. Spectry. USSR* 18:538, 1965].

Weaver, L. D., and Hughes, R. H., *J. Chem. Phys.* 47:346, 1967.

Wiese, W. L., Smith, M. W., and Glennon, B. M., *Atomic Transition Probabilities: Vol. I–Hydrogen Through Neon,* NSRDS-NBS4, U.S. Government Printing Office, Washington, D. C., 1966.

Appendix A

Analysis of the Helium Data

```
 N=  256     FIRST= 54     LAST=216     BACKGROUND=      22000.000     CHANNEL WIDTH=   0.33330

  1) 176682.    2) 156975.    3) 157084.    4) 149799.    5) 141987.    6) 134831.    7) 129266.    8) 124186.
  9) 115509.   10) 117546.   11) 111598.   12) 108074.   13) 107049.   14) 102232.   15) 99660.   16) 97564.
 17) 94438.    18) 91819.    19) 91644.    20) 89205.    21) 87101.    22) 86440.    23) 84245.    24) 82192.
 25) 79611.    26) 78060.    27) 77232.    28) 76976.    29) 75761.    30) 74809.    31) 72681.    32) 72666.
 33) 70637.    34) 70373.    35) 67980.    36) 69680.    37) 68574.    38) 66305.    39) 65252.    40) 66040.
 41) 64424.    42) 63207.    43) 63417.    44) 62578.    45) 61777.    46) 60963.    47) 60339.    48) 60075.
 49) 59593.    50) 58881.    51) 57965.    52) 57497.    53) 57534.    54) 56907.    55) 56128.    56) 55474.
 57) 55551.    58) 54733.    59) 54369.    60) 53826.    61) 53831.    62) 52291.    63) 51237.    64) 52364.
 65) 50959.    66) 52174.    67) 50801.    68) 50962.    69) 49675.    70) 49144.    71) 49780.    72) 49006.
 73) 48626.    74) 49056.    75) 48818.    76) 48270.    77) 48308.    78) 47758.    79) 46900.    80) 48289.
 81) 46670.    82) 46933.    83) 45280.    84) 46198.    85) 46178.    86) 45431.    87) 45368.    88) 44631.
 89) 45339.    90) 45989.    91) 42994.    92) 44585.    93) 43584.    94) 43886.    95) 42782.    96) 44531.
 97) 43497.    98) 42610.    99) 42892.   100) 42868.   101) 41816.   102) 40754.   103) 41844.   104) 41562.
105) 41358.   106) 40716.   107) 41594.   108) 40364.   109) 40540.   110) 39997.   111) 39699.   112) 39679.
113) 39116.   114) 40136.   115) 40365.   116) 40366.   117) 39761.   118) 39756.   119) 38652.   120) 38677.
121) 39892.   122) 38020.   123) 39678.   124) 38836.   125) 38358.   126) 37845.   127) 37867.   128) 37710.
129) 37710.   130) 36951.   131) 38325.   132) 37764.   133) 36423.   134) 36951.   135) 37628.   136) 37262.
137) 37189.   138) 37461.   139) 36606.   140) 36460.   141) 36479.   142) 36999.   143) 35841.   144) 35656.
145) 36532.   146) 35618.   147) 35860.   148) 35409.   149) 35845.   150) 35787.   151) 34873.   152) 34694.
153) 35132.   154) 35876.   155) 35081.   156) 34830.   157) 34273.   158) 34569.   159) 34637.   160) 34207.
161) 34511.   162) 34061.   163) 34033.
```

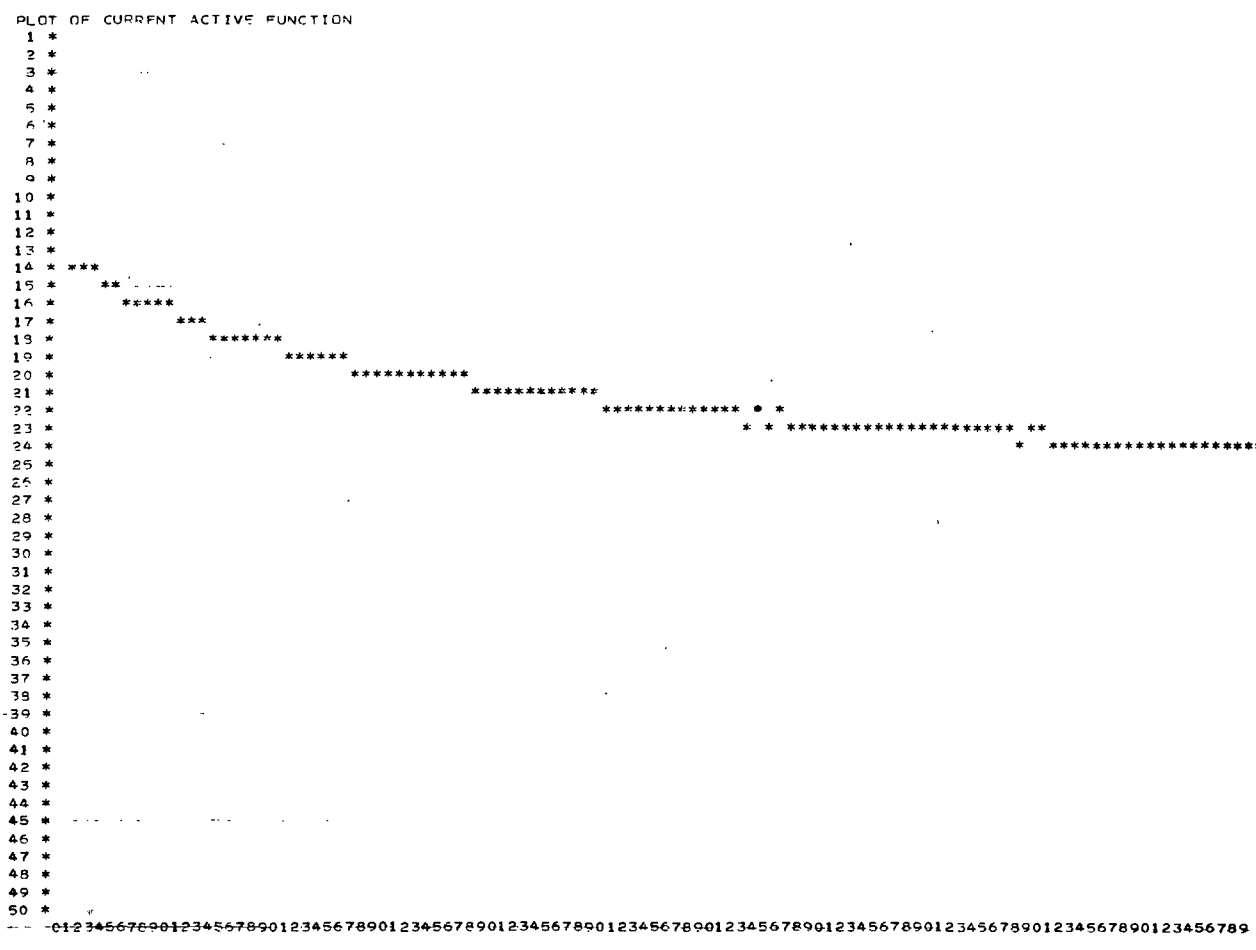

```
 INPUT TAU=      0.02488690      START=110      END=163

   1) 154682.    2) 144975.    3) 135084.    4) 127799.    5) 119987.    6) 112831.    7) 107266.    8) 102186.
   9) 96509.    10) 95546.    11) 89598.    12) 86074.    13) 85049.    14) 80232.    15) 76660.    16) 75564.
  17) 72438.    18) 69818.    19) 69644.    20) 67205.    21) 65101.    22) 64440.    23) 62245.    24) 60192.
  25) 57611.    26) 56060.    27) 55282.    28) 54976.    29) 53761.    30) 52809.    31) 50581.    32) 50666.
  33) 48637.    34) 48373.    35) 45980.    36) 47650.    37) 46574.    38) 44305.    39) 43252.    40) 44040.
  41) 42424.    42) 41207.    43) 41417.    44) 40578.    45) 39773.    46) 38963.    47) 38339.    48) 38075.
  49) 37593.    50) 36881.    51) 35965.    52) 35497.    53) 35574.    54) 34907.    55) 34128.    56) 33474.
  57) 33551.    58) 32733.    59) 32369.    60) 31826.    61) 31831.    62) 30291.    63) 29237.    64) 30364.
  65) 28959.    66) 30174.    67) 28801.    68) 28962.    69) 27875.    70) 27144.    71) 27780.    72) 27006.
  73) 26626.    74) 27066.    75) 26819.    76) 26270.    77) 26308.    78) 25758.    79) 24900.    80) 26289.
  81) 24670.    82) 24933.    83) 23280.    84) 24198.    85) 24178.    86) 23431.    87) 23368.    88) 22631.
  89) 23329.    90) 23380.    91) 20984.    92) 22585.    93) 21584.    94) 21886.    95) 20782.    96) 22531.
  97) 21497.    98) 20610.    99) 20892.   100) 20968.   101) 19818.   102) 18764.   103) 19844.   104) 19562.
 105) 19358.   106) 18716.   107) 19594.   108) 18364.   109) 18540.   110) 17897.   111) 17699.   112) 17679.
 113) 17116.   114) 18136.   115) 18365.   116) 18366.   117) 17761.   118) 17756.   119) 15652.   120) 16477.
 121) 16892.   122) 16020.   123) 16678.   124) 14836.   125) 16358.   126) 15845.   127) 15867.   128) 15710.
 129) 15710.   130) 14951.   131) 16325.   132) 15764.   133) 14423.   134) 14951.   135) 15528.   136) 15262.
 137) 15186.   138) 15461.   139) 14606.   140) 14460.   141) 14479.   142) 14999.   143) 13841.   144) 13656.
 145) 14532.   146) 13618.   147) 13860.   148) 13499.   149) 13845.   150) 13787.   151) 12873.   152) 12694.
 153) 13172.   154) 12876.   155) 13081.   156) 12830.   157) 12273.   158) 12569.   159) 12637.   160) 12297.
 161) 12511.   162) 12061.   163) 12023.

PLOT OF CURRENT ACTIVE FUNCTION
```

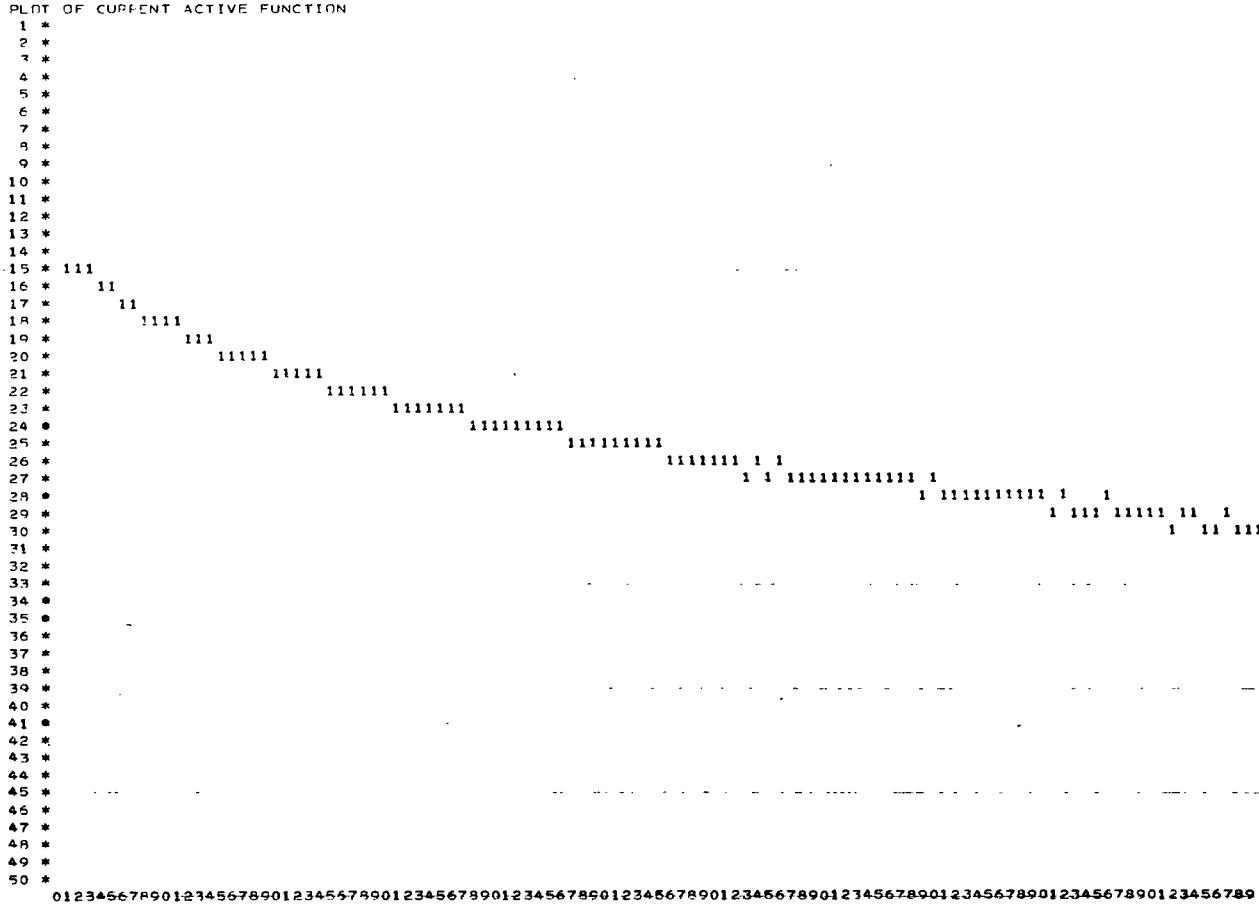

```
    01234567890123456789012345678901234567890123456789012345678901234567890123456789012345678901234567890123456789
```

LEAST SQUARES RESULT -	SLOPE= -0.22687983E-01	XINTER=	10.63257	AOLD=	0.22000000E 05
LEAST SQUARES RESULT -	SLOPE= -0.26553614E-01	XINTER=	10.65047	AOLD=	0.24199984E 05
LEAST SQUARES RESULT -	SLOPE= -0.22687983E-01	XINTER=	10.63257	AOLD=	0.21999996E 05
LEAST SQUARES RESULT -	SLOPE= -0.23018453E-01	XINTER=	10.63277	AOLD=	0.22219977E 05
LEAST SQUARES RESULT -	SLOPE= -0.23361634E-01	XINTER=	10.63298	AOLD=	0.22442160E 05
LEAST SQUARES RESULT -	SLOPE= -0.23717523E-01	XINTER=	10.63318	AOLD=	0.22666563E 05
LEAST SQUARES RESULT -	SLOPE= -0.24088832E-01	XINTER=	10.63440	AOLD=	0.22893211E 05
LEAST SQUARES RESULT -	SLOPE= -0.24543695E-01	XINTER=	10.63765	AOLD=	0.23122125E 05
LEAST SQUARES RESULT -	SLOPE= -0.24963137E-01	XINTER=	10.63948	AOLD=	0.23353328E 05
LEAST SQUARES RESULT -	SLOPE= -0.24543695E-01	XINTER=	10.63765	AOLD=	0.23122121E 05
LEAST SQUARES RESULT -	SLOPE= -0.24594538E-01	XINTER=	10.63847	AOLD=	0.23145230E 05
LEAST SQUARES RESULT -	SLOPE= -0.24619959E-01	XINTER=	10.63765	AOLD=	0.23168359E 05
LEAST SQUARES RESULT -	SLOPE= -0.24658001E-01	XINTER=	10.63806	AOLD=	0.23191512E 05
LEAST SQUARES RESULT -	SLOPE= -0.24706970E-01	XINTER=	10.63826	AOLD=	0.23214688E 05
LEAST SQUARES RESULT -	SLOPE= -0.24759773E-01	XINTER=	10.63908	AOLD=	0.23237887E 05
LEAST SQUARES RESULT -	SLOPE= -0.24785195E-01	XINTER=	10.63847	AOLD=	0.23261109E 05
LEAST SQUARES RESULT -	SLOPE= -0.24848744E-01	XINTER=	10.63908	AOLD=	0.23284355E 05
LEAST SQUARES RESULT -	SLOPE= -0.24861455E-01	XINTER=	10.63806	AOLD=	0.23307625E 05
LEAST SQUARES RESULT -	SLOPE= -0.24912298E-01	XINTER=	10.63867	AOLD=	0.23330918E 05
LEAST SQUARES RESULT -	SLOPE= -0.24861455E-01	XINTER=	10.63806	AOLD=	0.23307621E 05
LEAST SQUARES RESULT -	SLOPE= -0.24859587E-01	XINTER=	10.64030	AOLD=	0.23309930E 05
LEAST SQUARES RESULT -	SLOPE= -0.24861455E-01	XINTER=	10.63806	AOLD=	0.23307617E 05
LEAST SQUARES RESULT -	SLOPE= -0.24861455E-01	XINTER=	10.63826	AOLD=	0.23307836E 05
LEAST SQUARES RESULT -	SLOPE= -0.24861455E-01	XINTER=	10.63847	AOLD=	0.23308055E 05
LEAST SQUARES RESULT -	SLOPE= -0.24861455E-01	XINTER=	10.63847	AOLD=	0.23308273E 05
LEAST SQUARES RESULT -	SLOPE= -0.24848744E-01	XINTER=	10.63826	AOLD=	0.23308492E 05
LEAST SQUARES RESULT -	SLOPE= -0.24874166E-01	XINTER=	10.63887	AOLD=	0.23308711E 05
LEAST SQUARES RESULT -	SLOPE= -0.24874166E-01	XINTER=	10.63867	AOLD=	0.23308930E 05
LEAST SQUARES RESULT -	SLOPE= -0.24874166E-01	XINTER=	10.63826	AOLD=	0.23309148E 05
LEAST SQUARES RESULT -	SLOPE= -0.24874166E-01	XINTER=	10.63867	AOLD=	0.23309367E 05
LEAST SQUARES RESULT -	SLOPE= -0.24886876E-01	XINTER=	10.63948	AOLD=	0.23309586E 05
LEAST SQUARES RESULT -	SLOPE= -0.24899587E-01	XINTER=	10.63989	AOLD=	0.23309805E 05

COMPUTED LINE - DATA Y(I)

I= 110	9.735	9.716	0.019
I= 111	9.727	9.704	0.023
I= 112	9.719	9.703	0.016
I= 113	9.710	9.668	0.042
I= 114	9.702	9.731	-0.029
I= 115	9.694	9.744	-0.050
I= 116	9.686	9.744	-0.059
I= 117	9.677	9.708	-0.031
I= 118	9.669	9.708	-0.039
I= 119	9.661	9.638	0.022
I= 120	9.652	9.640	0.012
I= 121	9.644	9.654	-0.010
I= 122	9.636	9.596	0.039
I= 123	9.627	9.640	-0.013
I= 124	9.619	9.512	0.107
I= 125	9.611	9.619	-0.008
I= 126	9.603	9.584	0.018
I= 127	9.594	9.586	0.008
I= 128	9.586	9.575	0.011
I= 129	9.578	9.575	0.003
I= 130	9.569	9.521	0.048
I= 131	9.561	9.617	-0.056
I= 132	9.553	9.579	-0.026
I= 133	9.544	9.481	0.063
I= 134	9.536	9.521	0.015
I= 135	9.528	9.569	-0.041
I= 136	9.520	9.543	-0.024
I= 137	9.511	9.538	-0.027
I= 138	9.503	9.558	-0.055
I= 139	9.495	9.495	-0.001
I= 140	9.486	9.484	0.002
I= 141	9.478	9.486	-0.008
I= 142	9.470	9.524	-0.055
I= 143	9.461	9.436	0.025
I= 144	9.453	9.421	0.032
I= 145	9.445	9.490	-0.045
I= 146	9.437	9.418	0.019
I= 147	9.428	9.437	-0.009
I= 148	9.420	9.408	0.012

I= 149	9.412	9.436	-0.025
I= 150	9.403	9.432	-0.028
I= 151	9.395	9.356	0.039
I= 152	9.387	9.340	0.047
I= 153	9.378	9.378	0.001
I= 154	9.370	9.439	-0.069
I= 155	9.362	9.374	-0.012
I= 156	9.354	9.352	0.002
I= 157	9.345	9.302	0.043
I= 158	9.337	9.329	0.008
I= 159	9.328	9.335	-0.006
I= 160	9.320	9.304	0.016
I= 161	9.312	9.324	-0.012
I= 162	9.304	9.283	0.021
I= 163	9.295	9.279	0.016

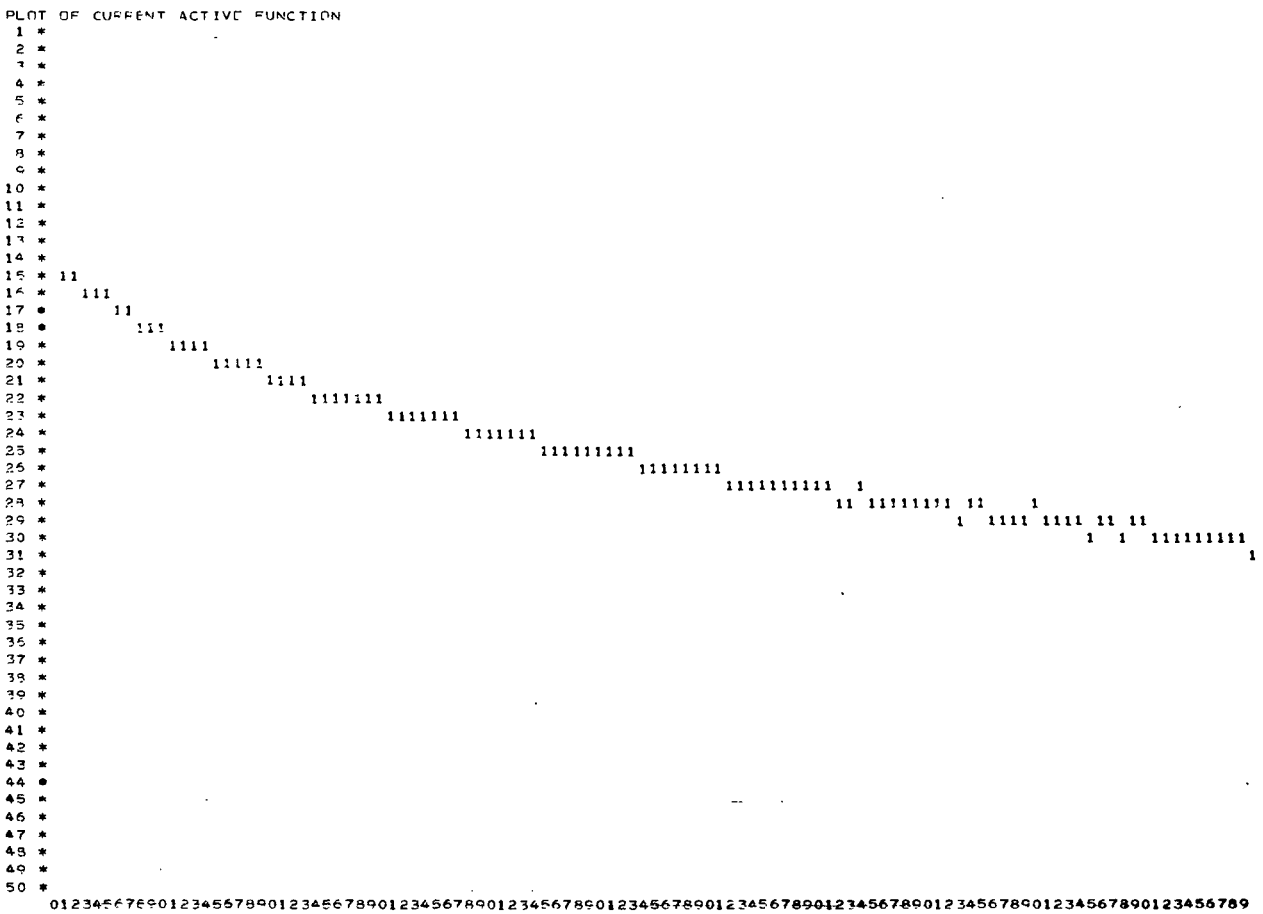

RESULT FOR GIVEN TAU = 0.02488690 COMPUTED COEFFICIENT (INTERCEPT EXP(10.63989)) = 41768.1641

INPUT TAU= 0.07052143 START= 65 END= 93

1)	111604.	2)	102242.	3)	92693.	4)	85748.	5)	78272.	6)	71450.	7)	66216.	8)	61464.
9)	56113.	10)	55473.	11)	49845.	12)	46638.	13)	45928.	14)	41424.	15)	38161.	16)	37373.
17)	34551.	18)	32233.	19)	32359.	20)	30217.	21)	28408.	22)	28039.	23)	26134.	24)	24369.
25)	22073.	26)	20804.	27)	20307.	28)	20279.	29)	19340.	30)	18661.	31)	16805.	32)	17059.
33)	15296.	34)	15297.	35)	13166.	36)	15127.	37)	14279.	38)	12266.	39)	11466.	40)	12506.
41)	11140.	42)	10170.	43)	10626.	44)	10031.	45)	9467.	46)	8897.	47)	8510.	48)	8482.
49)	8233.	50)	7753.	51)	7067.	52)	6827.	53)	7090.	54)	6687.	55)	6130.	56)	5697.
57)	5092.	58)	5301.	59)	5242.	60)	4912.	61)	5129.	62)	3799.	63)	2953.	64)	4286.
65)	3086.	66)	4503.	67)	3332.	68)	3692.	69)	2803.	70)	2268.	71)	3099.	72)	2518.
73)	2330.	74)	2960.	75)	2901.	76)	2539.	77)	2762.	78)	2396.	79)	1720.	80)	3289.
81)	1850.	82)	2290.	83)	813.	84)	1906.	85)	2060.	86)	1484.	87)	1592.	88)	1024.
89)	1900.	90)	2716.												

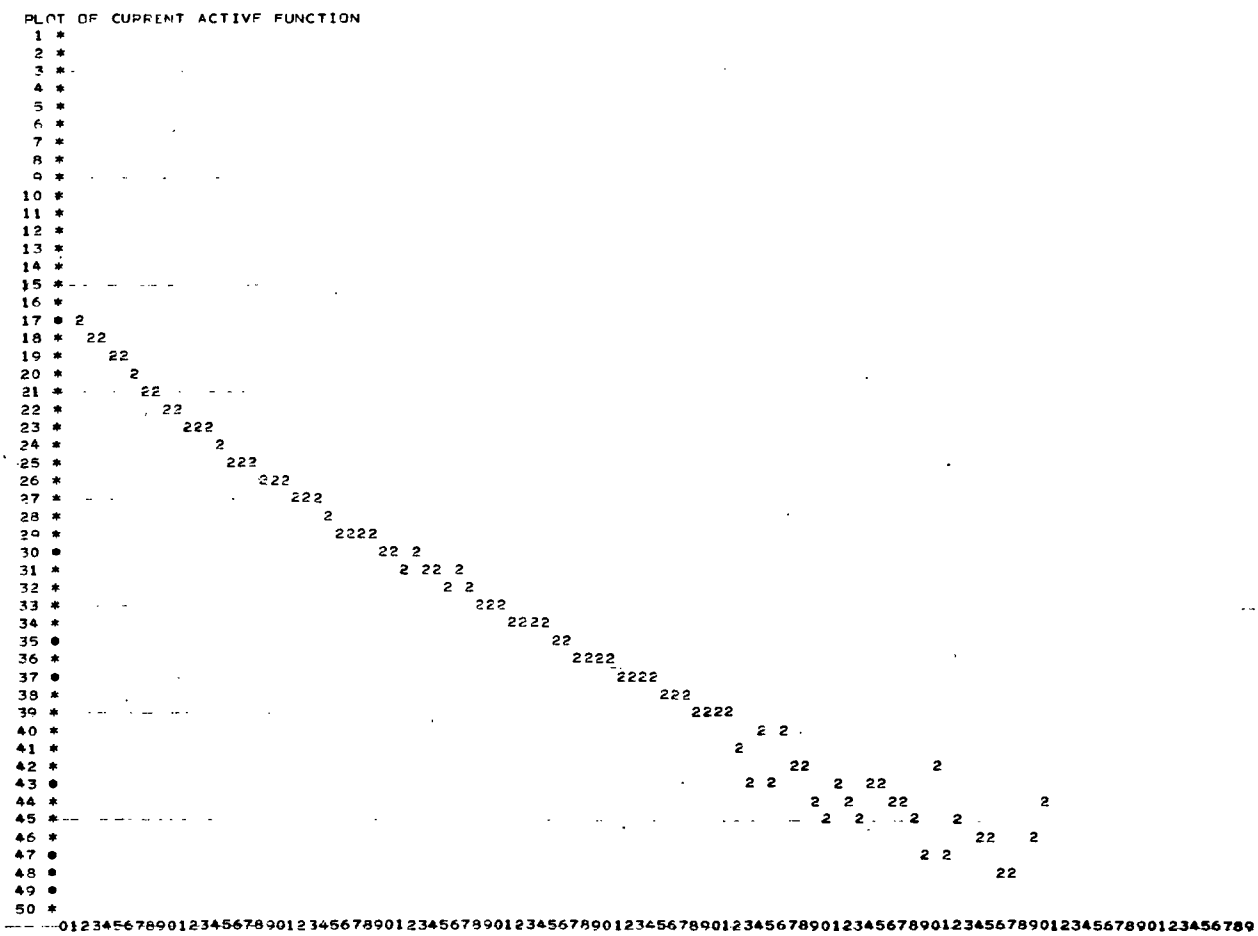

LEAST SQUARES RESULT -	SLOPE= -0.10139179E 00	XINTER=	10.32857	AOLD=	0.41768164E 05
LEAST SQUARES RESULT -	SLOPE= -0.62077533E-01	XINTER=	10.01310	AOLD=	0.37591348E 05
LEAST SQUARES RESULT -	SLOPE= -0.10139179E 00	XINTER=	10.32857	AOLD=	0.41768160E 05
LEAST SQUARES RESULT -	SLOPE= -0.93789279E-01	XINTER=	10.23154	AOLD=	0.41350477E 05
LEAST SQUARES RESULT -	SLOPE= -0.87739766E-01	XINTER=	10.16362	AOLD=	0.40936969E 05
LEAST SQUARES RESULT -	SLOPE= -0.82725644E-01	XINTER=	10.11392	AOLD=	0.40527598E 05
LEAST SQUARES RESULT -	SLOPE= -0.78539789E-01	XINTER=	10.07842	AOLD=	0.40122320E 05
LEAST SQUARES RESULT -	SLOPE= -0.75019538E-01	XINTER=	10.05429	AOLD=	0.39721094E 05
LEAST SQUARES RESULT -	SLOPE= -0.71898699E-01	XINTER=	10.03559	AOLD=	0.39323883E 05
LEAST SQUARES RESULT -	SLOPE= -0.69265902E-01	XINTER=	10.02517	AOLD=	0.38930641E 05
LEAST SQUARES RESULT -	SLOPE= -0.71898699E-01	XINTER=	10.03559	AOLD=	0.39323879E 05
LEAST SQUARES RESULT -	SLOPE= -0.71602881E-01	XINTER=	10.03393	AOLD=	0.39284555E 05
LEAST SQUARES RESULT -	SLOPE= -0.71307063E-01	XINTER=	10.03227	AOLD=	0.39245270E 05
LEAST SQUARES RESULT -	SLOPE= -0.71095155E-01	XINTER=	10.03227	AOLD=	0.39206023E 05
LEAST SQUARES RESULT -	SLOPE= -0.70904179E-01	XINTER=	10.03062	AOLD=	0.39166816E 05
LEAST SQUARES RESULT -	SLOPE= -0.70537925E-01	XINTER=	10.02943	AOLD=	0.39127648E 05
LEAST SQUARES RESULT -	SLOPE= -0.70804179E-01	XINTER=	10.03085	AOLD=	0.39166813E 05
LEAST SQUARES RESULT -	SLOPE= -0.70789337E-01	XINTER=	10.03085	AOLD=	0.39162895E 05
LEAST SQUARES RESULT -	SLOPE= -0.70774555E-01	XINTER=	10.03109	AOLD=	0.39158977E 05
LEAST SQUARES RESULT -	SLOPE= -0.70715427E-01	XINTER=	10.03038	AOLD=	0.39155059E 05
LEAST SQUARES RESULT -	SLOPE= -0.70744991E-01	XINTER=	10.03156	AOLD=	0.39151145E 05
LEAST SQUARES RESULT -	SLOPE= -0.70671022E-01	XINTER=	10.03014	AOLD=	0.39147230E 05
LEAST SQUARES RESULT -	SLOPE= -0.70671022E-01	XINTER=	10.03062	AOLD=	0.39143316E 05
LEAST SQUARES RESULT -	SLOPE= -0.70597053E-01	XINTER=	10.02920	AOLD=	0.39139402E 05
LEAST SQUARES RESULT -	SLOPE= -0.70671022E-01	XINTER=	10.03085	AOLD=	0.39143313E 05
LEAST SQUARES RESULT -	SLOPE= -0.70626676E-01	XINTER=	10.02967	AOLD=	0.39142922E 05
LEAST SQUARES RESULT -	SLOPE= -0.70556240E-01	XINTER=	10.03038	AOLD=	0.39142531E 05
LEAST SQUARES RESULT -	SLOPE= -0.70641458E-01	XINTER=	10.03014	AOLD=	0.39142141E 05
LEAST SQUARES RESULT -	SLOPE= -0.70671022E-01	XINTER=	10.03062	AOLD=	0.39141750E 05
LEAST SQUARES RESULT -	SLOPE= -0.70641458E-01	XINTER=	10.03038	AOLD=	0.39141359E 05
LEAST SQUARES RESULT -	SLOPE= -0.70626676E-01	XINTER=	10.03014	AOLD=	0.39140969E 05
LEAST SQUARES RESULT -	SLOPE= -0.70626676E-01	XINTER=	10.02991	AOLD=	0.39140578E 05
LEAST SQUARES RESULT -	SLOPE= -0.70626676E-01	XINTER=	10.02967	AOLD=	0.39140188E 05
LEAST SQUARES RESULT -	SLOPE= -0.70626676E-01	XINTER=	10.03014	AOLD=	0.39139797E 05
LEAST SQUARES RESULT -	SLOPE= -0.70582271E-01	XINTER=	10.02896	AOLD=	0.39139406E 05

COMPUTED LINE - DATA Y(I)

I=	65	8.523	8.441	0.083
I=	66	8.500	8.706	-0.206
I=	67	8.476	8.487	-0.011
I=	68	8.453	8.556	-0.104
I=	69	8.429	8.366	0.063
I=	70	8.406	8.230	0.176
I=	71	8.382	8.427	-0.045
I=	72	8.359	8.288	0.070
I=	73	8.335	8.237	0.099
I=	74	8.312	8.388	-0.076
I=	75	8.288	8.372	-0.084
I=	76	8.265	8.281	-0.017
I=	77	8.241	8.334	-0.093
I=	78	8.218	8.238	-0.021
I=	79	8.194	8.038	0.156
I=	80	8.170	8.446	-0.275
I=	81	8.147	8.072	0.075
I=	82	8.123	8.198	-0.074
I=	83	8.100	7.671	0.429
I=	84	8.076	8.079	-0.003
I=	85	8.053	8.122	-0.070
I=	86	8.029	7.931	0.098
I=	87	8.006	7.966	0.040
I=	88	7.982	7.741	0.241
I=	89	7.959	8.060	-0.102
I=	90	7.935	8.287	-0.352

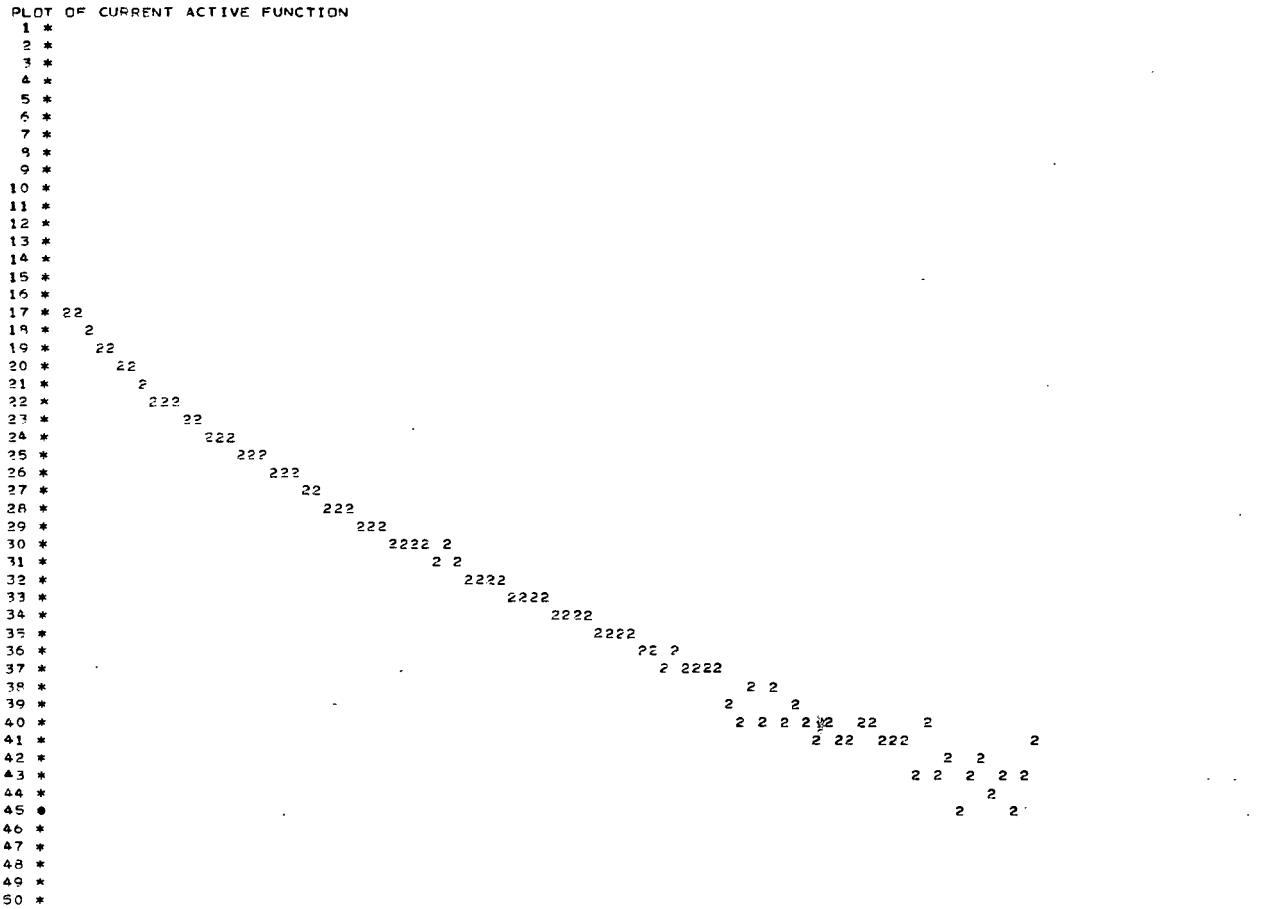

RESULT FOR GIVEN TAU = 0.07062143 COMPUTED COEFFICIENT (INTERCEPT EXP(10.02896)) = 22673.6836

```
 INPUT TAU=      0.22075051      START= 25      END= 55

  1)  91556.    2)  82703.    3)  73648.    4)  67184.    5)  60179.    6)  53816.    7)  49030.    8)  44715.
  9)  40791.   10)  38567.   11)  34346.   12)  31526.   13)  31214.   14)  27087.   15)  24194.   16)  23765.
 17)  21295.   18)  19320.   19)  19780.   20)  17965.   21)  16475.   22)  16417.   23)  14815.   24)  13346.
 25)  11336.   26)  10353.   27)  10130.   28)  10371.   29)   9694.   30)   9271.   31)   7664.   32)   8161.
 33)   6636.   34)   6869.   35)   4964.   36)   7145.   37)   6512.   38)   4709.   39)   4115.   40)   5354.
 41)   4183.   42)   3404.   43)   4045.   44)   3630.   45)   3243.   46)   2845.   47)   2626.   48)   2762.
 49)   2673.   50)   2349.   51)   1814.   52)   1723.   53)   2130.   54)   1868.   55)   1449.   56)   1150.
 57)   1576.   58)   1102.   59)   1078.   60)    869.   61)   1204.

PLOT OF CURRENT ACTIVE FUNCTION
 1 *
 2 *
 3 *
 4 *
 5 *
 6 *
 7 *
 8 *
 9 *
10 *
11 *
12 *
13 *
14 *
15 *
16 *
17 *
18 * 3
19 *  3
20 *   3
21 *    33
22 *      3
23 *       33
24 *         33
25 *           3
26 *            33
27 *              3
28 *               33
29 *                 3 3
30 *                  3 3
31 *                    333
32 *                       3
33 *                        3
34 *                       333
35 *                          33
36 *                            33
37 *                              33 33
38 *
39 *                                 3    3
40 *                                   3
41 *                                    3 3 3
42 *                                       3 33
43 *                                          3
44 *                                           333
45 *                                              3
46 *                                                33
47 *                                               33
48 *                                                  3 3
49 *
50 *                                                    3 33 3
   -01234567890123456789012345678901234567890123456789012345678901234567890123456789012345678901234567890123456789012345678901234567890123456789
```

```
LEAST SQUARES RESULT -    SLOPE= -0.20032489E 00    XINTER=    11.00312    AOLD=  0.22673684E 05
LEAST SQUARES RESULT -    SLOPE= -0.23796630E 00    XINTER=    11.23552    AOLD=  0.24941035E 05
LEAST SQUARES RESULT -    SLOPE= -0.20032489E 00    XINTER=    11.00312    AOLD=  0.22673680E 05
LEAST SQUARES RESULT -    SLOPE= -0.20322990E 00    XINTER=    11.01845    AOLD=  0.22900398E 05
LEAST SQUARES RESULT -    SLOPE= -0.20630330E 00    XINTER=    11.03520    AOLD=  0.23129383E 05
LEAST SQUARES RESULT -    SLOPE= -0.20954155E 00    XINTER=    11.05381    AOLD=  0.23360656E 05
LEAST SQUARES RESULT -    SLOPE= -0.21307200E 00    XINTER=    11.07395    AOLD=  0.23594242E 05
LEAST SQUARES RESULT -    SLOPE= -0.21680397E 00    XINTER=    11.09631    AOLD=  0.23830164E 05
LEAST SQUARES RESULT -    SLOPE= -0.22081399E 00    XINTER=    11.12137    AOLD=  0.24068445E 05
LEAST SQUARES RESULT -    SLOPE= -0.21680397E 00    XINTER=    11.09631    AOLD=  0.23830160E 05
LEAST SQUARES RESULT -    SLOPE= -0.21719182E 00    XINTER=    11.09877    AOLD=  0.23853977E 05
LEAST SQUARES RESULT -    SLOPE= -0.21759427E 00    XINTER=    11.10123    AOLD=  0.23877816E 05
LEAST SQUARES RESULT -    SLOPE= -0.21798211E 00    XINTER=    11.10369    AOLD=  0.23901680E 05
LEAST SQUARES RESULT -    SLOPE= -0.21838456E 00    XINTER=    11.10603    AOLD=  0.23925566E 05
LEAST SQUARES RESULT -    SLOPE= -0.21878701E 00    XINTER=    11.10849    AOLD=  0.23949477E 05
LEAST SQUARES RESULT -    SLOPE= -0.21918947E 00    XINTER=    11.11118    AOLD=  0.23973410E 05
LEAST SQUARES RESULT -    SLOPE= -0.21959192E 00    XINTER=    11.11364    AOLD=  0.23997367E 05
LEAST SQUARES RESULT -    SLOPE= -0.22000903E 00    XINTER=    11.11622    AOLD=  0.24021348E 05
LEAST SQUARES RESULT -    SLOPE= -0.22041881E 00    XINTER=    11.11879    AOLD=  0.24045355E 05
LEAST SQUARES RESULT -    SLOPE= -0.22084326E 00    XINTER=    11.12137    AOLD=  0.24069387E 05
LEAST SQUARES RESULT -    SLOPE= -0.22041881E 00    XINTER=    11.11879    AOLD=  0.24045352E 05
LEAST SQUARES RESULT -    SLOPE= -0.22046274E 00    XINTER=    11.11903    AOLD=  0.24047734E 05
LEAST SQUARES RESULT -    SLOPE= -0.22049934E 00    XINTER=    11.11926    AOLD=  0.24050117E 05
LEAST SQUARES RESULT -    SLOPE= -0.22054321E 00    XINTER=    11.11949    AOLD=  0.24052500E 05
LEAST SQUARES RESULT -    SLOPE= -0.22057980E 00    XINTER=    11.11985    AOLD=  0.24054883E 05
LEAST SQUARES RESULT -    SLOPE= -0.22062373E 00    XINTER=    11.12008    AOLD=  0.24057266E 05
LEAST SQUARES RESULT -    SLOPE= -0.22066760E 00    XINTER=    11.12043    AOLD=  0.24059648E 05
LEAST SQUARES RESULT -    SLOPE= -0.22070420E 00    XINTER=    11.12055    AOLD=  0.24062031E 05
LEAST SQUARES RESULT -    SLOPE= -0.22074813E 00    XINTER=    11.12090    AOLD=  0.24064414E 05
LEAST SQUARES RESULT -    SLOPE= -0.22079200E 00    XINTER=    11.12113    AOLD=  0.24066801E 05
LEAST SQUARES RESULT -    SLOPE= -0.22074813E 00    XINTER=    11.12090    AOLD=  0.24064410E 05
LEAST SQUARES RESULT -    SLOPE= -0.22075546E 00    XINTER=    11.12078    AOLD=  0.24064637E 05
```

COMPUTED LINE - DATA Y(I)

```
I=  25    9.355    9.264    0.091
I=  26    9.281    9.167    0.114
I=  27    9.208    9.146    0.062
I=  28    9.134    9.173   -0.039
I=  29    9.061    9.102   -0.042
I=  30    8.987    9.056   -0.069
I=  31    8.913    8.850    0.063
I=  32    8.840    8.921   -0.082
I=  33    8.766    8.696    0.070
I=  34    8.693    8.737   -0.044
I=  35    8.619    8.375    0.244
I=  36    8.546    8.785   -0.239
I=  37    8.472    8.685   -0.213
I=  38    8.398    8.325    0.073
I=  39    8.325    8.174    0.151
I=  40    8.251    8.476   -0.225
I=  41    8.178    8.200   -0.022
I=  42    8.104    7.963    0.141
I=  43    8.031    8.168   -0.138
I=  44    7.957    8.047   -0.090
I=  45    7.883    7.919   -0.036
I=  46    7.810    7.768    0.042
I=  47    7.736    7.676    0.061
I=  48    7.663    7.741   -0.079
I=  49    7.589    7.707   -0.118
I=  50    7.515    7.555   -0.039
I=  51    7.442    7.234    0.208
I=  52    7.368    7.173    0.195
I=  53    7.295    7.451   -0.156
I=  54    7.221    7.292   -0.071
I=  55    7.148    6.965    0.183
```

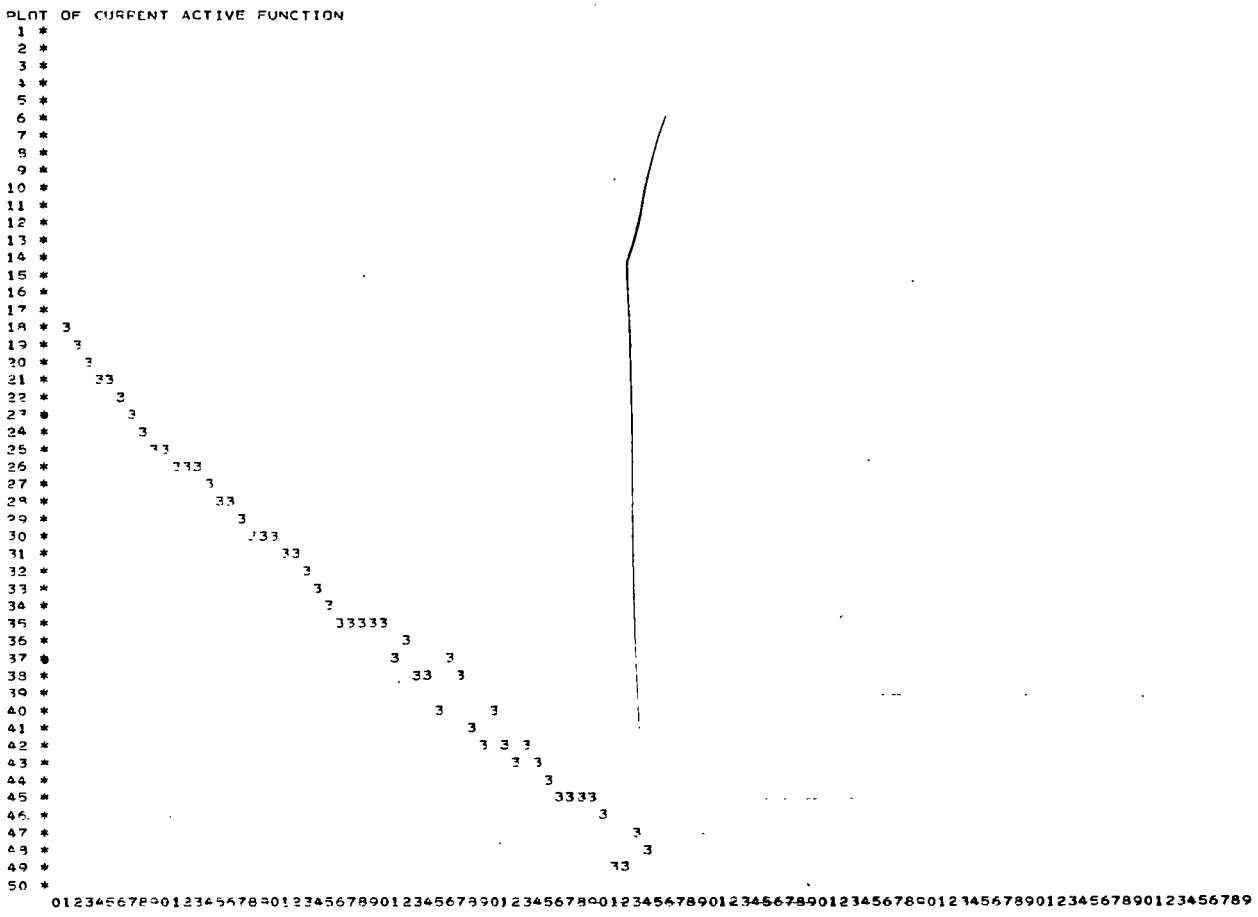

RESULT FOR GIVEN TAU = 0.22075051 COMPUTED COEFFICIENT (INTERCEPT EXP(11.12078)) = 67560.7500

```
 INPUT TAU=      0.44247782      START=  8      END= 18

 1)  22608.    2)  18576.    3)  14005.    4)  11709.    5)   8577.    6)   5814.    7)   4374.    8)   3169.
 9)   1136.   10)   3599.   11)    876.   12)    388.   13)   2223.   14)    103.
```

PLOT OF CURRENT ACTIVE FUNCTION

```
 LEAST SQUARES RESULT -    SLOPE= -0.11951199E 01    XINTER=      10.89265    AOLD=  0.67560750E 05
 LEAST SQUARES RESULT -    SLOPE= -0.38665960E 00    XINTER=       9.74054    AOLD=  0.60804676E 05
 LEAST SQUARES RESULT -    SLOPE= -0.11950073E 01    XINTER=      10.89233    AOLD=  0.67560688E 05
 LEAST SQUARES RESULT -    SLOPE= -0.81393929E 00    XINTER=      10.01647    AOLD=  0.66885063E 05
 LEAST SQUARES RESULT -    SLOPE= -0.67102456E 00    XINTER=       9.77533    AOLD=  0.66216188E 05
 LEAST SQUARES RESULT -    SLOPE= -0.58933014E 00    XINTER=       9.68026    AOLD=  0.65554000E 05
 LEAST SQUARES RESULT -    SLOPE= -0.53499424E 00    XINTER=       9.64277    AOLD=  0.64898457E 05
 LEAST SQUARES RESULT -    SLOPE= -0.49581772E 00    XINTER=       9.63434    AOLD=  0.64249473E 05
 LEAST SQUARES RESULT -    SLOPE= -0.46605968E 00    XINTER=       9.64115    AOLD=  0.63606977E 05
 LEAST SQUARES RESULT -    SLOPE= -0.44252455E 00    XINTER=       9.65676    AOLD=  0.62970906E 05
 LEAST SQUARES RESULT -    SLOPE= -0.42349690E 00    XINTER=       9.67793    AOLD=  0.62341195E 05
 LEAST SQUARES RESULT -    SLOPE= -0.44252455E 00    XINTER=       9.65676    AOLD=  0.62970902E 05
 LEAST SQUARES RESULT -    SLOPE= -0.44048393E 00    XINTER=       9.65891    AOLD=  0.62907930E 05
 LEAST SQUARES RESULT -    SLOPE= -0.44252455E 00    XINTER=       9.65676    AOLD=  0.62970898E 05
 LEAST SQUARES RESULT -    SLOPE= -0.44234520E 00    XINTER=       9.65712    AOLD=  0.62964602E 05
 LEAST SQUARES RESULT -    SLOPE= -0.44255823E 00    XINTER=       9.65694    AOLD=  0.62970995E 05
 LEAST SQUARES RESULT -    SLOPE= -0.44253582E 00    XINTER=       9.65694    AOLD=  0.62970266E 05
 LEAST SQUARES RESULT -    SLOPE= -0.44251335E 00    XINTER=       9.65694    AOLD=  0.62969637E 05
 LEAST SQUARES RESULT -    SLOPE= -0.44250214E 00    XINTER=       9.65712    AOLD=  0.62969008E 05
 LEAST SQUARES RESULT -    SLOPE= -0.44246852E 00    XINTER=       9.65694    AOLD=  0.62968379E 05
```

COMPUTED LINE - DATA Y(I)

I=	9	8.625	8.685	-0.060
I=	9	8.477	8.212	0.265
I=	10	8.330	8.694	-0.364
I=	11	8.182	8.031	0.151
I=	12	8.035	7.797	0.238
I=	13	7.887	8.324	-0.437
I=	14	7.740	7.533	0.207

PLOT OF CURRENT ACTIVE FUNCTION

RESULT FOR GIVEN TAU = 0.44247782 COMPUTED COEFFICIENT (INTERCEPT EXP(9.65694)) = 15629.9063

```
 INPUT TAU=      1.24871635      START= 1      END= 4

 1)  11570.    2)   9356.    3)   6331.    4)   5350.    5)   3334.    6)   1516.    7)    876.    8)    346.


PLOT OF CURRENT ACTIVE FUNCTION .
 1 *
 2 *
 3 *
 4 *
 5 *
 6 *
 7 *
 8 *
 9 *
10 *
11 *
12 *
13 *
14 *
15 *
16 *
17 *
18 *
19 *
20 *
21 *
22 *
23 *
24 *
25 *
26 *
27 *
28 *
29 *
30 *
31 *
32 *
33 * *
34 *
35 *  *
36 *
37 *
38 *   *
39 *    *
40 *
41 *
42 *     *
43 *
44 *
45 *
46 *
47 *
48 *       *
49 *
50 *
   01234567890123456789012345678901234567890123456789012345678901234567890123456789012345678901234567890123456789012345678901234567890...

    LEAST SQUARES RESULT -      SLOPE= -0.81146926E 00     XINTER=       9.36519     AOLD=  0.15629906E 05
    LEAST SQUARES RESULT -      SLOPE= -0.88218737E 00     XINTER=       9.22260     AOLD=  0.17192887E 05
    LEAST SQUARES RESULT -      SLOPE= -0.10004444E 01     XINTER=       9.03888     AOLD=  0.18912164E 05
    LEAST SQUARES RESULT -      SLOPE= -0.12387714E 01     XINTER=       8.79141     AOLD=  0.20803367E 05
    LEAST SQUARES RESULT -      SLOPE= -0.20119667E 01     XINTER=       8.45078     AOLD=  0.22883691E 05
    LEAST SQUARES RESULT -      SLOPE= -0.12387648E 01     XINTER=       8.79141     AOLD=  0.20803363E 05
    LEAST SQUARES RESULT -      SLOPE= -0.12785711E 01     XINTER=       8.76050     AOLD=  0.21011379E 05
    LEAST SQUARES RESULT -      SLOPE= -0.12387648E 01     XINTER=       8.79141     AOLD=  0.20803359E 05
    LEAST SQUARES RESULT -      SLOPE= -0.12425556E 01     XINTER=       8.78834     AOLD=  0.20824148E 05
    LEAST SQUARES RESULT -      SLOPE= -0.12464161E 01     XINTER=       8.78530     AOLD=  0.20844961E 05
    LEAST SQUARES RESULT -      SLOPE= -0.12502890E 01     XINTER=       8.78221     AOLD=  0.20865793E 05
    LEAST SQUARES RESULT -      SLOPE= -0.12464161E 01     XINTER=       8.78530     AOLD=  0.20844957E 05
    LEAST SQUARES RESULT -      SLOPE= -0.12468004E 01     XINTER=       8.78499     AOLD=  0.20847023E 05
    LEAST SQUARES RESULT -      SLOPE= -0.12471714E 01     XINTER=       8.78468     AOLD=  0.20849090E 05
    LEAST SQUARES RESULT -      SLOPE= -0.12475624E 01     XINTER=       8.78438     AOLD=  0.20851156E 05
    LEAST SQUARES RESULT -      SLOPE= -0.12479334E 01     XINTER=       8.78407     AOLD=  0.20853223E 05
    LEAST SQUARES RESULT -      SLOPE= -0.12483387E 01     XINTER=       8.78377     AOLD=  0.20855289E 05
    LEAST SQUARES RESULT -      SLOPE= -0.12487030E 01     XINTER=       8.78345     AOLD=  0.20857355E 05
    LEAST SQUARES RESULT -      SLOPE= -0.12490940E 01     XINTER=       8.78315     AOLD=  0.20859422E 05
    LEAST SQUARES RESULT -      SLOPE= -0.12487164E 01     XINTER=       8.78345     AOLD=  0.20857352E 05
```

COMPUTED LINE - DATA Y(I)

I=	1	8.783	8.755	0.028
I=	2	8.367	8.486	-0.118
I=	3	7.951	7.799	0.152
I=	4	7.535	7.596	-0.062

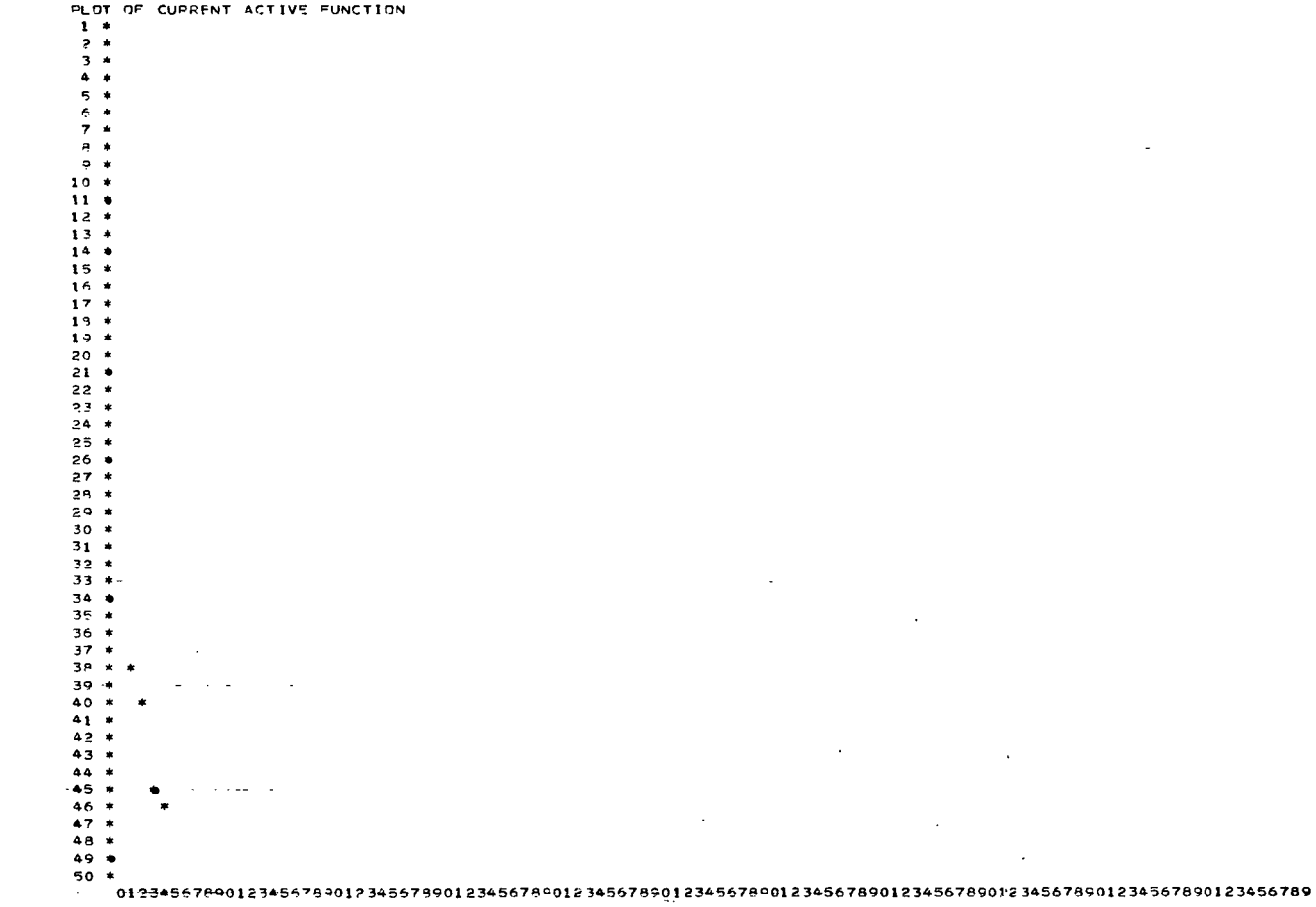

RESULT FOR GIVEN TAU = 1.24871635 COMPUTED COEFFICIENT (INTERCEPT EXP(8.78345)) = 6525.3628

FINAL CURVE Y = SUM OVER I OF A(I)*EXP(TAU(I)) WHERE

A(1) =	41768.16406250	TAU(1) =	0.02488690
A(2) =	22673.68359375	TAU(2) =	0.07062143
A(3) =	67560.75000000	TAU(3) =	0.22075051
A(4) =	15629.90625000	TAU(4) =	0.44247782
A(5) =	6525.38281250	TAU(5) =	1.24871635

INDEX	COMPUTED	ORIGINAL	DIFFERENCE
1	176157.81	175682.00	524.19
2	166128.19	166975.00	846.81
3	157503.81	157084.00	-419.81
4	149652.56	149739.00	-163.56
5	143277.00	141987.00	-1290.00
6	137284.06	134831.00	-2453.06
7	131864.44	129266.00	-2598.44
8	126922.69	124186.00	-2742.69
9	122408.50	118509.00	-3899.50
10	118250.19	117546.00	-704.19
11	114410.94	111598.00	-2812.94
12	110855.19	108074.00	-2781.19
13	107553.81	107049.00	-504.81
14	104481.56	102232.00	-2249.56
15	101617.00	98660.00	-2957.00
16	98941.19	97564.00	-1377.19
17	96437.56	94438.00	-1999.56
18	94081.50	91813.00	-2273.50
19	91849.88	91644.00	-205.88
20	89820.81	89205.00	-615.81
21	87873.69	87101.00	-772.69
22	86039.06	86440.00	400.94
23	84308.06	84245.00	-63.06
24	82672.94	82192.00	-480.94
25	81126.25	79611.00	-1515.25
26	79661.69	78060.00	-1601.69
27	78273.13	77282.00	-991.13
28	76955.13	76976.00	20.88
29	75702.56	75761.00	58.44
30	74510.94	74809.00	298.06
31	73375.94	72681.00	-694.94
32	72293.81	72665.00	372.19
33	71260.81	70637.00	-623.81
34	70273.75	70373.00	99.25
35	69329.50	67980.00	-1349.50
36	68425.31	69680.00	1254.69
37	67558.63	68574.00	1015.38
38	66727.06	66305.00	-422.06
39	65928.25	65252.00	-676.25
40	65160.45	66040.00	879.55
41	64421.47	64424.00	2.53
42	63709.68	63207.00	-502.68
43	63023.45	63417.00	393.55
44	62361.26	62578.00	216.74
45	61721.71	61773.00	51.29
46	61103.50	60963.00	-140.50
47	60505.42	60339.00	-166.42
48	59926.35	60075.00	148.65
49	59365.22	59593.00	227.78
50	58821.09	58881.00	59.91
51	58293.02	57965.00	-328.02
52	57780.19	57497.00	-283.19
53	57281.79	57534.00	252.21
54	56797.07	56907.00	109.93
55	56325.35	56128.00	-197.35
56	55866.02	55474.00	-392.02
57	55418.44	55551.00	132.56
58	54982.06	54733.00	-249.06
59	54556.35	54369.00	-187.35
60	54140.82	53826.00	-314.82
61	53735.02	53831.00	95.98
62	53339.46	52291.00	-1047.46
63	52950.32	51237.00	-1713.82
64	52571.66	52364.00	-207.66
65	52200.54	50959.00	-1241.64
66	51837.43	52174.00	336.57
67	51481.70	50801.00	-680.70
68	51133.15	50962.00	-171.15
69	50791.49	49875.00	-916.49
70	50456.50	49144.00	-1312.50
71	50127.89	49780.00	-347.89
72	49805.45	49006.00	-799.45
73	49488.94	48626.00	-862.94
74	49179.16	49066.00	-112.16
75	48872.91	48819.00	-53.91
76	48572.99	48270.00	-302.99
77	48278.25	48308.00	29.75
78	47988.51	47758.00	-230.51
79	47703.61	46900.00	-803.61
80	47423.40	48289.00	865.60

INDEX	COMPUTED	ORIGINAL	DIFFERENCE
81	47147.73	46670.00	-477.73
82	46879.46	46933.00	56.54
83	46609.49	45280.00	-1329.49
84	46346.67	46198.00	-148.67
85	46087.89	46178.00	90.11
86	45833.05	45431.00	-402.05
87	45582.02	45368.00	-214.02
88	45334.73	44631.00	-703.73
89	45091.04	45339.00	247.96
90	44850.89	45988.00	1138.11
91	44614.20	42984.00	-1630.20
92	44380.86	44585.00	204.14
93	44150.80	43584.00	-566.80
94	43923.95	43886.00	-37.95
95	43700.21	42782.00	-918.21
96	43479.56	44531.00	1051.45
97	43261.84	43497.00	235.16
98	43047.07	42610.00	-437.07
99	42835.17	42892.00	56.83
100	42626.05	42868.00	241.95
101	42419.69	41818.00	-601.69
102	42215.99	40764.00	-1451.99
103	42014.91	41844.00	-170.91
104	41816.41	41562.00	-254.41
105	41620.44	41358.00	-262.44
106	41426.94	40716.00	-710.94
107	41235.87	41594.00	358.13
108	41047.17	40364.00	-683.17
109	40860.80	40540.00	-320.80
110	40676.74	39897.00	-779.74
111	40494.91	39699.00	-795.91
112	40315.30	39679.00	-636.30
113	40137.87	39116.00	-1021.87
114	39962.56	40136.00	173.44
115	39789.34	40365.00	575.66
116	39618.18	40366.00	747.82
117	39449.04	39761.00	311.96
118	39281.90	39756.00	474.10
119	39116.71	38652.00	-464.71
120	38953.44	38677.00	-276.44
121	38792.07	38892.00	99.93
122	38632.56	38020.00	-612.56
123	38474.87	38678.00	203.13
124	38319.00	36836.00	-1483.00
125	38164.89	38358.00	193.11
126	38012.52	37845.00	-167.52
127	37861.89	37867.00	5.11
128	37712.93	37710.00	-2.93
129	37565.65	37710.00	144.35
130	37420.00	36951.00	-469.00
131	37275.98	38325.00	1049.02
132	37133.54	37764.00	630.46
133	36992.68	36423.00	-569.68
134	36853.35	36951.00	97.65
135	36715.56	37628.00	912.44
136	36579.26	37262.00	682.74
137	36444.44	37189.00	744.56
138	36311.09	37461.00	1149.92
139	36179.17	36606.00	426.83
140	36048.66	36460.00	411.34
141	35919.55	36470.00	550.45
142	35791.93	36999.00	1207.17
143	35665.45	35841.00	175.55
144	35540.42	35656.00	115.58
145	35416.70	36532.00	1115.30
146	35294.30	35618.00	323.70
147	35173.18	35860.00	686.82
148	35053.33	35499.00	445.67
149	34934.73	35845.00	910.27
150	34817.36	35787.00	969.64
151	34701.21	34873.00	171.79
152	34586.26	34694.00	107.74
153	34472.50	35132.00	659.50
154	34359.91	35876.00	1516.09
155	34248.46	35081.00	832.54
156	34138.17	34830.00	691.83
157	34029.00	34273.00	244.00
158	33920.95	34569.00	648.05
159	33813.98	34637.00	823.02
160	33708.10	34297.00	588.90

INDEX	COMPUTED	ORIGINAL	DIFFERENCE
161	33607.30	34511.00	907.70
162	33499.54	34061.00	561.46
163	33396.83	34023.00	626.17

CHI-SQUARE= 33396.82813 ABSOLUTE DIFFERENCE= 0.01224

Appendix B

Time-Shifted Analysis of the Helium Data

N= 256 FIRST= 49 LAST=216 BACKGROUND= 22000.000 CHANNEL WIDTH= 0.33330

1)	237511.	2)	220635.	3)	210161.	4)	197067.	5)	183403.	6)	176682.	7)	166975.	8)	157084.
9)	149799.	10)	141987.	11)	134831.	12)	129266.	13)	124186.	14)	118509.	15)	117546.	16)	111598.
17)	108074.	18)	107049.	19)	102232.	20)	98660.	21)	97564.	22)	94438.	23)	91818.	24)	91644.
25)	89205.	26)	87101.	27)	85440.	28)	84245.	29)	82192.	30)	79611.	31)	78060.	32)	77282.
33)	76976.	34)	75761.	35)	74809.	36)	72681.	37)	72666.	38)	70637.	39)	70373.	40)	67980.
41)	69580.	42)	68574.	43)	66305.	44)	65252.	45)	66040.	46)	64424.	47)	63207.	48)	63417.
49)	62578.	50)	61773.	51)	60963.	52)	60339.	53)	60075.	54)	59593.	55)	58881.	56)	57965.
57)	57497.	58)	57534.	59)	56907.	60)	56128.	61)	55474.	62)	55551.	63)	54733.	64)	54369.
65)	53826.	66)	53831.	67)	52291.	68)	51237.	69)	52364.	70)	50959.	71)	52174.	72)	50801.
73)	50962.	74)	49875.	75)	49144.	76)	49780.	77)	49006.	78)	48626.	79)	49066.	80)	48819.
81)	48270.	82)	48308.	83)	47758.	84)	46900.	85)	48289.	86)	46670.	87)	46933.	88)	45280.
89)	46198.	90)	46178.	91)	45431.	92)	45168.	93)	44631.	94)	45339.	95)	45989.	96)	42984.
97)	44585.	98)	43584.	99)	43886.	100)	42782.	101)	44531.	102)	43497.	103)	42610.	104)	42892.
105)	42868.	106)	41818.	107)	40764.	108)	41844.	109)	41562.	110)	41358.	111)	40716.	112)	41594.
113)	40364.	114)	40540.	115)	39897.	116)	39699.	117)	39679.	118)	39116.	119)	40136.	120)	40365.
121)	40366.	122)	39761.	123)	39756.	124)	38652.	125)	38677.	126)	38892.	127)	38020.	128)	38678.
129)	36836.	130)	38358.	131)	37845.	132)	37867.	133)	37710.	134)	37710.	135)	36951.	136)	38325.
137)	37764.	138)	36423.	139)	36951.	140)	37628.	141)	37262.	142)	37189.	143)	37461.	144)	36606.
145)	36460.	146)	36479.	147)	36999.	148)	35841.	149)	35656.	150)	36532.	151)	35618.	152)	35860.
153)	35499.	154)	35845.	155)	35787.	156)	34873.	157)	34694.	158)	35132.	159)	35876.	160)	35081.
161)	34830.	162)	34273.	163)	34569.	164)	34637.	165)	34297.	166)	34511.	167)	34061.	168)	34023.

PLOT OF CURRENT ACTIVE FUNCTION

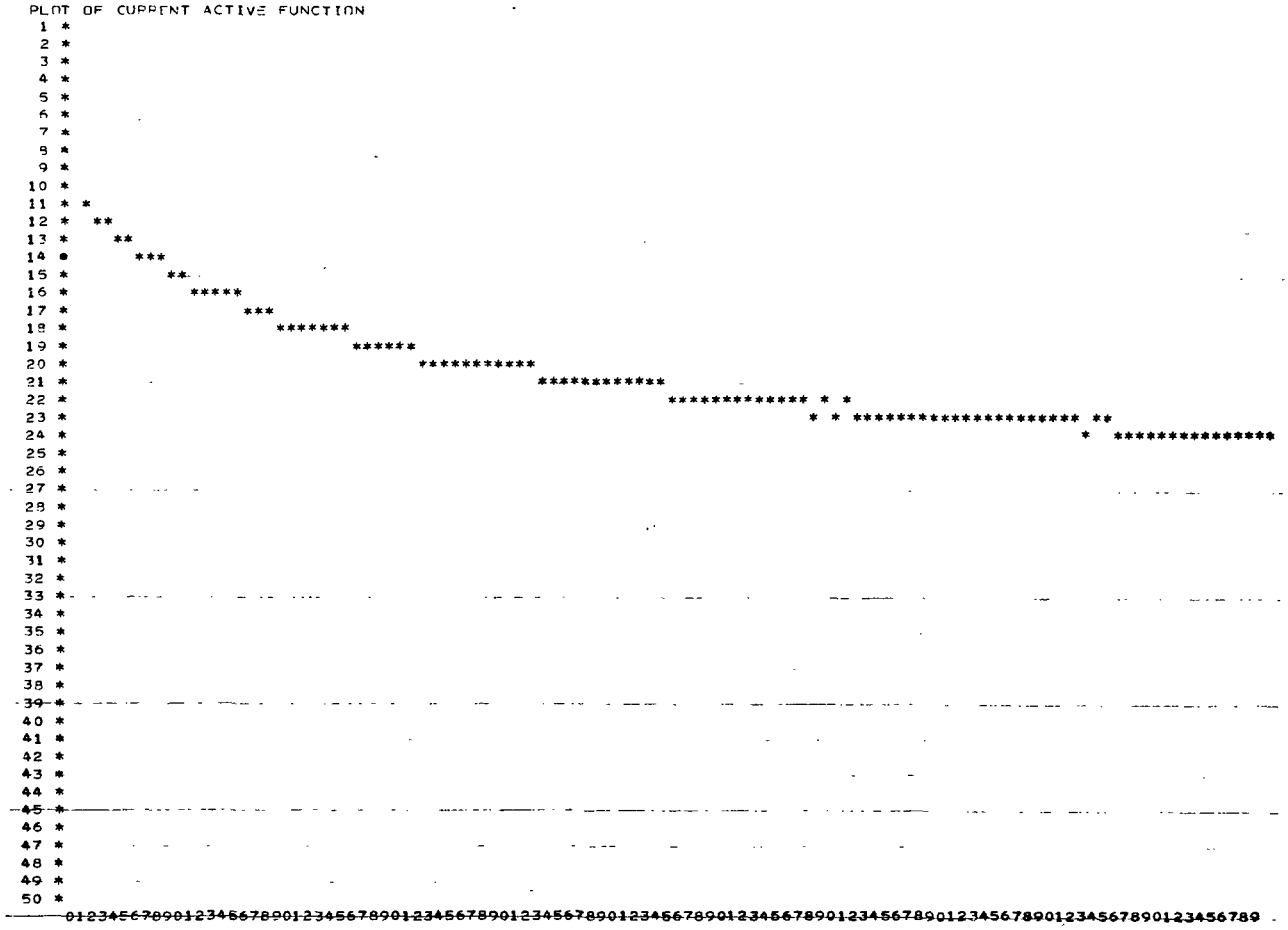

INPUT TAU= 0.02488690 START=110 END=163

1)	215511.	2)	198635.	3)	188161.	4)	175067.	5)	161403.	6)	154682.	7)	144975.	8)	135084.
9)	127796.	10)	119397.	11)	112831.	12)	107266.	13)	102186.	14)	96509.	15)	95546.	16)	89598.
17)	86074.	18)	85049.	19)	80232.	20)	75660.	21)	75564.	22)	72438.	23)	69818.	24)	69644.
25)	67205.	26)	65101.	27)	64440.	28)	62245.	29)	60192.	30)	57611.	31)	56060.	32)	55282.
33)	54976.	34)	53761.	35)	52809.	36)	50681.	37)	50666.	38)	48637.	39)	48373.	40)	45980.
41)	47680.	42)	46574.	43)	44305.	44)	43252.	45)	44040.	46)	42424.	47)	41207.	48)	41417.
49)	40578.	50)	39773.	51)	38963.	52)	38339.	53)	38075.	54)	37593.	55)	36881.	56)	35965.
57)	35497.	58)	35534.	59)	34907.	60)	34128.	61)	33474.	62)	33551.	63)	32733.	64)	32369.
65)	31826.	66)	31831.	67)	30291.	68)	29237.	69)	30364.	70)	28959.	71)	30174.	72)	28801.
73)	29962.	74)	27875.	75)	27144.	76)	27780.	77)	27006.	78)	26626.	79)	27066.	80)	26819.
81)	26270.	82)	26308.	83)	25758.	84)	24900.	85)	26289.	86)	24670.	87)	24933.	88)	23280.
89)	24198.	90)	24178.	91)	23431.	92)	23368.	93)	22631.	94)	23339.	95)	23989.	96)	20984.
97)	22585.	98)	21584.	99)	21886.	100)	20782.	101)	22531.	102)	21497.	103)	20610.	104)	20892.
105)	20868.	106)	19818.	107)	18764.	108)	19844.	109)	19562.	110)	19358.	111)	18716.	112)	19594.
113)	18364.	114)	18540.	115)	17897.	116)	17699.	117)	17679.	118)	17116.	119)	18136.	120)	18365.
121)	19366.	122)	17761.	123)	17756.	124)	16652.	125)	16677.	126)	16892.	127)	16020.	128)	16678.
129)	14836.	130)	16358.	131)	15845.	132)	15867.	133)	15710.	134)	15710.	135)	14951.	136)	16325.
137)	15764.	138)	14423.	139)	14951.	140)	15628.	141)	15262.	142)	15189.	143)	15461.	144)	14606.
145)	14460.	146)	14479.	147)	14999.	148)	13841.	149)	13656.	150)	14532.	151)	13618.	152)	13860.
153)	13499.	154)	13846.	155)	13787.	156)	12973.	157)	12694.	158)	13132.	159)	13876.	160)	13081.
161)	12830.	162)	12273.	163)	12569.	164)	12637.	165)	12297.	166)	12511.	167)	12061.	168)	12023.

PLOT OF CURRENT ACTIVE FUNCTION

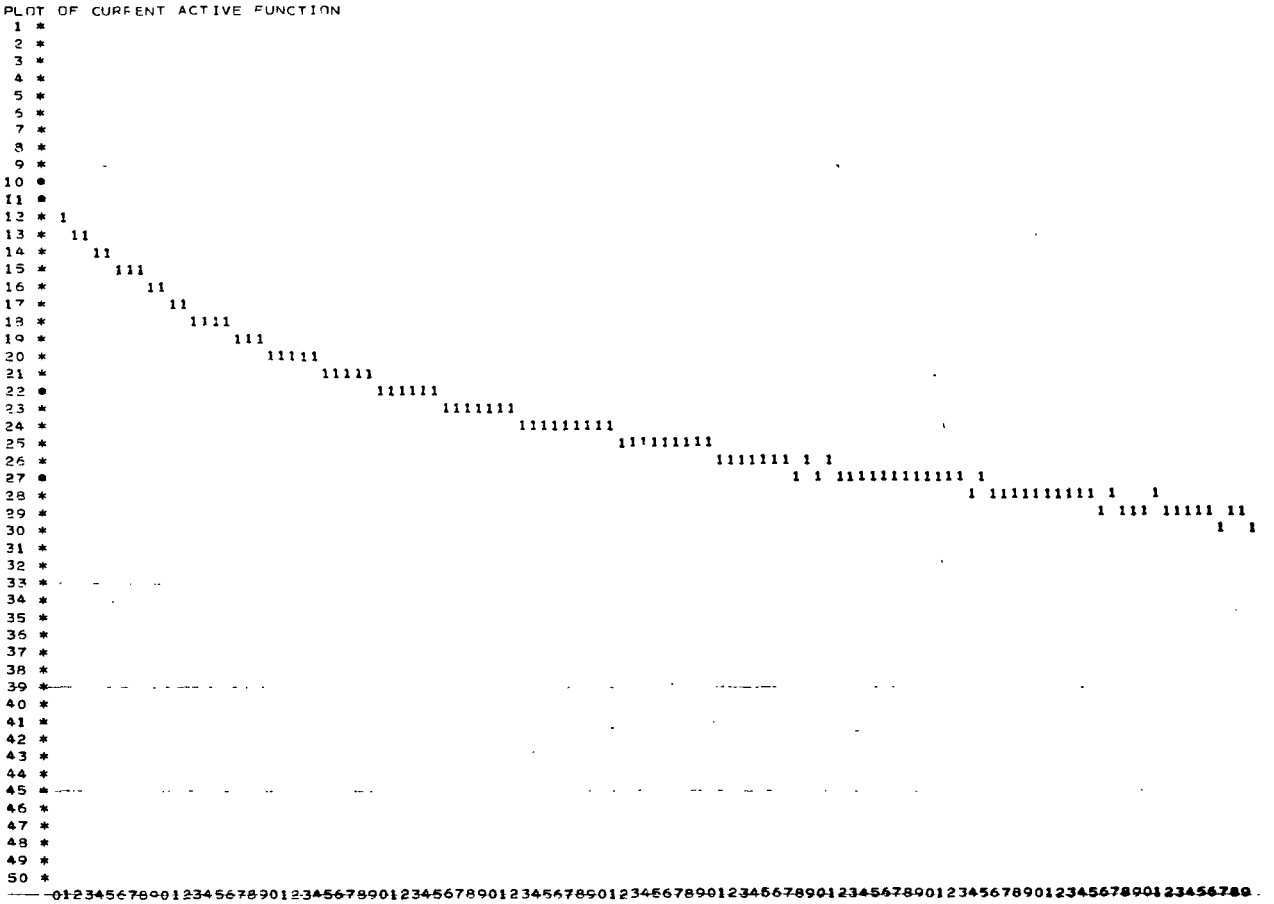

LEAST SQUARES RESULT -	SLOPE= -0.22929482E-01	XINTER=	10.68321	AOLD=	0.22000000E 05	
LEAST SQUARES RESULT -	SLOPE= -0.26755299E-01	XINTER=	10.70131	AOLD=	0.24199984E 05	
LEAST SQUARES RESULT -	SLOPE= -0.22929482E-01	XINTER=	10.68321	AOLD=	0.21999996E 05	
LEAST SQUARES RESULT -	SLOPE= -0.23285370E-01	XINTER=	10.68504	AOLD=	0.22219977E 05	
LEAST SQUARES RESULT -	SLOPE= -0.23603130E-01	XINTER=	10.68483	AOLD=	0.22442160E 05	
LEAST SQUARES RESULT -	SLOPE= -0.23933601E-01	XINTER=	10.68483	AOLD=	0.22666563E 05	
LEAST SQUARES RESULT -	SLOPE= -0.24314910E-01	XINTER=	10.68646	AOLD=	0.22893211E 05	
LEAST SQUARES RESULT -	SLOPE= -0.24734352E-01	XINTER=	10.68931	AOLD=	0.23122125E 05	
LEAST SQUARES RESULT -	SLOPE= -0.25128372E-01	XINTER=	10.69073	AOLD=	0.23353328E 05	
LEAST SQUARES RESULT -	SLOPE= -0.24734352E-01	XINTER=	10.68931	AOLD=	0.23122121E 05	
LEAST SQUARES RESULT -	SLOPE= -0.24772484E-01	XINTER=	10.68951	AOLD=	0.23145230E 05	
LEAST SQUARES RESULT -	SLOPE= -0.24823323E-01	XINTER=	10.69032	AOLD=	0.23168359E 05	
LEAST SQUARES RESULT -	SLOPE= -0.24848744E-01	XINTER=	10.68971	AOLD=	0.23191512E 05	
LEAST SQUARES RESULT -	SLOPE= -0.24899587E-01	XINTER=	10.68992	AOLD=	0.23214688E 05	
LEAST SQUARES RESULT -	SLOPE= -0.24848744E-01	XINTER=	10.68971	AOLD=	0.23191508E 05	
LEAST SQUARES RESULT -	SLOPE= -0.24874166E-01	XINTER=	10.69053	AOLD=	0.23193805E 05	
LEAST SQUARES RESULT -	SLOPE= -0.24861455E-01	XINTER=	10.68971	AOLD=	0.23196102E 05	
LEAST SQUARES RESULT -	SLOPE= -0.24848744E-01	XINTER=	10.68910	AOLD=	0.23198398E 05	
LEAST SQUARES RESULT -	SLOPE= -0.24848744E-01	XINTER=	10.68910	AOLD=	0.23200699E 05	
LEAST SQUARES RESULT -	SLOPE= -0.24874166E-01	XINTER=	10.68971	AOLD=	0.23203000E 05	
LEAST SQUARES RESULT -	SLOPE= -0.24874166E-01	XINTER=	10.68992	AOLD=	0.23205301E 05	
LEAST SQUARES RESULT -	SLOPE= -0.24886876E-01	XINTER=	10.69012	AOLD=	0.23207602E 05	
LEAST SQUARES RESULT -	SLOPE= -0.24874166E-01	XINTER=	10.68971	AOLD=	0.23209902E 05	
LEAST SQUARES RESULT -	SLOPE= -0.24861455E-01	XINTER=	10.68890	AOLD=	0.23212203E 05	
LEAST SQUARES RESULT -	SLOPE= -0.24886876E-01	XINTER=	10.68931	AOLD=	0.23214504E 05	
LEAST SQUARES RESULT -	SLOPE= -0.24912298E-01	XINTER=	10.69032	AOLD=	0.23216805E 05	
LEAST SQUARES RESULT -	SLOPE= -0.24886876E-01	XINTER=	10.68931	AOLD=	0.23214500E 05	
LEAST SQUARES RESULT -	SLOPE= -0.24899587E-01	XINTER=	10.68992	AOLD=	0.23214719E 05	

COMPUTED LINE - DATA Y(I)

I= 110	9.785	9.806	-0.021
I= 111	9.777	9.770	0.007
I= 112	9.769	9.819	-0.050
I= 113	9.760	9.750	0.011
I= 114	9.752	9.760	-0.008
I= 115	9.744	9.722	0.022
I= 116	9.736	9.710	0.025
I= 117	9.727	9.709	0.018
I= 118	9.719	9.674	0.045
I= 119	9.711	9.736	-0.026
I= 120	9.702	9.750	-0.047
I= 121	9.694	9.750	-0.056
I= 122	9.686	9.714	-0.028
I= 123	9.677	9.714	-0.036
I= 124	9.669	9.645	0.025
I= 125	9.661	9.646	0.015
I= 126	9.653	9.660	-0.007
I= 127	9.644	9.603	0.042
I= 128	9.636	9.646	-0.010
I= 129	9.628	9.519	0.108
I= 130	9.619	9.625	-0.006
I= 131	9.611	9.591	0.020
I= 132	9.603	9.592	0.010
I= 133	9.594	9.582	0.013
I= 134	9.586	9.582	0.005
I= 135	9.578	9.528	0.050
I= 136	9.570	9.623	-0.054
I= 137	9.561	9.585	-0.024
I= 138	9.553	9.489	0.064
I= 139	9.545	9.528	0.017
I= 140	9.536	9.576	-0.040
I= 141	9.528	9.550	-0.022
I= 142	9.520	9.545	-0.025
I= 143	9.511	9.564	-0.053
I= 144	9.503	9.502	0.001
I= 145	9.495	9.491	0.003
I= 146	9.487	9.493	-0.006
I= 147	9.478	9.531	-0.053
I= 148	9.470	9.444	0.026
I= 149	9.462	9.429	0.033
I= 150	9.453	9.497	-0.043
I= 151	9.445	9.426	0.019
I= 152	9.437	9.445	-0.008
I= 153	9.428	9.416	0.012
I= 154	9.420	9.444	-0.024
I= 155	9.412	9.439	-0.027
I= 156	9.404	9.364	0.040
I= 157	9.395	9.348	0.047
I= 158	9.387	9.386	0.001
I= 159	9.379	9.446	-0.068
I= 160	9.370	9.381	-0.011
I= 161	9.362	9.360	0.002
I= 162	9.354	9.311	0.043
I= 163	9.345	9.337	0.008

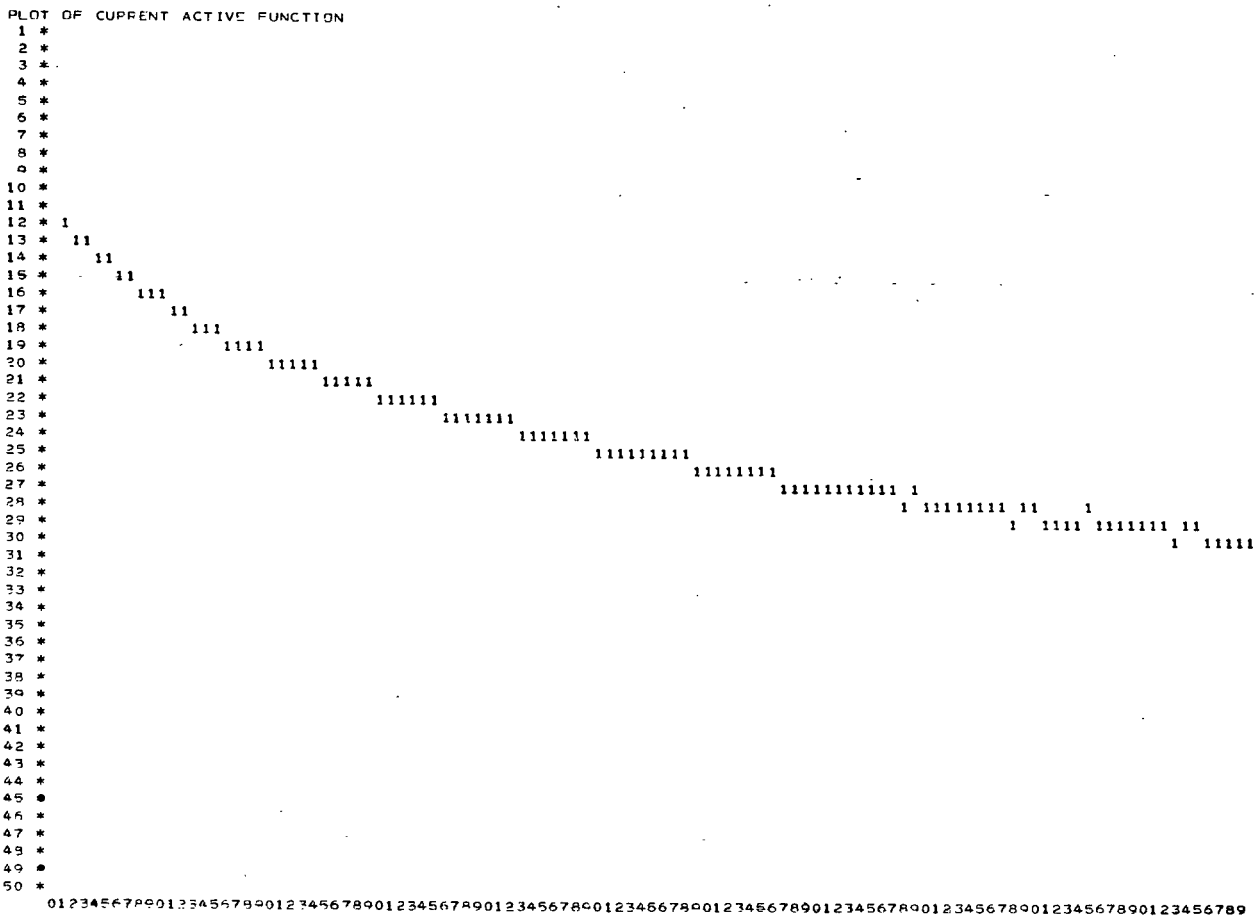

RESULT FOR GIVEN TAU = 0.02488690 COMPUTED COEFFICIENT (INTERCEPT EXP(10.68992)) = 43910.8867

```
 INPUT TAU=      0.07062143      START= 70      END= 98

  1) 170385.    2) 153872.    3) 143758.    4) 131021.    5) 117710.    6) 111340.    7) 101981.    8)  92436.
  9)  85493.   10)  78030.   11)  71201.   12)  65970.   13)  61221.   14)  55872.   15)  55235.   16)  49610.
 17)  46406.   18)  45699.   19)  41197.   20)  37937.   21)  37151.   22)  34332.   23)  32017.   24)  32145.
 25)  30006.   26)  28199.   27)  27833.   28)  25930.   29)  24167.   30)  21874.   31)  20608.   32)  20113.
 33)  20087.   34)  19150.   35)  18474.   36)  16620.   37)  16876.   38)  15116.   39)  15119.   40)  12991.
 41)  14953.   42)  14108.   43)  12097.   44)  11300.   45)  12342.   46)  10977.   47)  10010.   48)  10468.
 49)   9874.   50)   9313.   51)   8745.   52)   8360.   53)   8334.   54)   8087.   55)   7609.   56)   6925.
 57)   6687.   58)   6952.   59)   6551.   60)   5996.   61)   5564.   62)   5862.   63)   5263.   64)   5115.
 65)   4788.   66)   5006.   67)   3677.   68)   2833.   69)   4168.   70)   2970.   71)   4389.   72)   3219.
 73)   3582.   74)   2694.   75)   2161.   76)   2993.   77)   2414.   78)   2227.   79)   2859.   80)   2802.
 81)   2441.   82)   2666.   83)   2301.   84)   1627.   85)   3198.   86)   1760.   87)   2202.   88)    727.
 89)   1821.   90)   1976.   91)   1402.   92)   1511.   93)    945.   94)   1822.   95)   2639.
```

PLOT OF CURRENT ACTIVE FUNCTION

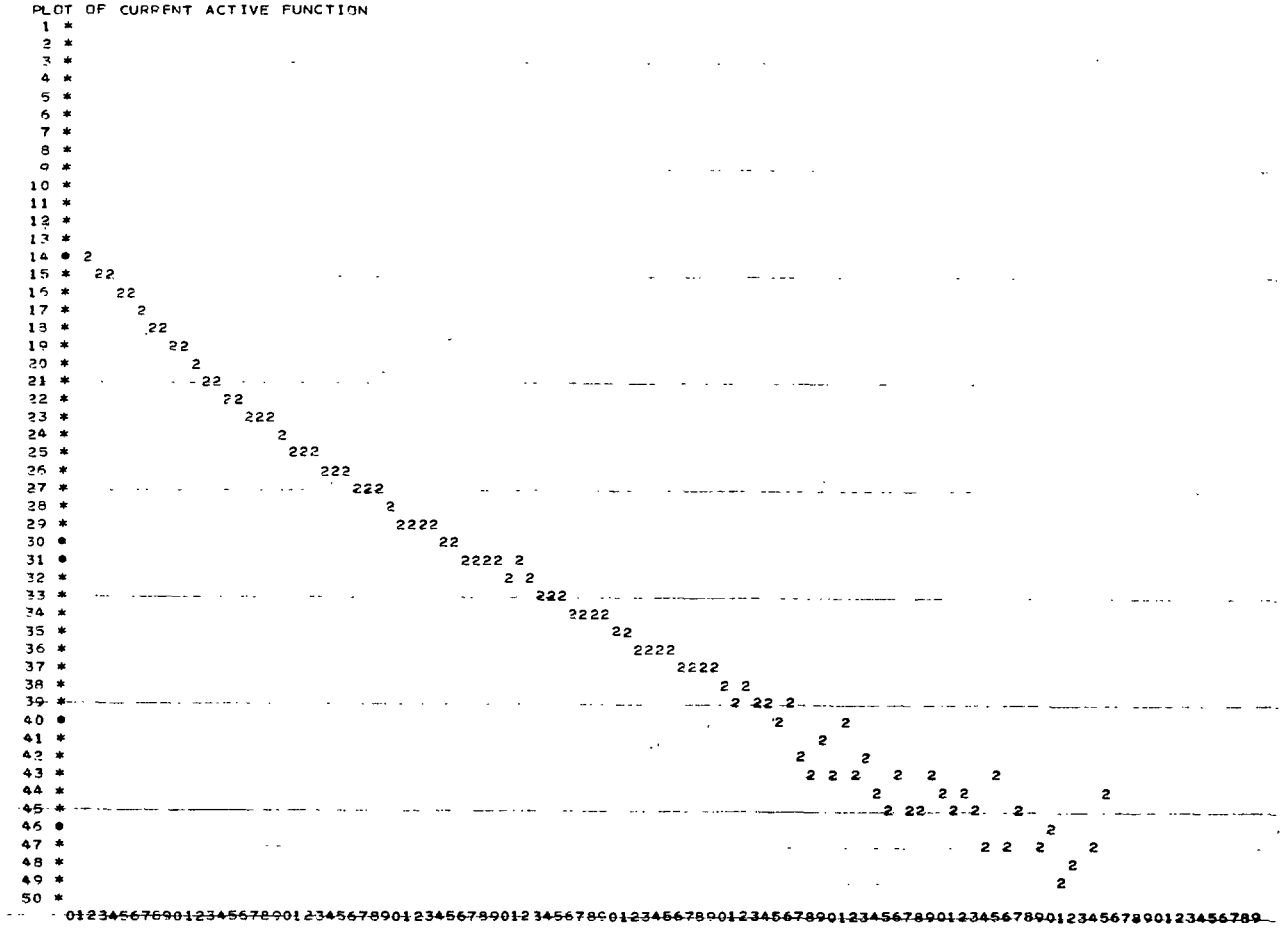

```
LEAST SQUARES RESULT -     SLOPE= -0.10416323E 00     XINTER=     10.52831     AOLD=  0.43910887E 05
LEAST SQUARES RESULT -     SLOPE= -0.62234711E-01     XINTER=     10.10379     AOLD=  0.39519797E 05
LEAST SQUARES RESULT -     SLOPE= -0.10410410E 00     XINTER=     10.52713     AOLD=  0.43910983E 05
LEAST SQUARES RESULT -     SLOPE= -0.95777512E-01     XINTER=     10.40290     AOLD=  0.43471773E 05
LEAST SQUARES RESULT -     SLOPE= -0.89196146E-01     XINTER=     10.31511     AOLD=  0.43037055E 05
LEAST SQUARES RESULT -     SLOPE= -0.83857119E-01     XINTER=     10.25145     AOLD=  0.42606684E 05
LEAST SQUARES RESULT -     SLOPE= -0.79390645E-01     XINTER=     10.20436     AOLD=  0.42180613E 05
LEAST SQUARES RESULT -     SLOPE= -0.75634062E-01     XINTER=     10.17052     AOLD=  0.41758905E 05
LEAST SQUARES RESULT -     SLOPE= -0.72409928E-01     XINTER=     10.14568     AOLD=  0.41341215E 05
LEAST SQUARES RESULT -     SLOPE= -0.69644272E-01     XINTER=     10.12911     AOLD=  0.40927801E 05
LEAST SQUARES RESULT -     SLOPE= -0.72409928E-01     XINTER=     10.14568     AOLD=  0.41341211E 05
LEAST SQUARES RESULT -     SLOPE= -0.72143734E-01     XINTER=     10.14426     AOLD=  0.41299867E 05
LEAST SQUARES RESULT -     SLOPE= -0.71933134E-01     XINTER=     10.14213     AOLD=  0.41258566E 05
LEAST SQUARES RESULT -     SLOPE= -0.71552157E-01     XINTER=     10.14047     AOLD=  0.41217305E 05
LEAST SQUARES RESULT -     SLOPE= -0.71226776E-01     XINTER=     10.13739     AOLD=  0.41176086E 05
LEAST SQUARES RESULT -     SLOPE= -0.71034491E-01     XINTER=     10.13787     AOLD=  0.41134910E 05
LEAST SQUARES RESULT -     SLOPE= -0.70723951E-01     XINTER=     10.13527     AOLD=  0.41093773E 05
LEAST SQUARES RESULT -     SLOPE= -0.70398569E-01     XINTER=     10.13243     AOLD=  0.41052680E 05
LEAST SQUARES RESULT -     SLOPE= -0.70723951E-01     XINTER=     10.13527     AOLD=  0.41093770E 05
LEAST SQUARES RESULT -     SLOPE= -0.70649991E-01     XINTER=     10.13408     AOLD=  0.41089660E 05
LEAST SQUARES RESULT -     SLOPE= -0.70636200E-01     XINTER=     10.13456     AOLD=  0.41085551E 05
LEAST SQUARES RESULT -     SLOPE= -0.70635200E-01     XINTER=     10.13456     AOLD=  0.41081441E 05
LEAST SQUARES RESULT -     SLOPE= -0.70605576E-01     XINTER=     10.13432     AOLD=  0.41077332E 05
LEAST SQUARES RESULT -     SLOPE= -0.70635200E-01     XINTER=     10.13456     AOLD=  0.41081438E 05
LEAST SQUARES RESULT -     SLOPE= -0.70605576E-01     XINTER=     10.13408     AOLD=  0.41081027E 05
```

COMPUTED LINE - DATA Y(I)

I=	70	8.510	8.426	0.084
I=	71	8.487	8.695	-0.208
I=	72	8.463	8.474	-0.011
I=	73	8.440	8.545	-0.105
I=	74	8.416	8.352	0.064
I=	75	8.393	8.214	0.178
I=	76	8.369	8.415	-0.046
I=	77	8.346	8.274	0.072
I=	78	8.322	8.222	0.100
I=	79	8.299	8.376	-0.077
I=	80	8.275	8.360	-0.085
I=	81	8.251	8.268	-0.017
I=	82	8.228	8.321	-0.094
I=	83	8.204	8.225	-0.021
I=	84	8.181	8.022	0.158
I=	85	8.157	8.436	-0.278
I=	86	8.134	8.058	0.076
I=	87	8.110	8.186	-0.075
I=	88	8.087	7.651	0.436
I=	89	8.063	8.066	-0.003
I=	90	8.040	8.110	-0.071
I=	91	8.016	7.917	0.099
I=	92	7.993	7.952	0.041
I=	93	7.969	7.725	0.244
I=	94	7.946	8.049	-0.103
I=	95	7.922	8.278	-0.356

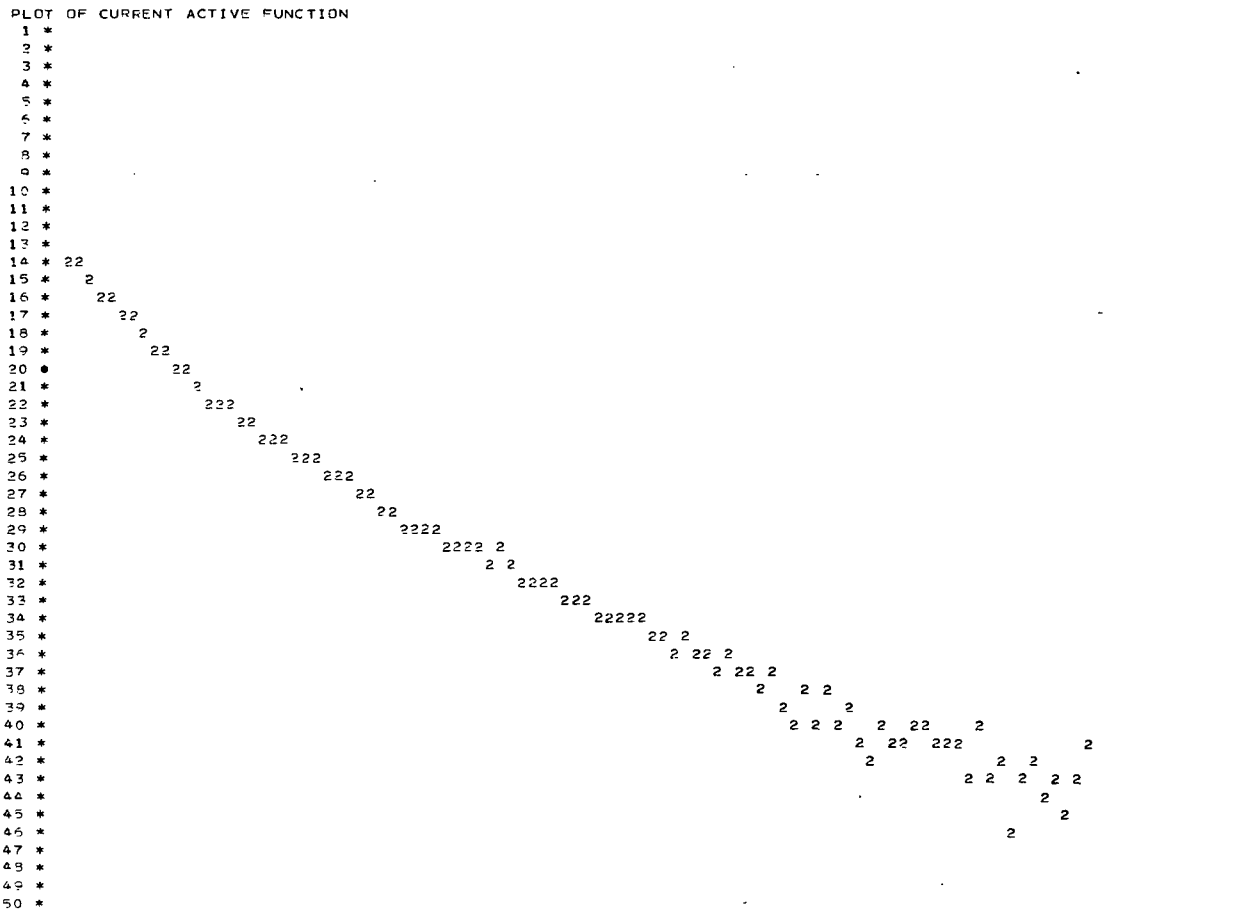

RESULT FOR GIVEN TAU = 0.07062143 COMPUTED COEFFICIENT (INTERCEPT EXP(10.13408)) = 25186.9648

```
 INPUT TAU=      0.22075051      START= 30      END= 60

  1) 148028.    2) 132078.    3) 122513.    4) 110311.    5)  97524.    6)  91665.    7)  82804.    8)  73745.
  9)  67277.   10)  60268.   11)  53901.   12)  49111.   13)  44793.   14)  39865.   15)  39638.   16)  34414.
 17)  31601.   18)  31275.   19)  27146.   20)  24250.   21)  23818.   22)  21346.   23)  19368.   24)  19826.
 25)  18008.   26)  16516.   27)  16456.   28)  14852.   29)  13381.   30)  11372.   31)  10384.   32)  10159.
 33)  10398.   34)   9719.   35)   9295.   36)   7686.   37)   8182.   38)   6656.   39)   6887.   40)   4981.
 41)   7160.   42)   6526.   43)   4722.   44)   4127.   45)   5365.   46)   4193.   47)   3413.   48)   4053.
 49)   3637.   50)   3249.   51)   2850.   52)   2631.   53)   2766.   54)   2677.   55)   2352.   56)   1817.
 57)   1724.   58)   2131.   59)   1869.   60)   1449.   61)   1150.   62)   1576.   63)   1102.   64)   1077.
 65)    868.   66)   1202.
```

PLOT OF CURRENT ACTIVE FUNCTION

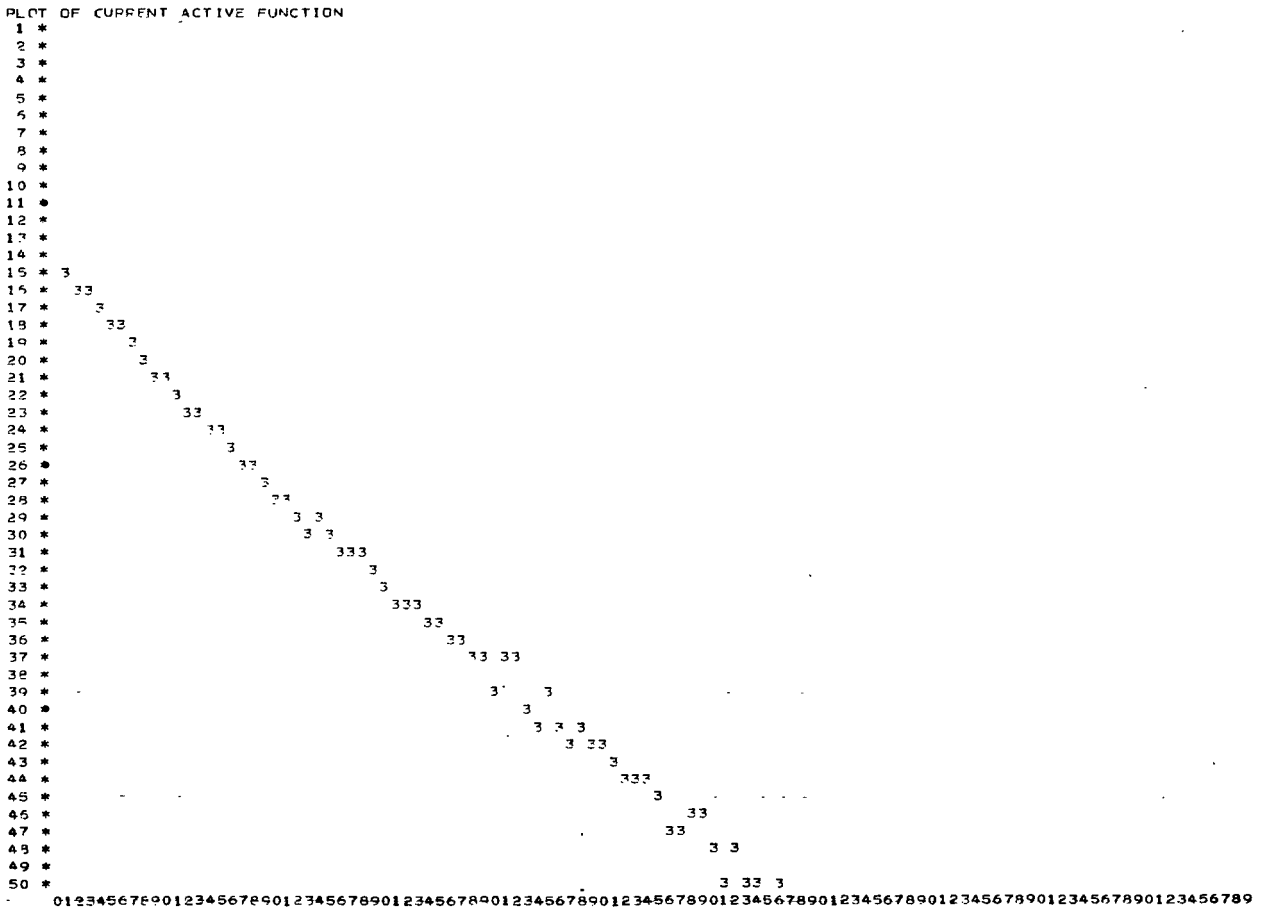

LEAST SQUARES RESULT -	SLOPE=	-0.2005561 0E 00	XINTER=	11.34248	AOLD=	0.25186965E	05
LEAST SQUARES RESULT -	SLOPE=	-0.23754573E 00	XINTER=	11.63225	AOLD=	0.27705645F	05
LEAST SQUARES RESULT -	SLOPE=	-0.2005561 0E 00	XINTER=	11.34248	AOLD=	0.25186961E	05
LEAST SQUARES RESULT -	SLOPE=	-0.2034171 9E 00	XINTER=	11.36227	AOLD=	0.25438809E	05
LEAST SQUARES RESULT -	SLOPE=	-0.20644655E 00	XINTER=	11.38381	AOLD=	0.25693176E	05
LEAST SQUARES RESULT -	SLOPE=	-0.20969825E 00	XINTER=	11.40770	AOLD=	0.25950086E	05
LEAST SQUARES RESULT -	SLOPE=	-0.2131201 0E 00	XINTER=	11.43322	AOLD=	0.26209566E	05
LEAST SQUARES RESULT -	SLOPE=	-0.21679348E 00	XINTER=	11.46155	AOLD=	0.26471641E	05
LEAST SQUARES RESULT -	SLOPE=	-0.22073758E 00	XINTER=	11.49258	AOLD=	0.26736336E	05
LEAST SQUARES RESULT -	SLOPE=	-0.22497437E 00	XINTER=	11.52665	AOLD=	0.27003680F	05
LEAST SQUARES RESULT -	SLOPE=	-0.22073756E 00	XINTER=	11.49258	AOLD=	0.26736332E	05
LEAST SQUARES RESULT -	SLOPE=	-0.22115469E 00	XINTER=	11.49586	AOLD=	0.26767051E	05
LEAST SQUARES RESULT -	SLOPE=	-0.22073758E 00	XINTER=	11.49258	AOLD=	0.26736328E	05
LEAST SQUARES RESULT -	SLOPE=	-0.22077417E 00	XINTER=	11.49281	AOLD=	0.26738977E	05
LEAST SQUARES RESULT -	SLOPE=	-0.22073758E 00	XINTER=	11.49246	AOLD=	0.26736324E	05
LEAST SQUARES RESULT -	SLOPE=	-0.22073758E 00	XINTER=	11.49258	AOLD=	0.26736578F	05
LEAST SQUARES RESULT -	SLOPE=	-0.22074491E 00	XINTER=	11.49258	AOLD=	0.26736832E	05
LEAST SQUARES RESULT -	SLOPE=	-0.22075951F 00	XINTER=	11.49270	AOLD=	0.26737086E	05

COMPUTED LINE - DATA Y(I)

I=	30	9.359	9.268	0.091
I=	31	9.285	9.171	0.114
I=	32	9.212	9.150	0.062
I=	33	9.138	9.177	-0.038
I=	34	9.065	9.106	-0.041
I=	35	8.991	9.059	-0.068
I=	36	8.917	8.855	0.063
I=	37	8.844	8.925	-0.081
I=	38	8.770	8.701	0.070
I=	39	8.697	8.741	-0.044
I=	40	8.623	8.381	0.242
I=	41	8.550	8.788	-0.239
I=	42	8.476	8.689	-0.213
I=	43	8.402	8.330	0.073
I=	44	8.329	8.178	0.150
I=	45	8.255	8.479	-0.224
I=	46	8.182	8.204	-0.022
I=	47	8.108	7.968	0.140
I=	48	8.034	8.172	-0.137
I=	49	7.961	8.051	-0.090
I=	50	7.887	7.923	-0.036
I=	51	7.814	7.772	0.042
I=	52	7.740	7.680	0.060
I=	53	7.667	7.745	-0.078
I=	54	7.593	7.710	-0.117
I=	55	7.519	7.558	-0.039
I=	56	7.446	7.238	0.207
I=	57	7.372	7.177	0.195
I=	58	7.299	7.454	-0.155
I=	59	7.225	7.295	-0.070
I=	60	7.152	6.969	0.183

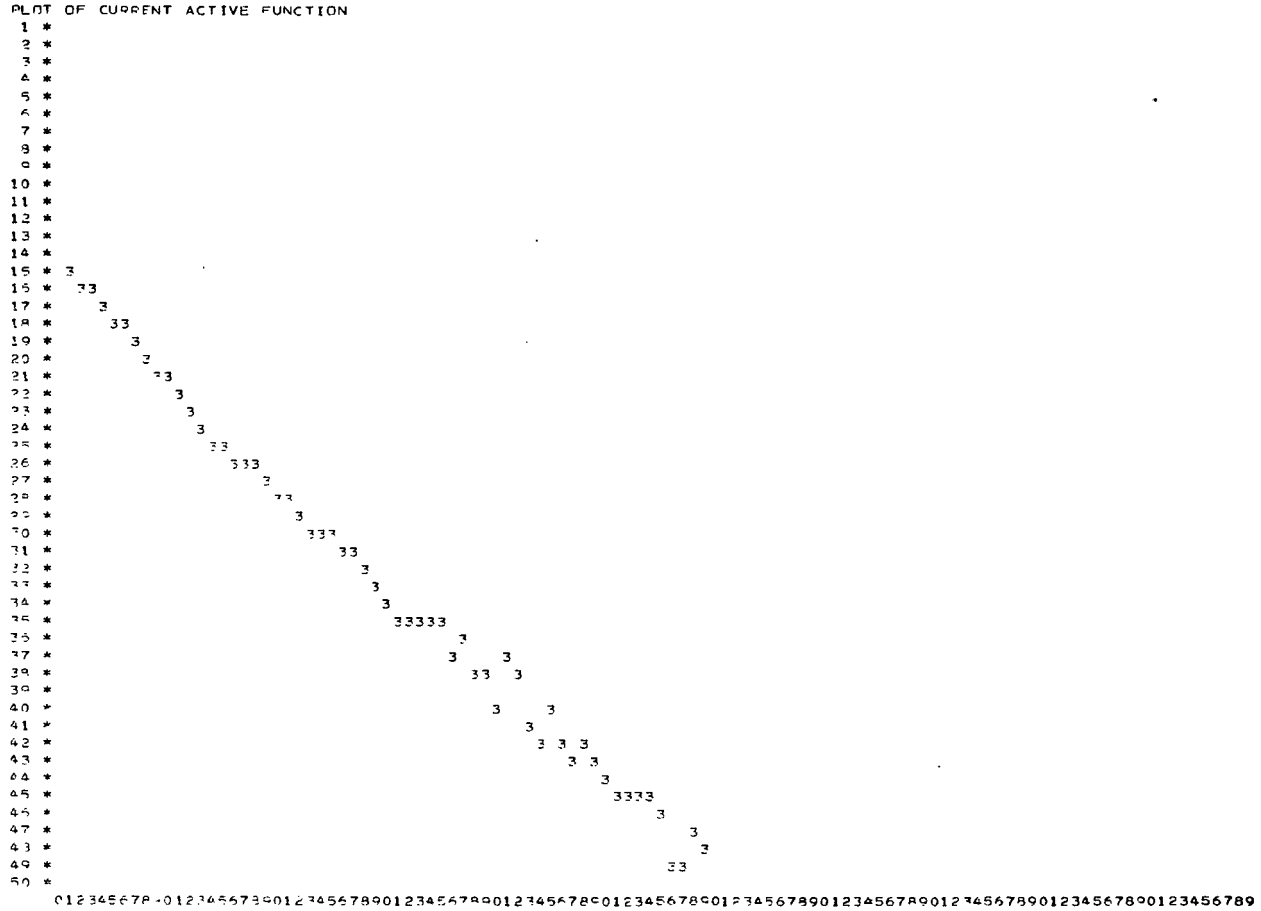
PLOT OF CURRENT ACTIVE FUNCTION
0123456789012345678901234567890123456789012345678901234567890123456789012345678901234567890123456789
RESULT FOR GIVEN TAU = 0.22075051 COMPUTED COEFFICIENT (INTERCEPT EXP(11.49370)) = 97997.4375

```
 INPUT TAU=      0.44247762      START= 13      END= 23

  1)  48481.    2)  39518.    3)  36446.    4)  30279.    5)  23100.    6)  22453.    7)  18436.    8)  13879.
  9)  11595.   10)   8474.   11)   5721.   12)   4291.   13)   3095.   14)   1069.   15)   3540.   16)    823.
 17)    341.   18)   2182.   19)     67.

PLOT OF CURRENT ACTIVE FUNCTION
 1 *
 2 *
 3 *
 4 *
 5 *
 6 *
 7 *
 8 *
 9 *
10 *
11 *
12 *
13 *
14 *
15 *
16 *
17 *
18 *
19 *
20 *
21 *
22 *
23 * 4
24 *  4
25 *   4
26 *    4
27 *
28 *     44
29 *
30 *       4
31 *
32 *        4
33 *         4
34 *
35 *
36 *          4
37 *
38 *           4
39 *
40 *            4
41 *
42 *              4
43 *             4
44 *
45 *                 4
46 *
47 *
48 *
49 *
50 *
    -0123456789012345678901234567890123456789012345678901234567890123456789012345678901234567890123456789012345678901234567890123456789

      LEAST SQUARES RESULT -    SLOPE= -0.13308811E 01    XINTER=      13.45645    AOLD=  0.97997438E 05
      LEAST SQUARES RESULT -    SLOPE= -0.3885662OE 00    XINTER=      10.37905    AOLD=  0.88197688E 05
      LEAST SQUARES RESULT -    SLOPE= -0.13307915E 01    XINTER=      13.45609    AOLD=  0.97997375E 05
      LEAST SQUARES RESULT -    SLOPE= -0.84018743E 00    XINTER=      11.45986    AOLD=  0.97017375E 05
      LEAST SQUARES RESULT -    SLOPE= -0.68278545E 00    XINTER=      10.92170    AOLD=  0.96047188E 05
      LEAST SQUARES RESULT -    SLOPE= -0.59574848E 00    XINTER=      10.67037    AOLD=  0.95086688E 05
      LEAST SQUARES RESULT -    SLOPE= -0.53883755E 00    XINTER=      10.53404    AOLD=  0.94135813E 05
      LEAST SQUARES RESULT -    SLOPE= -0.49818367E 00    XINTER=      10.45582    AOLD=  0.93194438E 05
      LEAST SQUARES RESULT -    SLOPE= -0.46750825E 00    XINTER=      10.41080    AOLD=  0.92262438E 05
      LEAST SQUARES RESULT -    SLOPE= -0.44341415E 00    XINTER=      10.38604    AOLD=  0.91339813E 05
      LEAST SQUARES RESULT -    SLOPE= -0.42398417E 00    XINTER=      10.37492    AOLD=  0.90426375E 05
      LEAST SQUARES RESULT -    SLOPE= -0.44343662E 00    XINTER=      10.38622    AOLD=  0.91339750E 05
      LEAST SQUARES RESULT -    SLOPE= -0.44130635E 00    XINTER=      10.38443    AOLD=  0.91248375E 05
      LEAST SQUARES RESULT -    SLOPE= -0.44342542E 00    XINTER=      10.38622    AOLD=  0.91339588E 05
      LEAST SQUARES RESULT -    SLOPE= -0.44324601E 00    XINTER=      10.38622    AOLD=  0.91330500E 05
      LEAST SQUARES RESULT -    SLOPE= -0.44298816E 00    XINTER=      10.38586    AOLD=  0.91321313E 05
      LEAST SQUARES RESULT -    SLOPE= -0.44277513E 00    XINTER=      10.38586    AOLD=  0.91312125E 05
      LEAST SQUARES RESULT -    SLOPE= -0.44257331E 00    XINTER=      10.38568    AOLD=  0.91302938E 05
      LEAST SQUARES RESULT -    SLOPE= -0.44236028E 00    XINTER=      10.38533    AOLD=  0.91293750E 05
      LEAST SQUARES RESULT -    SLOPE= -0.44256210E 00    XINTER=      10.38568    AOLD=  0.91302875E 05
      LEAST SQUARES RESULT -    SLOPE= -0.44255090E 00    XINTER=      10.38550    AOLD=  0.91301938E 05
      LEAST SQUARES RESULT -    SLOPE= -0.44250602E 00    XINTER=      10.38550    AOLD=  0.91301000E 05
      LEAST SQUARES RESULT -    SLOPE= -0.44251722E 00    XINTER=      10.38550    AOLD=  0.91300063E 05
      LEAST SQUARES RESULT -    SLOPE= -0.44247240E 00    XINTER=      10.38550    AOLD=  0.91299125E 05
```

COMPUTED LINE - DATA Y(I)

I=	13	8.615	8.677	-0.061
I=	14	8.469	8.201	0.268
I=	15	8.321	8.688	-0.367
I=	16	8.173	8.021	0.152
I=	17	8.026	7.785	0.241
I=	18	7.879	8.319	-0.440
I=	19	7.731	7.522	0.209

PLOT OF CURRENT ACTIVE FUNCTION

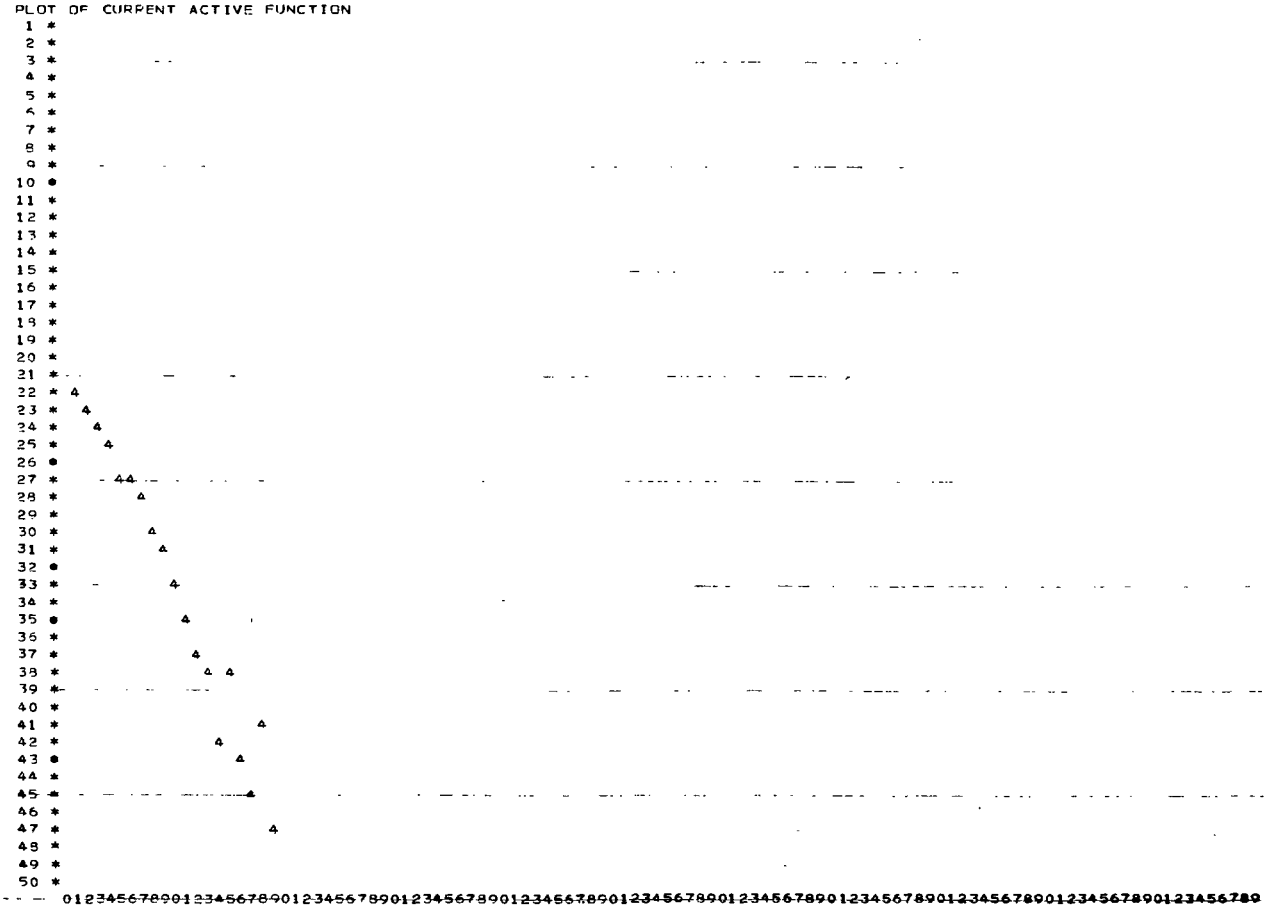

RESULT FOR GIVEN TAU = 0.44247782 COMPUTED COEFFICIENT (INTERCEPT EXP(-10.38550)) = 32386.7500

```
 INPUT TAU=      1.24871635      START=  6      END=  9

 1)  22793.    2)  17795.    3)  18114.    4)  14843.    5)  10137.    6)  11597.    7)  9376.    8)  6346.
 9)   5359.   10)   3340.   11)   1520.   12)    878.   13)    348.

PLOT OF CURRENT ACTIVE FUNCTION
```

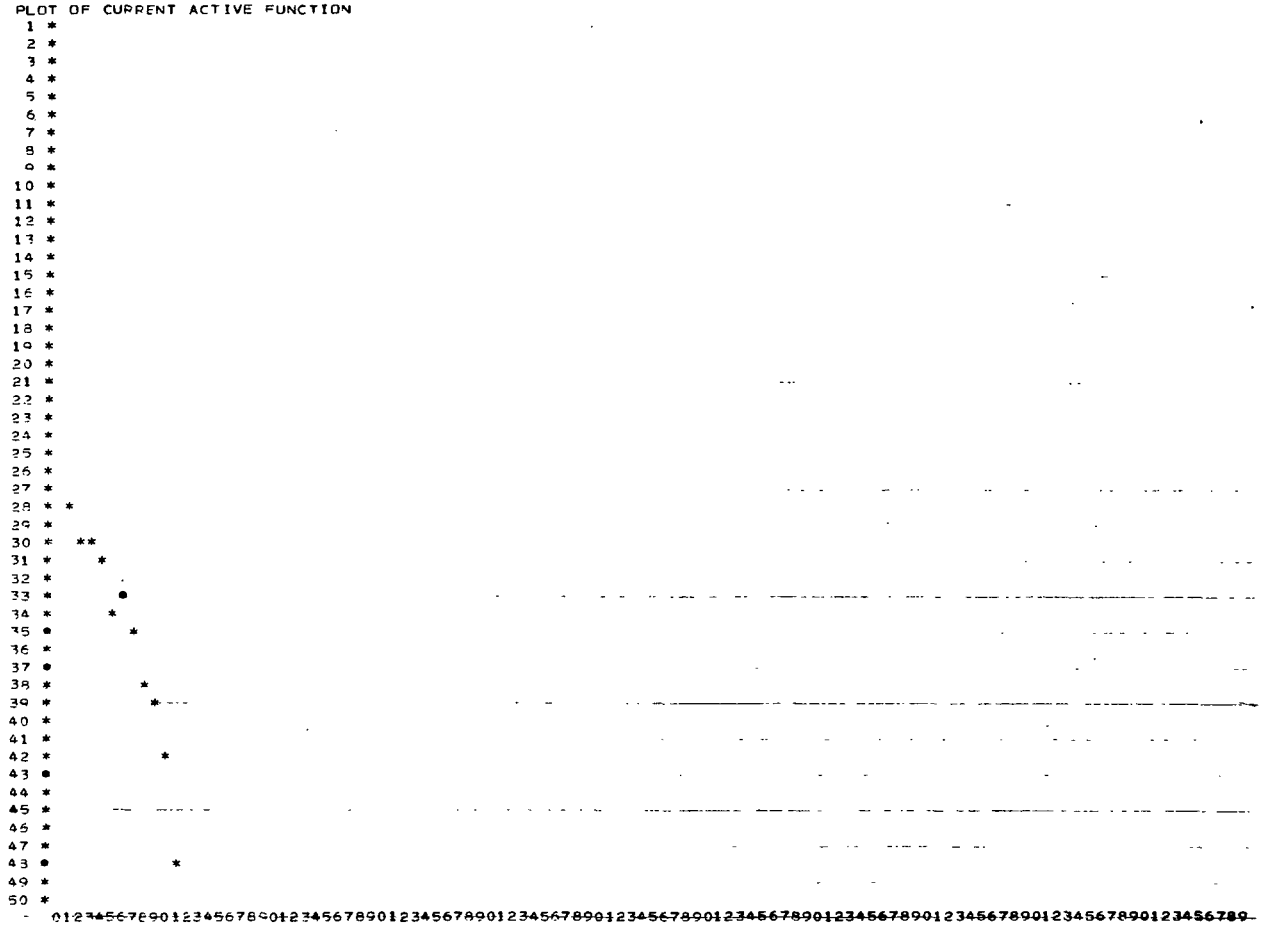

```
 LEAST SQUARES RESULT -     SLOPE= -0.81184024E 00     XINTER=     10.72040     AOLD=  0.32386750E 05
 LEAST SQUARES RESULT -     SLOPE= -0.88172793E 00     XINTER=     10.69623     AOLD=  0.35625406E 05
 LEAST SQUARES RESULT -     SLOPE= -0.99798769E 00     XINTER=     10.70853     AOLD=  0.39187926E 05
 LEAST SQUARES RESULT -     SLOPE= -0.12296276E 01     XINTER=     10.85149     AOLD=  0.43106695E 05
 LEAST SQUARES RESULT -     SLOPE= -0.19547405E 01     XINTER=     11.72476     AOLD=  0.47417340E 05
 LEAST SQUARES RESULT -     SLOPE= -0.12296276E 01     XINTER=     10.85149     AOLD=  0.43106691E 05
 LEAST SQUARES RESULT -     SLOPE= -0.12678680E 01     XINTER=     10.88490     AOLD=  0.43537727E 05
 LEAST SQUARES RESULT -     SLOPE= -0.12296276E 01     XINTER=     10.85149     AOLD=  0.43106688E 05
 LEAST SQUARES RESULT -     SLOPE= -0.12332535E 01     XINTER=     10.85446     AOLD=  0.43149770E 05
 LEAST SQUARES RESULT -     SLOPE= -0.12369900E 01     XINTER=     10.85776     AOLD=  0.43192895E 05
 LEAST SQUARES RESULT -     SLOPE= -0.12407265E 01     XINTER=     10.86095     AOLD=  0.43236063E 05
 LEAST SQUARES RESULT -     SLOPE= -0.12444620E 01     XINTER=     10.86402     AOLD=  0.43279273E 05
 LEAST SQUARES RESULT -     SLOPE= -0.12484179E 01     XINTER=     10.86754     AOLD=  0.43322527E 05
 LEAST SQUARES RESULT -     SLOPE= -0.12521544E 01     XINTER=     10.87094     AOLD=  0.43365824E 05
 LEAST SQUARES RESULT -     SLOPE= -0.12484179E 01     XINTER=     10.86754     AOLD=  0.43322523E 05
 LEAST SQUARES RESULT -     SLOPE= -0.12486382E 01     XINTER=     10.86765     AOLD=  0.43326816E 05
 LEAST SQUARES RESULT -     SLOPE= -0.12490778E 01     XINTER=     10.86809     AOLD=  0.43331113E 05
 LEAST SQUARES RESULT -     SLOPE= -0.12486382E 01     XINTER=     10.86765     AOLD=  0.43326813E 05
 LEAST SQUARES RESULT -     SLOPE= -0.12487478E 01     XINTER=     10.86798     AOLD=  0.43327223E 05
```

COMPUTED LINE - DATA Y(I)

I= 6	8.787	8.758	0.029
I= 7	8.371	8.489	-0.118
I= 8	7.955	7.803	0.151
I= 9	7.538	7.599	-0.061

PLOT OF CURRENT ACTIVE FUNCTION

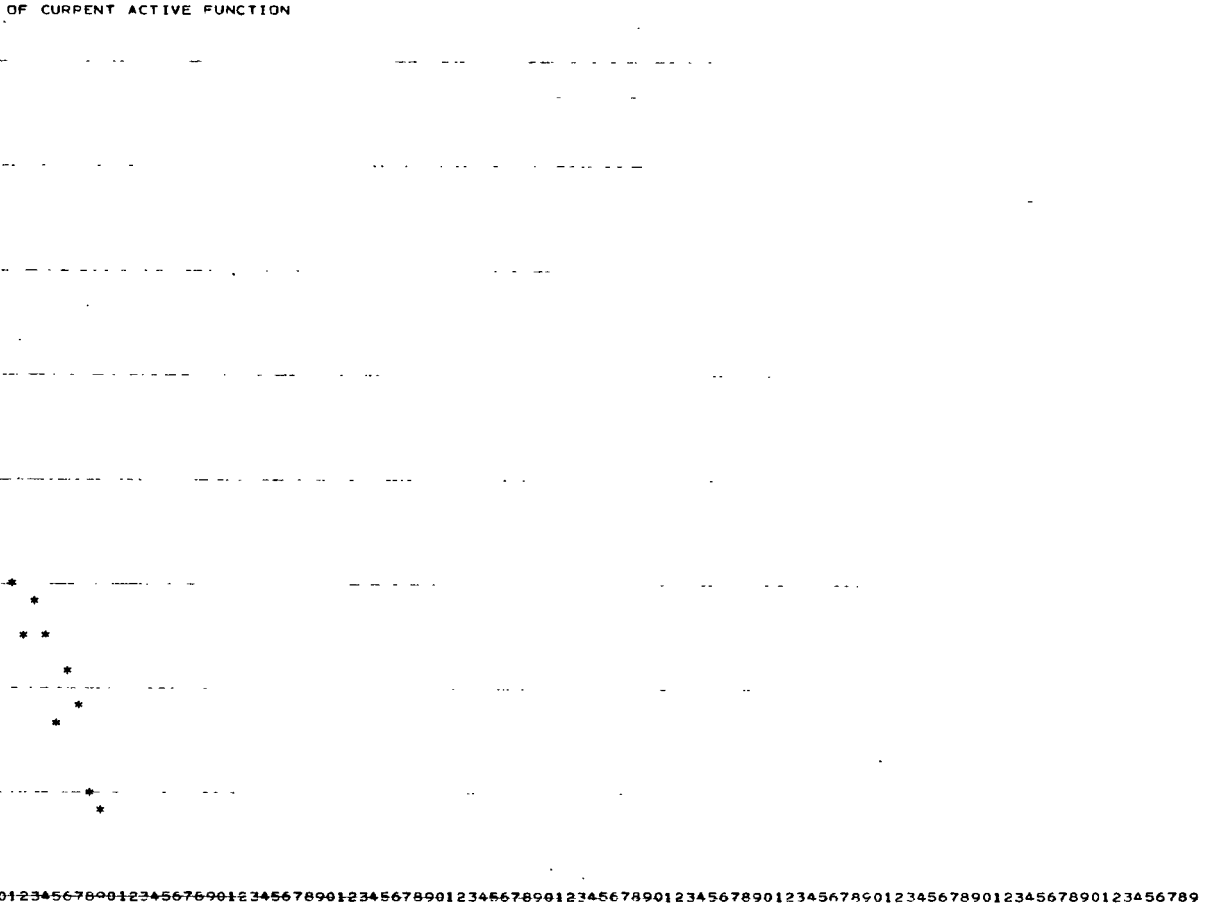

RESULT FOR GIVEN TAU = 1.24871635 COMPUTED COEFFICIENT (INTERCEPT EXP(10.86798)) = 52469.0156

FINAL CURVE Y = SUM OVER I OF A(I)*EXP(TAU(I)) WHERE

A(1) = 43910.88671875	TAU(1) = 0.02488690
A(2) = 25186.96484375	TAU(2) = 0.07062143
A(3) = 97997.43750000	TAU(3) = 0.22075051
A(4) = 32386.75000000	TAU(4) = 0.44247782
A(5) = 52469.01562500	TAU(5) = 1.24871635

INDEX	COMPUTED	ORIGINAL	DIFFERENCE
1	273951.00	237511.00	-36440.00
2	243746.94	220635.00	-23111.94
3	220743.13	210161.00	-10582.13
4	202750.19	197067.00	-5683.19
5	188297.75	183403.00	-4894.75
6	176392.31	176682.00	289.69
7	166357.81	166975.00	617.19
8	157730.06	157084.00	-646.06
9	150186.06	149799.00	-387.06
10	143498.00	141987.00	-1511.00
11	137502.75	134831.00	-2671.75
12	132080.75	129266.00	-2814.75
13	127142.63	124186.00	-2956.63
14	122619.88	118509.00	-4110.88
15	118459.06	117546.00	-913.06
16	114617.19	111598.00	-3019.19
17	111058.81	108074.00	-2984.81
18	107754.81	107049.00	-705.81
19	104680.00	102232.00	-2448.00
20	101812.91	98660.00	-3152.81
21	99134.63	97564.00	-1570.63
22	96628.69	94438.00	-2190.69
23	94280.31	91818.00	-2462.31
24	92076.50	91644.00	-432.50
25	90005.38	89205.00	-800.38
26	88056.31	87101.00	-955.31
27	86219.81	86440.00	220.19
28	84487.13	84245.00	-242.13
29	82850.25	82192.00	-658.25
30	81302.06	79611.00	-1691.06
31	79836.06	78060.00	-1776.06
32	78446.13	77282.00	-1164.13
33	77126.88	76976.00	-150.88
34	75873.06	75761.00	-112.06
35	74680.38	74809.00	128.63
36	73544.38	72681.00	-863.38
37	72461.19	72666.00	204.81
38	71427.31	70637.00	-790.31
39	70439.44	70373.00	-66.44
40	69494.38	67980.00	-1514.38
41	68589.44	69680.00	1090.56
42	67722.06	68574.00	851.94
43	66889.81	66305.00	-584.81
44	66090.44	65252.00	-838.44
45	65322.05	66040.00	717.95
46	64582.53	64424.00	-158.53
47	63870.21	63207.00	-663.21
48	63183.47	63417.00	233.53
49	62520.80	62578.00	57.20
50	61880.79	61773.00	-107.79
51	61262.13	60963.00	-299.13
52	60663.61	60339.00	-324.61
53	60084.12	60075.00	-9.12
54	59522.58	59593.00	70.42
55	58978.01	58881.00	-97.01
56	58449.55	57965.00	-484.55
57	57936.30	57497.00	-439.30
58	57437.49	57534.00	96.51
59	56952.38	56907.00	-45.38
60	56480.28	56128.00	-352.28
61	56020.54	55474.00	-546.54
62	55572.53	55551.00	-21.53
63	55135.74	54733.00	-402.74
64	54709.62	54369.00	-340.62
65	54293.68	53826.00	-467.68
66	53887.44	53831.00	-56.44
67	53490.49	52291.00	-1199.49
68	53102.39	51237.00	-1865.39
69	52722.79	52364.00	-358.79
70	52351.32	50959.00	-1392.32
71	51987.64	52174.00	186.36
72	51631.46	50801.00	-830.46
73	51282.43	50962.00	-320.43
74	50940.32	49875.00	-1065.32
75	50604.84	49144.00	-1460.84
76	50275.72	49780.00	-495.72
77	49952.77	49006.00	-946.77
78	49635.76	48626.00	-1009.76
79	49324.46	49066.00	-258.46
80	49018.69	48819.00	-199.69

INDEX	COMPUTED	ORIGINAL	DIFFERENCE
81	48714.35	48270.00	-444.35
82	48422.95	48308.00	-114.95
83	48132.66	47758.00	-374.66
84	47847.91	46900.00	-947.91
85	47566.43	48289.00	722.57
86	47290.20	46670.00	-620.20
87	47018.36	46933.00	-85.36
88	46750.80	45280.00	-1470.80
89	46487.38	46198.00	-289.38
90	46238.00	46178.00	-60.00
91	45972.55	45431.00	-541.55
92	45720.92	45368.00	-352.92
93	45473.00	44631.00	-842.00
94	45229.70	45339.00	110.30
95	44987.93	45989.00	1001.07
96	44750.59	42984.00	-1766.59
97	44516.62	44585.00	68.38
98	44285.92	43584.00	-701.92
99	44058.41	43885.00	-172.41
100	43834.02	42782.00	-1052.02
101	43612.69	44531.00	918.31
102	43394.34	43497.00	102.66
103	43178.90	42610.00	-568.90
104	42966.32	42892.00	-74.32
105	42756.54	42868.00	111.46
106	42549.49	41818.00	-731.49
107	42345.11	40764.00	-1581.11
108	42143.36	41844.00	-299.36
109	41944.17	41542.00	-402.17
110	41747.51	41358.00	-389.51
111	41553.32	40716.00	-837.32
112	41361.55	41594.00	232.45
113	41172.16	40364.00	-808.16
114	40985.11	40540.00	-445.11
115	40800.34	39897.00	-903.34
116	40617.82	39699.00	-918.82
117	40437.50	39679.00	-758.50
118	40259.36	39116.00	-1143.36
119	40083.35	40136.00	52.65
120	39909.43	40765.00	855.57
121	39737.56	40366.00	628.44
122	39567.73	39761.00	193.27
123	39399.87	39756.00	356.13
124	39233.98	38652.00	-581.98
125	39070.00	38677.00	-393.00
126	38907.92	38892.00	-15.92
127	38747.71	38020.00	-727.71
128	38549.31	38673.00	88.69
129	38432.72	36826.00	-1606.72
130	38277.90	38359.00	80.10
131	38124.84	37845.00	-279.84
132	37973.49	37867.00	-106.49
133	37823.83	37710.00	-113.83
134	37675.84	37710.00	34.16
135	37529.51	36951.00	-578.51
136	37384.77	38325.00	940.23
137	37241.63	37764.00	522.37
138	37100.07	36423.00	-677.07
139	36960.05	36951.00	-9.05
140	36821.55	37628.00	806.45
141	36684.56	37262.00	577.44
142	36549.06	37199.00	649.94
143	36415.00	37461.00	1046.00
144	36282.39	36606.00	323.61
145	36151.20	36460.00	308.80
146	36021.41	36479.00	457.59
147	35893.00	36999.00	1106.00
148	35765.93	35941.00	75.07
149	35640.23	35655.00	15.77
150	35515.84	36532.00	1016.16
151	35392.75	35618.00	225.25
152	35270.96	35860.00	589.04
153	35150.44	35499.00	348.56
154	35031.16	35845.00	813.84
155	34913.13	35787.00	873.87
156	34796.31	34873.00	76.69
157	34680.70	34694.00	13.30
158	34566.29	35132.00	565.71
159	34453.04	35876.00	1422.96
160	34340.95	35081.00	740.05

INDEX	COMPUTED	ORIGINAL	DIFFERENCE
161	34230.00	34830.00	600.00
162	34120.18	34273.00	152.82
163	34011.48	34569.00	557.52
164	33903.87	34637.00	733.13
165	33797.36	34297.00	499.64
166	33691.91	34511.00	819.09
167	33587.52	34061.00	473.48
168	33484.19	34023.00	538.82

CHI-SQUARE= 33484.18359 ABSOLUTE DIFFERENCE= 0.01443

Appendix C

Analysis of the P-15 Phosphor Data

N= 256 FIRST= 63 LAST=170 BACKGROUND= 33126.000 CHANNEL WIDTH= 0.33330

1)	105055.	2)	92276.	3)	82525.	4)	73094.	5)	66347.	6)	61320.	7)	57050.	8)	55079.
9)	53618.	10)	52800.	11)	51370.	12)	50179.	13)	49435.	14)	48427.	15)	47701.	16)	47464.
17)	47331.	18)	46800.	19)	47377.	20)	46818.	21)	46775.	22)	45931.	23)	46173.	24)	46024.
25)	45675.	26)	44864.	27)	44857.	28)	45002.	29)	45437.	30)	45016.	31)	45040.	32)	44580.
33)	44526.	34)	44084.	35)	44330.	36)	43917.	37)	43671.	38)	43739.	39)	43912.	40)	43396.
41)	43672.	42)	43098.	43)	43074.	44)	43184.	45)	43607.	46)	43050.	47)	42996.	48)	42471.
49)	42796.	50)	42287.	51)	42473.	52)	42551.	53)	41749.	54)	41988.	55)	42730.	56)	42639.
57)	42455.	58)	41957.	59)	42123.	60)	41914.	61)	41574.	62)	41175.	63)	42149.	64)	41670.
65)	41497.	66)	41944.	67)	41250.	68)	40903.	69)	41356.	70)	41651.	71)	41479.	72)	41419.
73)	41665.	74)	41196.	75)	41344.	76)	41699.	77)	41981.	78)	40905.	79)	40455.	80)	41097.
81)	40744.	82)	40449.	83)	41719.	84)	41120.	85)	41055.	86)	40747.	87)	41164.	88)	41085.
89)	41328.	90)	41036.	91)	41652.	92)	41470.	93)	41078.	94)	40935.	95)	41060.	96)	40734.
97)	40293.	98)	40213.	99)	40134.	100)	40480.	101)	40190.	102)	40237.	103)	39836.	104)	40558.
105)	40429.	106)	40365.	107)	40462.	108)	40542.								

PLOT OF CURRENT ACTIVE FUNCTION

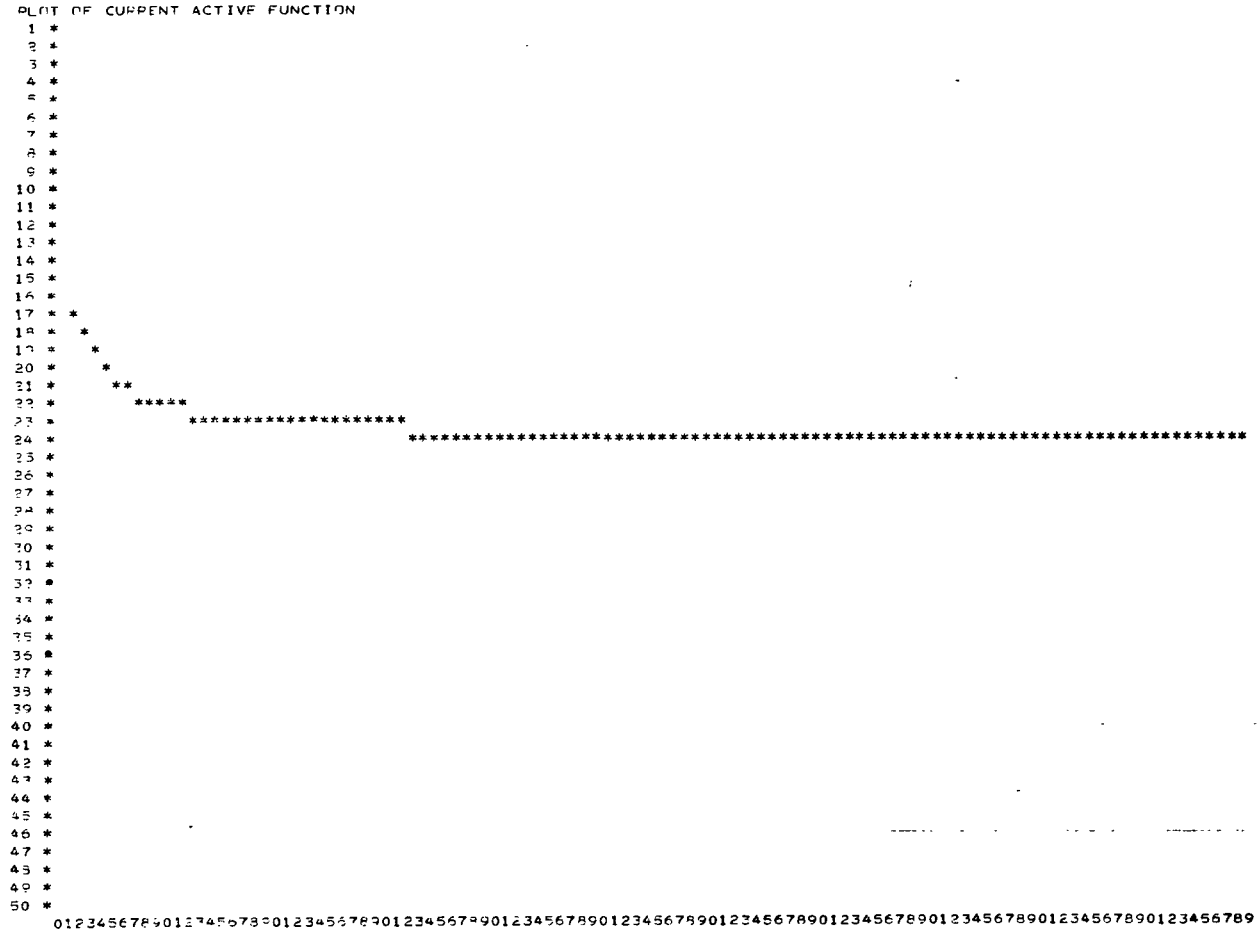

INPUT TAU= 0.01140230 START= 60 END=108

1)	71969.	2)	59150.	3)	49399.	4)	39968.	5)	33221.	6)	28194.	7)	24824.	8)	21953.
9)	20492.	10)	19674.	11)	18244.	12)	17053.	13)	16309.	14)	15301.	15)	14575.	16)	14338.
17)	14205.	18)	13574.	19)	14251.	20)	13632.	21)	13649.	22)	12705.	23)	13047.	24)	12898.
25)	12549.	26)	11736.	27)	11731.	28)	11870.	29)	12311.	30)	11890.	31)	11914.	32)	11454.
33)	11400.	34)	10958.	35)	11204.	36)	10791.	37)	10545.	38)	10613.	39)	10786.	40)	10270.
41)	10546.	42)	9972.	43)	9948.	44)	10058.	45)	10481.	46)	9924.	47)	9870.	48)	9345.
49)	9670.	50)	9131.	51)	9347.	52)	9425.	53)	8623.	54)	8862.	55)	9604.	56)	9513.
57)	9329.	58)	8831.	59)	8997.	60)	8796.	61)	8448.	62)	8049.	63)	9023.	64)	8544.
65)	8371.	66)	8818.	67)	8124.	68)	7776.	69)	8233.	70)	8525.	71)	8353.	72)	8293.
73)	8539.	74)	8070.	75)	8218.	76)	8573.	77)	8855.	78)	7779.	79)	7329.	80)	7971.
81)	7516.	82)	7323.	83)	8586.	84)	7494.	85)	7329.	86)	7621.	87)	8038.	88)	7959.
89)	8102.	90)	7910.	91)	8726.	92)	8344.	93)	7952.	94)	7809.	95)	7934.	96)	7608.
97)	7157.	98)	7087.	99)	7008.	100)	7294.	101)	7064.	102)	7111.	103)	6710.	104)	7432.
105)	7303.	106)	7239.	107)	7336.	108)	7416.								

PLOT OF CURRENT ACTIVE FUNCTION

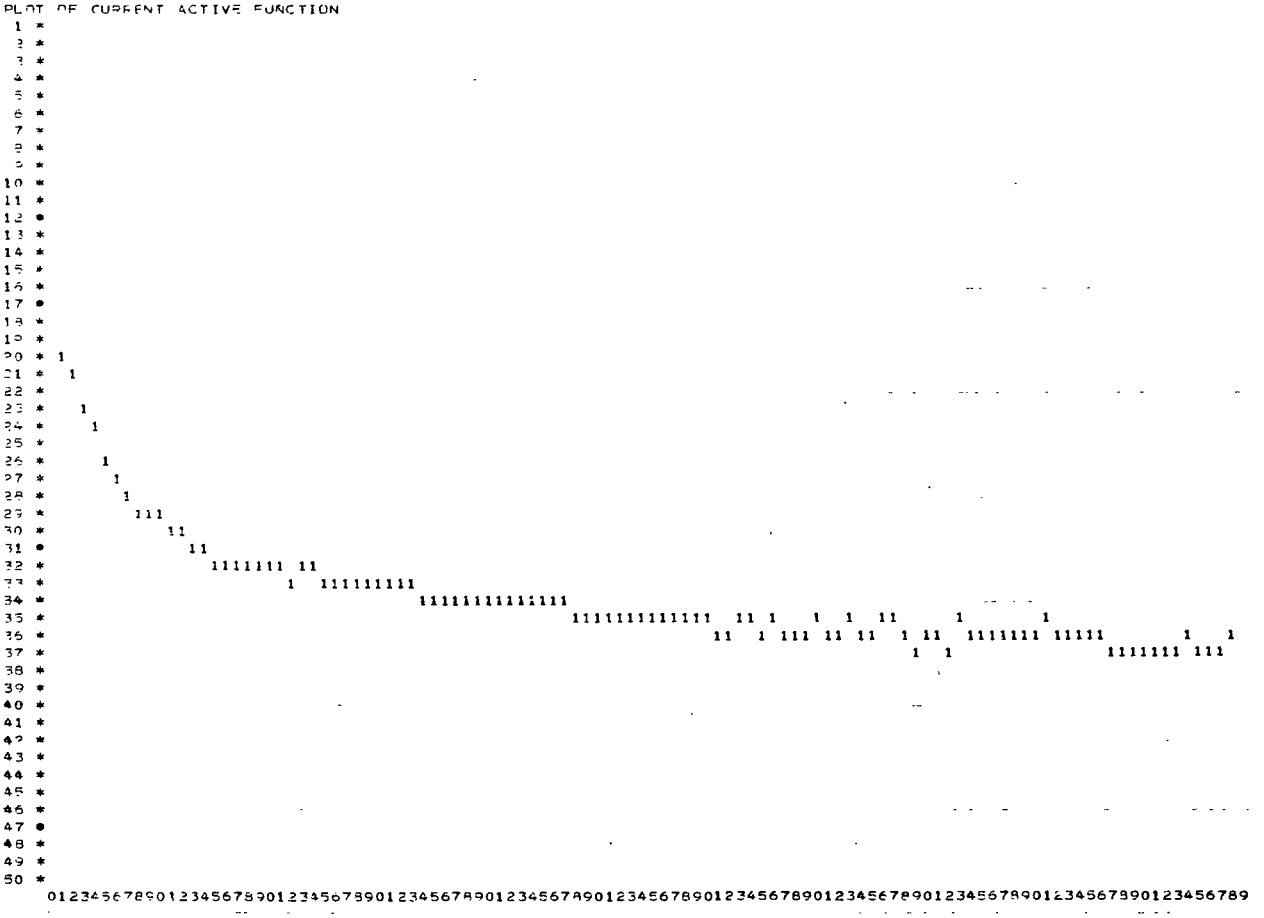

```
 LEAST SQUARES RESULT -    SLOPE= -0.11402823E-01    XINTER=    9.29044    AOLD=  0.33126000E 05
 LEAST SQUARES RESULT -    SLOPE= -0.79786964E-02    XINTER=    9.54638    AOLD=  0.29813398E 05
 LEAST SQUARES RESULT -    SLOPE= -0.11402823E-01    XINTER=    9.29044    AOLD=  0.33125996E 05
 LEAST SQUARES RESULT -    SLOPE= -0.10933075E-01    XINTER=    9.31858    AOLD=  0.32794734E 05
 LEAST SQUARES RESULT -    SLOPE= -0.11402823E-01    XINTER=    9.29044    AOLD=  0.33125992E 05
 LEAST SQUARES RESULT -    SLOPE= -0.11352453E-01    XINTER=    9.29318    AOLD=  0.33092863E 05
 LEAST SQUARES RESULT -    SLOPE= -0.11402823E-01    XINTER=    9.29044    AOLD=  0.33125988E 05
 LEAST SQUARES RESULT -    SLOPE= -0.11398140E-01    XINTER=    9.29074    AOLD=  0.33122676E 05
 LEAST SQUARES RESULT -    SLOPE= -0.11402823E-01    XINTER=    9.29044    AOLD=  0.33125984E 05
 LEAST SQUARES RESULT -    SLOPE= -0.11402823E-01    XINTER=    9.29054    AOLD=  0.33125652E 05
 LEAST SQUARES RESULT -    SLOPE= -0.11385255E-01    XINTER=    9.29005    AOLD=  0.33125320E 05

                    COMPUTED LINE - DATA Y(I)

 I=  60      9.066       9.081      -0.015
 I=  61      9.062       9.042       0.021
 I=  62      9.059       8.993       0.065
 I=  63      9.055       9.108      -0.053
 I=  64      9.051       9.053      -0.002
 I=  65      9.047       9.033       0.015
 I=  66      9.043       9.085      -0.041
 I=  67      9.040       9.003       0.037
 I=  68      9.036       8.959       0.077
 I=  69      9.032       9.016       0.016
 I=  70      9.028       9.051      -0.023
 I=  71      9.024       9.030      -0.006
 I=  72      9.021       9.023      -0.003
 I=  73      9.017       9.052      -0.036
 I=  74      9.013       8.996       0.017
 I=  75      9.009       9.014      -0.005
 I=  76      9.005       9.056      -0.051
 I=  77      9.002       9.089      -0.087
 I=  78      8.998       8.959       0.039
 I=  79      8.994       8.900       0.094
 I=  80      8.990       8.984       0.007
 I=  81      8.986       8.938       0.048
 I=  82      8.983       8.899       0.084
 I=  83      8.979       9.058      -0.079
 I=  84      8.975       8.987      -0.011
 I=  85      8.971       8.978      -0.007
 I=  86      8.967       8.939       0.029
 I=  87      8.964       8.992      -0.028
 I=  88      8.960       8.982      -0.022
 I=  89      8.956       9.000      -0.044
 I=  90      8.952       8.976      -0.024
 I=  91      8.949       9.074      -0.126
 I=  92      8.945       9.029      -0.085
 I=  93      8.941       8.981      -0.040
 I=  94      8.937       8.963      -0.026
 I=  95      8.933       8.979      -0.046
 I=  96      8.930       8.937      -0.007
 I=  97      8.926       8.876       0.050
 I=  98      8.922       8.866       0.056
 I=  99      8.918       8.855       0.063
 I= 100      8.914       8.895       0.019
 I= 101      8.911       8.863       0.048
 I= 102      8.907       8.869       0.037
 I= 103      8.903       8.811       0.092
 I= 104      8.899       8.914      -0.014
 I= 105      8.895       8.896      -0.001
 I= 106      8.892       8.887       0.004
 I= 107      8.888       8.901      -0.013
 I= 108      8.884       8.911      -0.027
```

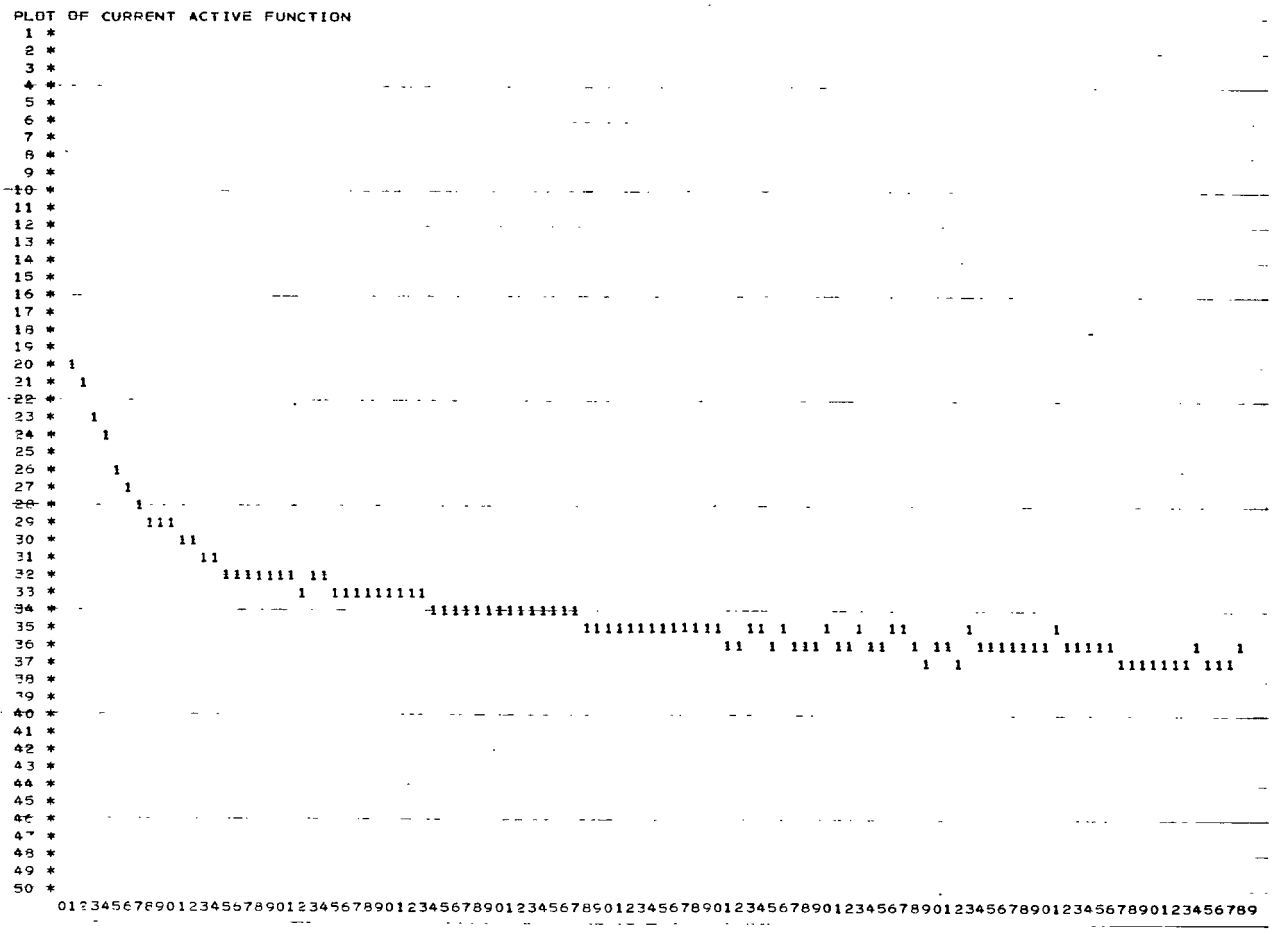

RESULT FOR GIVEN TAU = 0.01140280 COMPUTED COEFFICIENT (INTERCEPT EXP(9.29005)) = 10829.7109

```
 INPUT TAU=      0.15331995     START= 20     END= 35

  1)  61140.    2)  48362.    3)  38652.    4)  29262.    5)  22555.    6)  17569.    7)  14239.    8)  11408.
  9)   9987.   10)   9209.   11)   7819.   12)   6667.   13)   5963.   14)   4994.   15)   4307.   16)   4109.
 17)   4015.   18)   3523.   19)   4138.   20)   3617.   21)   3613.   22)   2707.   23)   3087.   24)   2975.
 25)   2664.   26)   1891.   27)   1921.   28)   2103.   29)   2575.   30)   2191.   31)   2252.   32)   1829.
 33)   1811.   34)   1405.   35)   1688.   36)   1311.   37)   1101.   38)   1205.   39)   1413.   40)    933.
 41)   1244.   42)    706.   43)    717.   44)    862.   45)   1320.   46)    797.   47)    778.   48)    288.
 49)    647.   50)    142.   51)    392.   52)    504.
```

PLOT OF CURRENT ACTIVE FUNCTION

```
  1 *
  2 *
  3 *
  4 *
  5 *
  6 *
  7 *
  8 *
  9 *
 10 *
 11 *
 12 *
 13 *
 14 *
 15 *
 16 *
 17 *
 18 *
 19 *
 20 *
 21 * 2
 22 *
 23 *  2
 24 *
 25 *   2
 26 *
 27 *    2
 28 *     2
 29 *
 30 *      2
 31 *
 32 *       2
 33 *        2
 34 *         2
 35 *          2
 36 *           2
 37 *            2
 38 *             2
 39 *              2
 40 *               2
 41 *                22 2
 42 *                  2 22
 43 *                     22
 44 *                    2  2   2
 45 *                        22
 46 *                   222
 47 *                       22 2
 48 *                          2
 49 *                        2 2   2   2
 50 *                           22
    01234567890123456789012345678901234567890123456789012345678901234567890123456789012345678901234567890123456789
```

LEAST SQUARES RESULT -	SLOPE= -0.15332007E 00	XINTER=	9.09941	AOLD=	0.10829711E 05
LEAST SQUARES RESULT -	SLOPE= -0.11140269E 00	XINTER=	9.08917	AOLD=	0.97467383E 04
LEAST SQUARES RESULT -	SLOPE= -0.15330714E 00	XINTER=	9.09930	AOLD=	0.10829707E 05
LEAST SQUARES RESULT -	SLOPE= -0.15967393E 00	XINTER=	9.11026	AOLD=	0.10939098E 05
LEAST SQUARES RESULT -	SLOPE= -0.15900815E 00	XINTER=	9.10902	AOLD=	0.10928156E 05
LEAST SQUARES RESULT -	SLOPE= -0.15836829E 00	XINTER=	9.10799	AOLD=	0.10917227E 05
LEAST SQUARES RESULT -	SLOPE= -0.15771544E 00	XINTER=	9.10685	AOLD=	0.10906309E 05
LEAST SQUARES RESULT -	SLOPE= -0.15706903E 00	XINTER=	9.10561	AOLD=	0.10895402E 05
LEAST SQUARES RESULT -	SLOPE= -0.15641624E 00	XINTER=	9.10437	AOLD=	0.10884504E 05
LEAST SQUARES RESULT -	SLOPE= -0.15580863E 00	XINTER=	9.10344	AOLD=	0.10873617E 05
LEAST SQUARES RESULT -	SLOPE= -0.15518165E 00	XINTER=	9.10240	AOLD=	0.10862742E 05
LEAST SQUARES RESULT -	SLOPE= -0.15454817E 00	XINTER=	9.10127	AOLD=	0.10851879E 05
LEAST SQUARES RESULT -	SLOPE= -0.15393412E 00	XINTER=	9.10023	AOLD=	0.10841023E 05
LEAST SQUARES RESULT -	SLOPE= -0.15333301E 00	XINTER=	9.09930	AOLD=	0.10830180E 05
LEAST SQUARES RESULT -	SLOPE= -0.15273833E 00	XINTER=	9.09847	AOLD=	0.10819348E 05
LEAST SQUARES RESULT -	SLOPE= -0.15333301E 00	XINTER=	9.09941	AOLD=	0.10830176E 05
LEAST SQUARES RESULT -	SLOPE= -0.15327483E 00	XINTER=	9.09920	AOLD=	0.10829090E 05
LEAST SQUARES RESULT -	SLOPE= -0.15333301E 00	XINTER=	9.09930	AOLD=	0.10830172E 05
LEAST SQUARES RESULT -	SLOPE= -0.15333301E 00	XINTER=	9.09941	AOLD=	0.10830063E 05
LEAST SQUARES RESULT -	SLOPE= -0.15332007E 00	XINTER=	9.09930	AOLD=	0.10829953E 05
LEAST SQUARES RESULT -	SLOPE= -0.15332007E 00	XINTER=	9.09930	AOLD=	0.10829844E 05
LEAST SQUARES RESULT -	SLOPE= -0.15330714E 00	XINTER=	9.09930	AOLD=	0.10829734E 05

COMPUTED LINE - DATA Y(I)

I= 20	8.128	8.194	-0.065
I= 21	8.077	8.192	-0.115
I= 22	8.026	7.903	0.123
I= 23	7.975	8.035	-0.060
I= 24	7.924	7.998	-0.074
I= 25	7.873	7.888	-0.015
I= 26	7.822	7.545	0.277
I= 27	7.771	7.561	0.210
I= 28	7.720	7.651	0.068
I= 29	7.669	7.854	-0.185
I= 30	7.617	7.692	-0.075
I= 31	7.566	7.720	-0.153
I= 32	7.515	7.511	0.004
I= 33	7.464	7.502	-0.037
I= 34	7.413	7.248	0.165
I= 35	7.362	7.431	-0.069

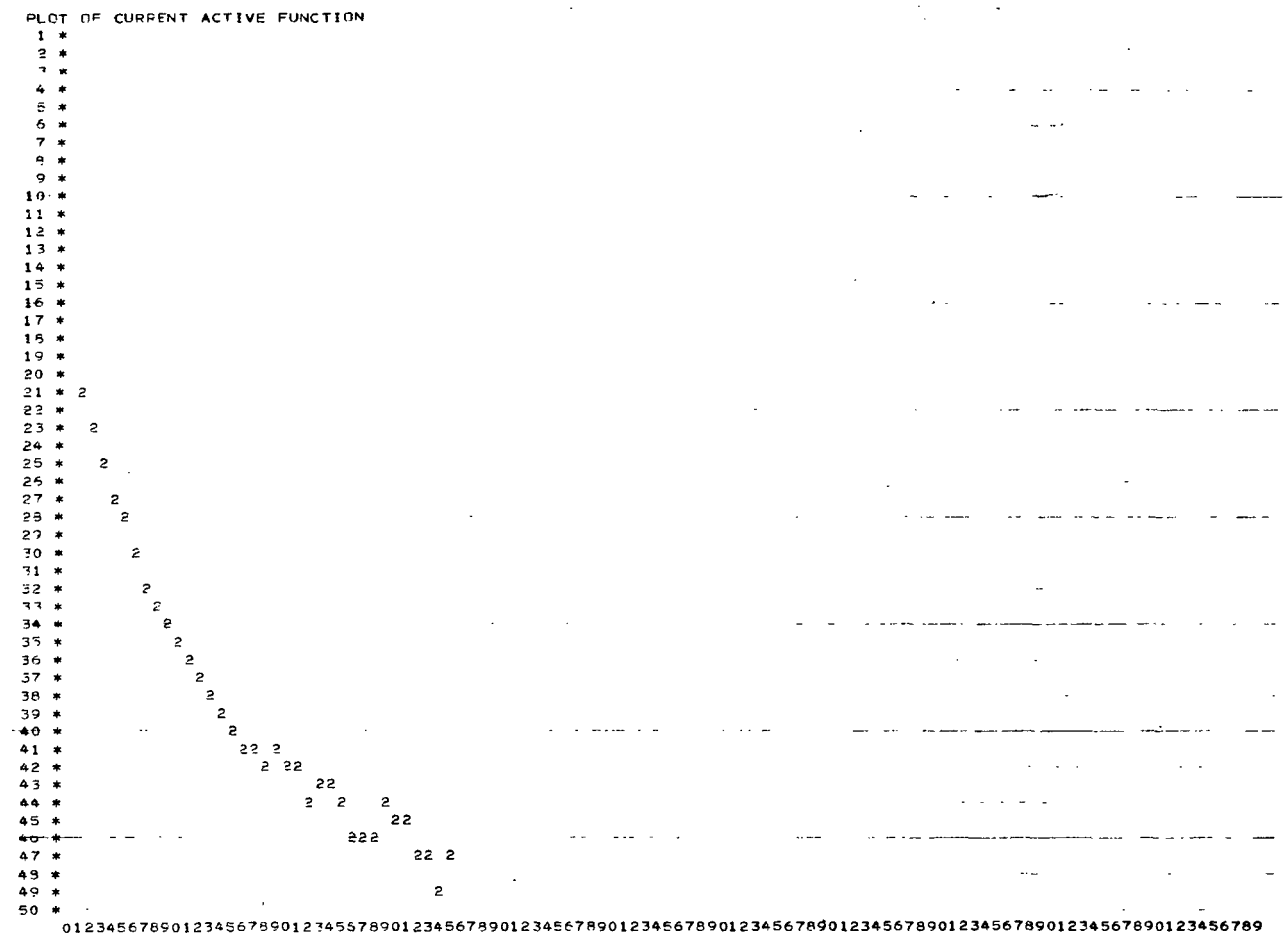

RESULT FOR GIVEN TAU = 0.15331995 COMPUTED COEFFICIENT (INTERCEPT EXP(9.09930)) = 8949.0469

```
 INPUT TAU=      0.96442997      START=  3      END= 13

 1)  52191.     2)  39859.     3)  30572.     4)  21585.     5)  15261.     6)  10638.     7)   7653.     8)   5150.
 9)   4041.    10)   3559.    11)   2450.    12)   1566.    13)   1116.    14)    389.


PLOT OF CURRENT ACTIVE FUNCTION
 1 *
 2 *                                 .
 3 *
 4 *
 5 *
 6 *                                    --  --
 7 *
 8 *
 9 *
10 *
11 *
12 *
13 *
14 *
15 *
16 *
17 *
18 *
19 *
20 *
21 *
22 *  3
23 *
24 *    3
25 *
26 *      3
27 *
28 *
29 *        3
30 *                                    .
31 *          3
32 *
33 *
34 *  --  --  -3   -  -  --  -  -  -  -  -----  -  -                                                  -  -  -
35 *
36 *           3                        .
37 *
38 *
39 *            3
40 *  -  -  -  --  --  ---  -  -  -----  --  ---  -  --                  -                  -  -  -  -  -  -
41 *             3
42 *              3
43 *
44 *
45 *                3
46 *  -  -  -  -  ---  ---  --  --  --  ---  ---  ---  -  -  -  --  --                  -                  -  -  ---  ---  --  --
47 *
48 *                  3
49 *
50 *                    3
    0123456789012345678901234567890123456789012345678901234567890123456789012345678901234567890123456789012345678901234567890123456789
    -  -  -  -  -  -  -  -  -  -  -  -  -  -  -  -  -  -  -  -  -  -  -  -  -  -  -  -  -  -  -  -  -  -  -  -  -  -  -  -  -  -  -  -


 LEAST SQUARES RESULT -      SLOPE= -0.96442831E 00      XINTER=       10.91938      AOLD=   0.89490469E 04
 LEAST SQUARES RESULT -      SLOPE= -0.11013708E 01      XINTER=       11.06233      AOLD=   0.98439453E 04
 LEAST SQUARES RESULT -      SLOPE= -0.96442288E 00      XINTER=       10.91938      AOLD=   0.89490430E 04
 LEAST SQUARES RESULT -      SLOPE= -0.97544681E 00      XINTER=       10.92973      AOLD=   0.90385234E 04
 LEAST SQUARES RESULT -      SLOPE= -0.96442467E 00      XINTER=       10.91938      AOLD=   0.89490391E 04
 LEAST SQUARES RESULT -      SLOPE= -0.96550173E 00      XINTER=       10.92034      AOLD=   0.89579805E 04
 LEAST SQUARES RESULT -      SLOPE= -0.96442288E 00      XINTER=       10.91938      AOLD=   0.89490352E 04
 LEAST SQUARES RESULT -      SLOPE= -0.96453184E 00      XINTER=       10.91947      AOLD=   0.89499219E 04
 LEAST SQUARES RESULT -      SLOPE= -0.96442288E 00      XINTER=       10.91938      AOLD=   0.89490313E 04
 LEAST SQUARES RESULT -      SLOPE= -0.96443194E 00      XINTER=       10.91938      AOLD=   0.89491133E 04
```

COMPUTED LINE - DATA Y(I)

I=	3	10.276	10.328	-0.051
I=	4	9.955	9.980	-0.025
I=	5	9.634	9.633	0.001
I=	6	9.312	9.272	0.040
I=	7	8.991	8.943	0.048
I=	8	8.669	8.547	0.122
I=	9	8.348	8.304	0.044
I=	10	8.026	8.177	-0.151
I=	11	7.705	7.804	-0.099
I=	12	7.383	7.357	0.027
I=	13	7.062	7.017	0.045

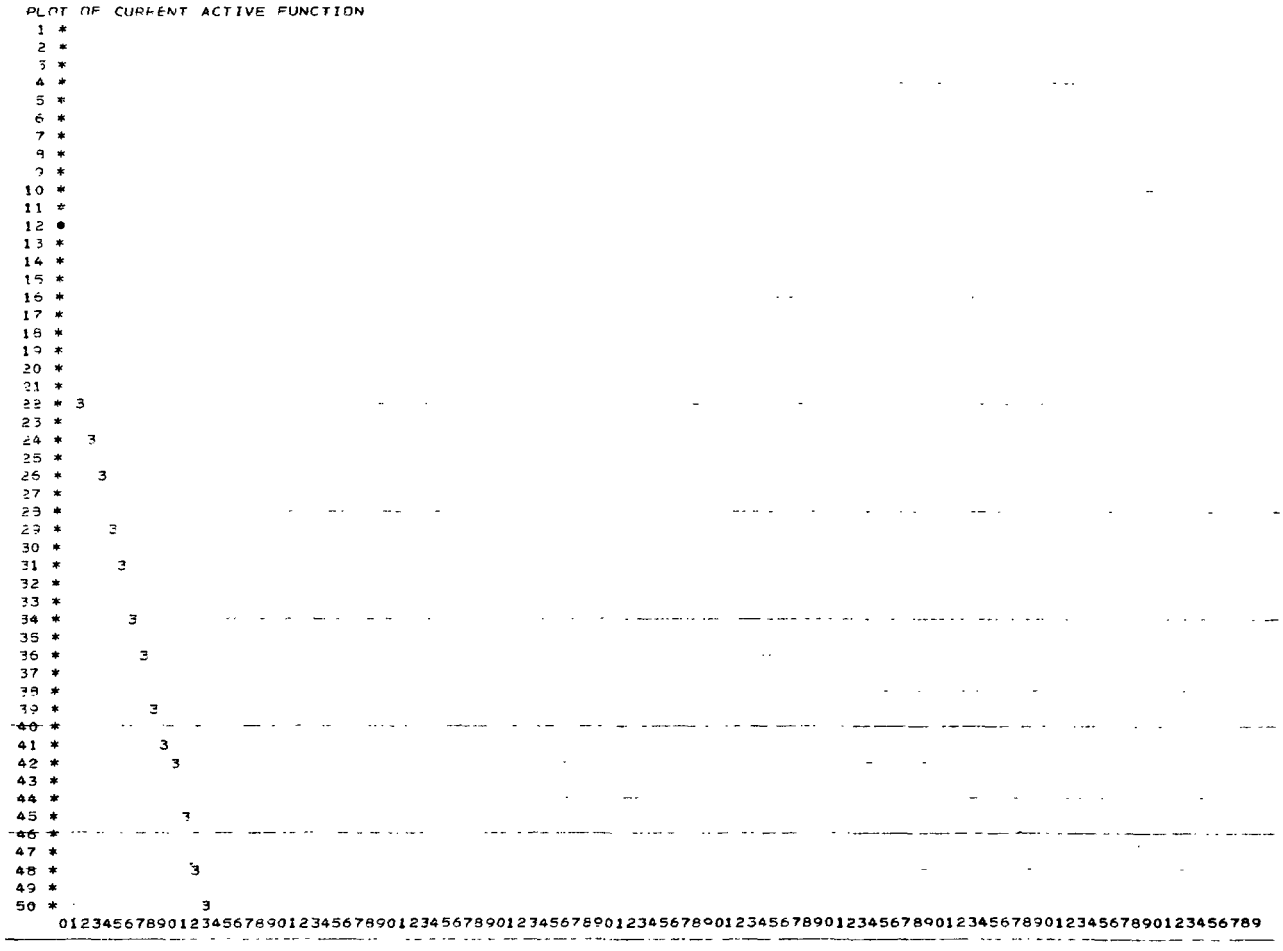

RESULT FOR GIVEN TAU = 0.96442997 COMPUTED COEFFICIENT (INTERCEPT EXP(-10.91938)) = 55236.7617

FINAL CURVE Y = SUM OVER I OF A(I)*EXP(TAU(I)) WHERE

A(1) = 10629.71093750 TAU(1) = 0.01140280

A(2) = 8949.04687500 TAU(2) = 0.15331995

A(3) = 55236.76171875 TAU(3) = 0.96442997

INDEX	COMPUTED	ORIGINAL	DIFFERENCE
1	108141.50	105095.00	[illegible]
2	92470.06	92276.00	-194.06
3	80995.19	82525.00	[illegible]
4	72568.31	73094.00	525.69
5	66356.38	66347.00	-9.38
6	61754.96	61320.00	-434.96
7	58325.71	57950.00	-375.71
8	55750.51	55079.00	-671.51
9	53798.49	53618.00	-180.49
10	52302.07	52800.00	497.93
11	51139.53	51370.00	230.47
12	50222.46	50179.00	-43.46
13	49436.57	49435.00	-51.57
14	48845.10	48427.00	-456.10
15	48393.99	47701.00	-692.99
16	47958.39	47464.00	-494.39
17	47590.16	47331.00	-259.16
18	47266.01	46800.00	-466.01
19	46976.19	47377.00	400.81
20	46713.50	46818.00	104.50
21	46472.64	46775.00	302.36
22	46249.62	45831.00	-418.62
23	46041.47	46173.00	131.53
24	45845.95	46024.00	178.05
25	45661.33	45675.00	13.67
26	45486.28	44864.00	-622.28
27	45319.75	44857.00	-462.75
28	45160.90	45002.00	-158.90
29	45009.05	45437.00	427.95
30	44863.65	45016.00	152.35
31	44724.21	45040.00	315.79
32	44590.32	44580.00	-10.32
33	44461.65	44526.00	64.35
34	44337.86	44084.00	-253.86
35	44218.68	44330.00	111.32
36	44103.86	43917.00	-186.86
37	43993.16	43671.00	-322.16
38	43886.36	43739.00	-147.36
39	43783.27	43912.00	128.73
40	43683.68	43396.00	-287.68
41	43587.44	43672.00	84.56
42	43494.38	43098.00	-396.38
43	43404.34	43074.00	-330.34
44	43317.18	43184.00	-133.18
45	43232.75	43607.00	374.25
46	43150.92	43050.00	-100.92
47	43071.57	42996.00	-75.57
48	42994.59	42471.00	-523.59
49	42919.85	42796.00	-123.85
50	42847.26	42257.00	-590.26
51	42776.70	42473.00	-303.70
52	42708.09	42551.00	-157.09
53	42641.34	41749.00	-892.34
54	42576.36	41988.00	-588.36
55	42513.06	42730.00	216.94
56	42451.37	42639.00	187.63
57	42391.21	42455.00	63.79
58	42332.52	41957.00	-375.52
59	42275.22	42123.00	-152.22
60	42219.26	41914.00	-305.26
61	42164.56	41574.00	-590.56
62	42111.08	41175.00	-936.08
63	42058.75	42149.00	90.25
64	42007.54	41670.00	-337.54
65	41957.38	41497.00	-460.38
66	41908.24	41944.00	35.76
67	41860.06	41250.00	-610.06

INDEX	COMPUTED	ORIGINAL	DIFFERENCE
68	41812.80	40902.00	-910.80
69	41766.43	41359.00	-407.43
70	41720.90	41651.00	-69.90
71	41676.18	41479.00	-197.18
72	41632.23	41419.00	-213.23
73	41589.02	41665.00	75.98
74	41546.52	41196.00	-350.52
75	41504.70	41344.00	-160.70
76	41463.53	41699.00	235.47
77	41422.98	41981.00	558.02
78	41383.04	40905.00	-478.04
79	41343.66	40455.00	-888.66
80	41304.84	41097.00	-207.84
81	41266.54	40744.00	-522.54
82	41228.76	40449.00	-779.76
83	41191.46	41712.00	520.54
84	41154.63	41120.00	-34.63
85	41118.25	41055.00	-63.25
86	41082.30	40747.00	-335.30
87	41046.77	41164.00	117.23
88	41011.64	41085.00	73.36
89	40976.89	41228.00	251.11
90	40942.52	41036.00	93.48
91	40908.51	41852.00	943.49
92	40874.84	41470.00	595.16
93	40841.52	41078.00	236.48
94	40808.51	40935.00	126.49
95	40775.81	41060.00	284.19
96	40743.41	40734.00	-9.41
97	40711.31	40283.00	-428.31
98	40679.49	40213.00	-466.49
99	40647.94	40134.00	-513.94
100	40616.65	40420.00	-196.65
101	40585.62	40190.00	-395.62
102	40554.84	40237.00	-317.84
103	40524.29	39836.00	-688.29
104	40493.99	40558.00	64.01
105	40463.91	40429.00	-34.91
106	40434.04	40365.00	-69.04
107	40404.39	40462.00	57.61
108	40374.96	40542.00	167.04

CHI-SQUARE= 40374.95703 ABSOLUTE DIFFERENCE= 0.00743

Appendix D

Time-Shifted Analysis of the P-15 Phosphor Data

N= 256 FIRST= 58 LAST=170 BACKGROUND= 33126.000 CHANNEL WIDTH= 0.33330

1)	154053.	2)	151572.	3)	142786.	4)	133039.	5)	119177.	6)	105095.	7)	92276.	8)	82525.
9)	73094.	10)	66347.	11)	61320.	12)	57950.	13)	56079.	14)	53618.	15)	52800.	16)	51370.
17)	50179.	18)	49435.	19)	48427.	20)	47701.	21)	47464.	22)	47331.	23)	46800.	24)	47377.
25)	46818.	26)	46775.	27)	45831.	28)	46173.	29)	46024.	30)	45675.	31)	44864.	32)	44857.
33)	45002.	34)	45437.	35)	45016.	36)	45040.	37)	44580.	38)	44526.	39)	44084.	40)	44330.
41)	43917.	42)	43671.	43)	43739.	44)	43912.	45)	43396.	46)	43672.	47)	43098.	48)	43074.
49)	43184.	50)	43607.	51)	43050.	52)	42996.	53)	42471.	54)	42796.	55)	42257.	56)	42473.
57)	42551.	58)	41749.	59)	41988.	60)	42730.	61)	42639.	62)	42455.	63)	41957.	64)	42123.
65)	41914.	66)	41574.	67)	41175.	68)	42149.	69)	41670.	70)	41497.	71)	41944.	72)	41250.
73)	40902.	74)	41359.	75)	41651.	76)	41479.	77)	41419.	78)	41665.	79)	41196.	80)	41344.
81)	41699.	82)	41981.	83)	40905.	84)	40455.	85)	41097.	86)	40744.	87)	40449.	88)	41712.
89)	41120.	90)	41055.	91)	40747.	92)	41164.	93)	41085.	94)	41228.	95)	41036.	96)	41852.
97)	41470.	98)	41078.	99)	40935.	100)	41060.	101)	40734.	102)	40283.	103)	40213.	104)	40134.
105)	40420.	106)	40190.	107)	40237.	108)	39836.	109)	40558.	110)	40429.	111)	40366.	112)	40462.
113)	40542.														

PLOT OF CURRENT ACTIVE FUNCTION

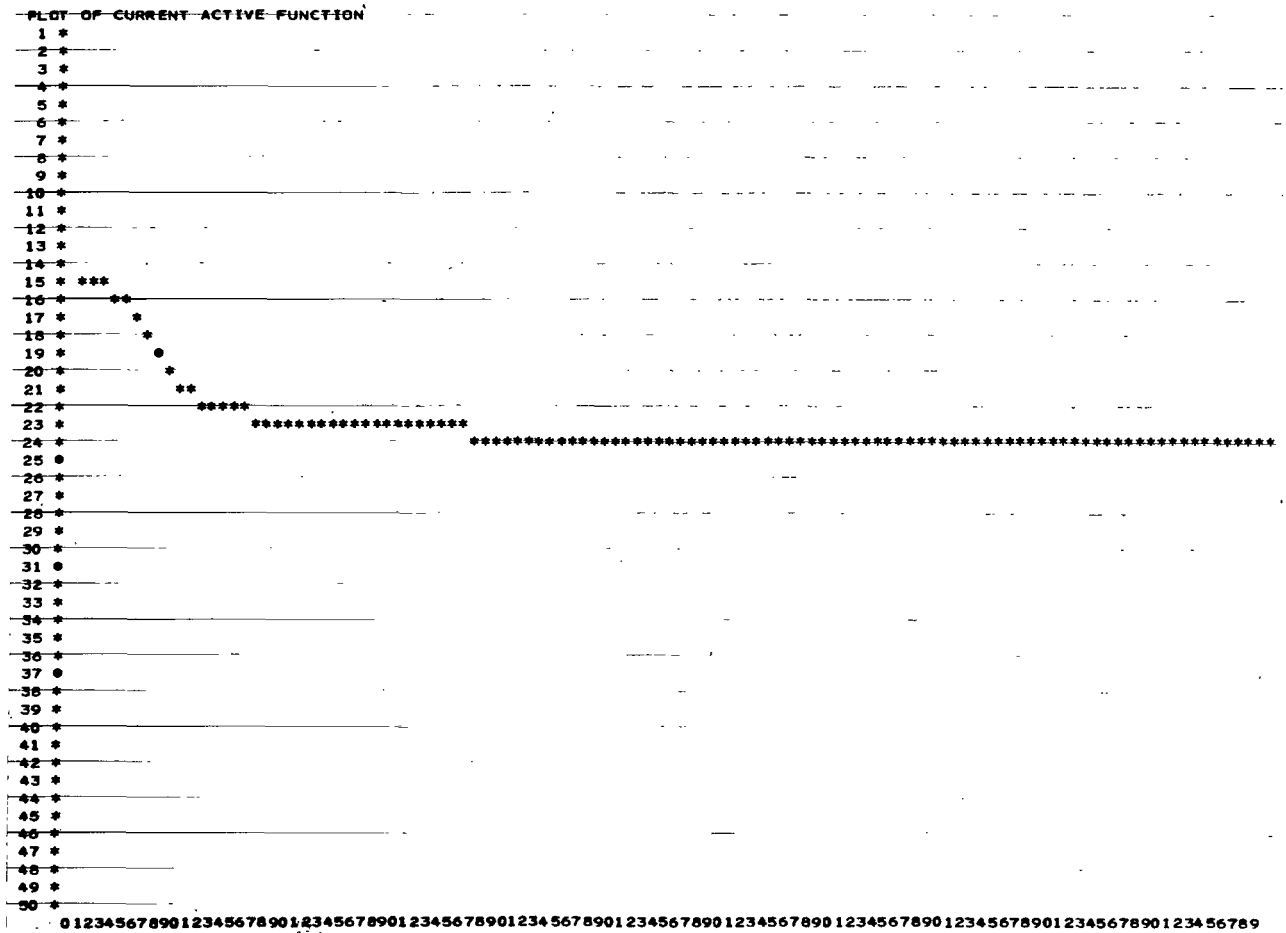

```
INPUT TAU=     0.01140260      START= 65      END=113

  1) 120927.    2) 118446.    3) 109660.    4)  99913.    5)  86051.    6)  71969.    7)  59150.    8)  49399.
  9)  39968.   10)  33221.   11)  28194.   12)  24824.   13)  21963.   14)  20492.   15)  19674.   16)  18244.
 17)  17053.   18)  16309.   19)  15301.   20)  14575.   21)  14338.   22)  14205.   23)  13674.   24)  14251.
 25)  13692.   26)  13649.   27)  12706.   28)  13047.   29)  12898.   30)  12649.   31)  11738.   32)  11731.
 33)  11876.   34)  12311.   35)  11890.   36)  11914.   37)  11454.   38)  11400.   39)  10958.   40)  11204.
 41)  10791.   42)  10545.   43)  10613.   44)  10786.   45)  10270.   46)  10546.   47)   9972.   48)   9948.
 49)  10058.   50)  10481.   51)   9924.   52)   9870.   53)   9345.   54)   9670.   55)   9131.   56)   9347.
 57)   9425.   58)   8623.   59)   8862.   60)   9604.   61)   9513.   62)   9329.   63)   8831.   64)   8997.
 65)   8788.   66)   8448.   67)   8049.   68)   9023.   69)   8544.   70)   8371.   71)   8818.   72)   8124.
 73)   7776.   74)   8233.   75)   8525.   76)   8363.   77)   8293.   78)   8539.   79)   8070.   80)   8218.
 81)   8573.   82)   8855.   83)   7779.   84)   7329.   85)   7971.   86)   7618.   87)   7323.   88)   8586.
 89)   7994.   90)   7929.   91)   7621.   92)   8038.   93)   7959.   94)   8102.   95)   7910.   96)   8726.
 97)   8344.   98)   7952.   99)   7809.  100)   7934.  101)   7608.  102)   7157.  103)   7087.  104)   7008.
105)   7294.  106)   7064.  107)   7111.  108)   6710.  109)   7432.  110)   7303.  111)   7239.  112)   7336.
113)   7416.
```

PLOT OF CURRENT ACTIVE FUNCTION

```
 1 *
 2 *
 3 *
 4 *
 5 *
 6 *
 7 *
 8 *
 9 *
10 *
11 *
12 *
13 *
14 *
15 *
16 * 11
17 *   1
18 *    1
19 *     1
20 *      1
21 *       1
22 *
23 *        1
24 *         1
25 *
26 *          1
27 *           1
28 *            1
29 *             111
30 *                11
31 *                  11
32 *                    1111111 11
33 *                           1  111111111
34 *                                       11111111111111
35 *                                                     1111111111111  11 1   1  1  11     1       1
36 *                                                                  11  1 111 11 11  1 11  1111111 11111       1
37 *                                                                                    1  1              1111111 1
38 *
39 *
40 *
41 *
42 *
43 *
44 *
45 *
46 *
47 *
48 *
49 *
50 *
    01234567890123456789012345678901234567890123456789012345678901234567890123456789012345678901234567890123456789
```

LEAST SQUARES RESULT -	SLOPE= -0.11393454E-01	XINTER=	9.30917	AOLD=	0.33126000E 05
LEAST SQUARES RESULT -	SLOPE= -0.19834872E-01	XINTER=	9.01048	AOLD=	0.36438578E 05
LEAST SQUARES RESULT -	SLOPE= -0.11393454E-01	XINTER=	9.30917	AOLD=	0.33125996E 05
LEAST SQUARES RESULT -	SLOPE= -0.11910059E-01	XINTER=	9.28128	AOLD=	0.33457230E 05
LEAST SQUARES RESULT -	SLOPE= -0.11393454E-01	XINTER=	9.30917	AOLD=	0.33125992E 05
LEAST SQUARES RESULT -	SLOPE= -0.11436798E-01	XINTER=	9.30647	AOLD=	0.33159098E 05
LEAST SQUARES RESULT -	SLOPE= -0.11393454E-01	XINTER=	9.30917	AOLD=	0.33125988E 05
LEAST SQUARES RESULT -	SLOPE= -0.11408683E-01	XINTER=	9.30947	AOLD=	0.33129273E 05
LEAST SQUARES RESULT -	SLOPE= -0.11393454E-01	XINTER=	9.30917	AOLD=	0.33125984E 05
LEAST SQUARES RESULT -	SLOPE= -0.11392280E-01	XINTER=	9.30917	AOLD=	0.33126297E 05
LEAST SQUARES RESULT -	SLOPE= -0.11391111E-01	XINTER=	9.30917	AOLD=	0.33126609E 05
LEAST SQUARES RESULT -	SLOPE= -0.11392280E-01	XINTER=	9.30917	AOLD=	0.33126922E 05
LEAST SQUARES RESULT -	SLOPE= -0.11393454E-01	XINTER=	9.30917	AOLD=	0.33127234E 05
LEAST SQUARES RESULT -	SLOPE= -0.11395797E-01	XINTER=	9.30917	AOLD=	0.33127547E 05
LEAST SQUARES RESULT -	SLOPE= -0.11403996E-01	XINTER=	9.30917	AOLD=	0.33127859E 05

COMPUTED LINE - DATA Y(I)

I= 65	9.066	9.081	-0.015
I= 66	9.062	9.041	0.021
I= 67	9.058	8.993	0.065
I= 68	9.055	9.107	-0.053
I= 69	9.051	9.053	-0.002
I= 70	9.047	9.032	0.015
I= 71	9.043	9.084	-0.041
I= 72	9.039	9.002	0.037
I= 73	9.035	8.959	0.077
I= 74	9.032	9.016	0.016
I= 75	9.028	9.051	-0.023
I= 76	9.024	9.030	-0.006
I= 77	9.020	9.023	-0.003
I= 78	9.016	9.052	-0.036
I= 79	9.013	8.996	0.017
I= 80	9.009	9.014	-0.005
I= 81	9.005	9.056	-0.051
I= 82	9.001	9.089	-0.087
I= 83	8.997	8.959	0.039
I= 84	8.994	8.899	0.094
I= 85	8.990	8.983	0.007
I= 86	8.986	8.938	0.048
I= 87	8.982	8.899	0.084
I= 88	8.978	9.058	-0.079
I= 89	8.976	8.986	-0.012
I= 90	8.971	8.978	-0.007
I= 91	8.967	8.938	0.029
I= 92	8.963	8.992	-0.028
I= 93	8.959	8.982	-0.022
I= 94	8.956	9.000	-0.044
I= 95	8.952	8.976	-0.024
I= 96	8.948	9.074	-0.126
I= 97	8.944	9.029	-0.085
I= 98	8.940	8.981	-0.040
I= 99	8.937	8.963	-0.026
I= 100	8.933	8.979	-0.046
I= 101	8.929	8.937	-0.008
I= 102	8.925	8.876	0.050
I= 103	8.921	8.866	0.056
I= 104	8.918	8.855	0.063
I= 105	8.914	8.895	0.019
I= 106	8.910	8.863	0.048
I= 107	8.906	8.869	0.037
I= 108	8.902	8.811	0.091
I= 109	8.899	8.913	-0.015
I= 110	8.895	8.896	-0.001
I= 111	8.891	8.887	0.004
I= 112	8.887	8.900	-0.013
I= 113	8.883	8.911	-0.028

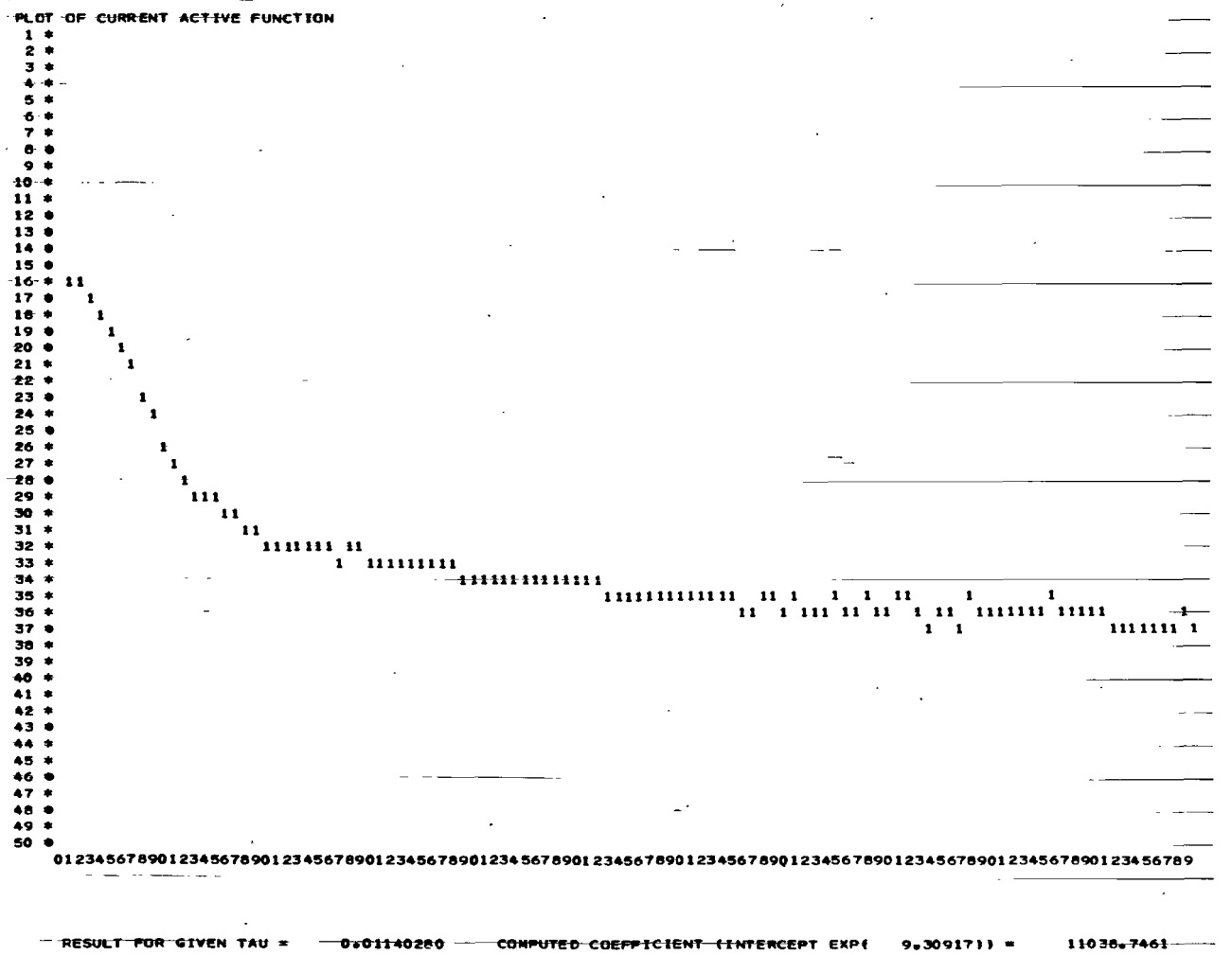

RESULT FOR GIVEN TAU = 0.01140280 COMPUTED COEFFICIENT (INTERCEPT EXP(9.30917)) = 11038.7461

```
 INPUT TAU=    0.15331995    START= 25    END= 40

     1) 109886.    2) 107447.    3)  98703.    4)  88998.    5)  75177.    6)  61136.    7)  48358.    8)  38648.
     9)  29258.   10)  22552.   11)  17665.   12)  14235.   13)  11405.   14)   9984.   15)   9205.   16)   7815.
    17)   6664.   18)   5959.   19)   4990.   20)   4303.   21)   4105.   22)   4011.   23)   3519.   24)   4134.
    25)   3614.   26)   3609.   27)   2703.   28)   3083.   29)   2972.   30)   2660.   31)   1887.   32)   1917.
    33)   2099.   34)   2572.   35)   2188.   36)   2248.   37)   1825.   38)   1807.   39)   1402.   40)   1684.
    41)   1307.   42)   1097.   43)   1201.   44)   1410.   45)    929.   46)   1241.   47)    702.   48)    713.
    49)    858.   50)   1316.   51)    794.   52)    774.   53)    284.   54)    643.   55)    139.   56)    389.
    57)    501.

 PLOT OF CURRENT ACTIVE FUNCTION
  1 *
  2 *
  3 *
  4 *
  5 *
  6 *
  7 *
  8 *
  9 *
 10 *
 11 *
 12 *
 13 *
 14 *
 15 *
 16 *
 17 * 22
 18 *  2
 19 *   2
 20 *    2
 21 *     2
 22 *
 23 *      2
 24 *
 25 *       2
 26 *
 27 *        2
 28 *         2
 29 *
 30 *          2
 31 *
 32 *           2
 33 *            2
 34 *             2
 35 *              2
 36 *               2
 37 *                2
 38 *                 2
 39 *                  2
 40 *                   2
 41 *                    22 2
 42 *                       2 22
 43 *                          22
 44 *                            2  2   2
 45 *                               22
 46 *                                 222
 47 *                                    22 2
 48 *
 49 *                                       2 2  2 2   2
 50 *                                          22
    01234567890123456789012345678901234567890123456789012345678901234567890123456789012345678901234567890123456789
```

LEAST SQUARES RESULT -	SLOPE= -0.15354633E 00	XINTER=	9.35568	AOLD=	0.11038746E 05
LEAST SQUARES RESULT -	SLOPE= -0.11153197E 00	XINTER=	9.27512	AOLD=	0.99348711E 04
LEAST SQUARES RESULT -	SLOPE= -0.15355277E 00	XINTER=	9.35578	AOLD=	0.11038742E 05
LEAST SQUARES RESULT -	SLOPE= -0.14776772E 00	XINTER=	9.33789	AOLD=	0.10928352E 05
LEAST SQUARES RESULT -	SLOPE= -0.15355277E 00	XINTER=	9.35578	AOLD=	0.11038738E 05
LEAST SQUARES RESULT -	SLOPE= -0.15294516E 00	XINTER=	9.35371	AOLD=	0.11027699E 05
LEAST SQUARES RESULT -	SLOPE= -0.15355921E 00	XINTER=	9.35578	AOLD=	0.11038734E 05
LEAST SQUARES RESULT -	SLOPE= -0.15347522E 00	XINTER=	9.35527	AOLD=	0.11037629E 05
LEAST SQUARES RESULT -	SLOPE= -0.15342999E 00	XINTER=	9.35527	AOLD=	0.11036523E 05
LEAST SQUARES RESULT -	SLOPE= -0.15335888E 00	XINTER=	9.35506	AOLD=	0.11034418E 05
LEAST SQUARES RESULT -	SLOPE= -0.15331364E 00	XINTER=	9.35506	AOLD=	0.11034313E 05
LEAST SQUARES RESULT -	SLOPE= -0.15336469E 00	XINTER=	9.35527	AOLD=	0.11035414E 05
LEAST SQUARES RESULT -	SLOPE= -0.15335238E 00	XINTER=	9.35506	AOLD=	0.11035301E 05
LEAST SQUARES RESULT -	SLOPE= -0.15335888E 00	XINTER=	9.35506	AOLD=	0.11035188E 05
LEAST SQUARES RESULT -	SLOPE= -0.15333945E 00	XINTER=	9.35485	AOLD=	0.11035074E 05
LEAST SQUARES RESULT -	SLOPE= -0.15335238E 00	XINTER=	9.35516	AOLD=	0.11034961E 05
LEAST SQUARES RESULT -	SLOPE= -0.15333301E 00	XINTER=	9.35496	AOLD=	0.11034848E 05
LEAST SQUARES RESULT -	SLOPE= -0.15332651E 00	XINTER=	9.35485	AOLD=	0.11034734E 05
LEAST SQUARES RESULT -	SLOPE= -0.15332007E 00	XINTER=	9.35485	AOLD=	0.11034621E 05
LEAST SQUARES RESULT -	SLOPE= -0.15333301E 00	XINTER=	9.35506	AOLD=	0.11034508E 05
LEAST SQUARES RESULT -	SLOPE= -0.15330070E 00	XINTER=	9.35475	AOLD=	0.11034395E 05

COMPUTED LINE - DATA Y(I)

I= 25	8.128	8.194	-0.065
I= 26	8.077	8.192	-0.115
I= 27	8.026	7.904	0.123
I= 28	7.975	8.035	-0.060
I= 29	7.924	7.998	-0.074
I= 30	7.873	7.888	-0.015
I= 31	7.822	7.545	0.277
I= 32	7.771	7.561	0.210
I= 33	7.720	7.651	0.068
I= 34	7.669	7.854	-0.185
I= 35	7.618	7.692	-0.075
I= 36	7.566	7.720	-0.153
I= 37	7.515	7.511	0.004
I= 38	7.464	7.502	-0.038
I= 39	7.413	7.248	0.165
I= 40	7.362	7.431	-0.069

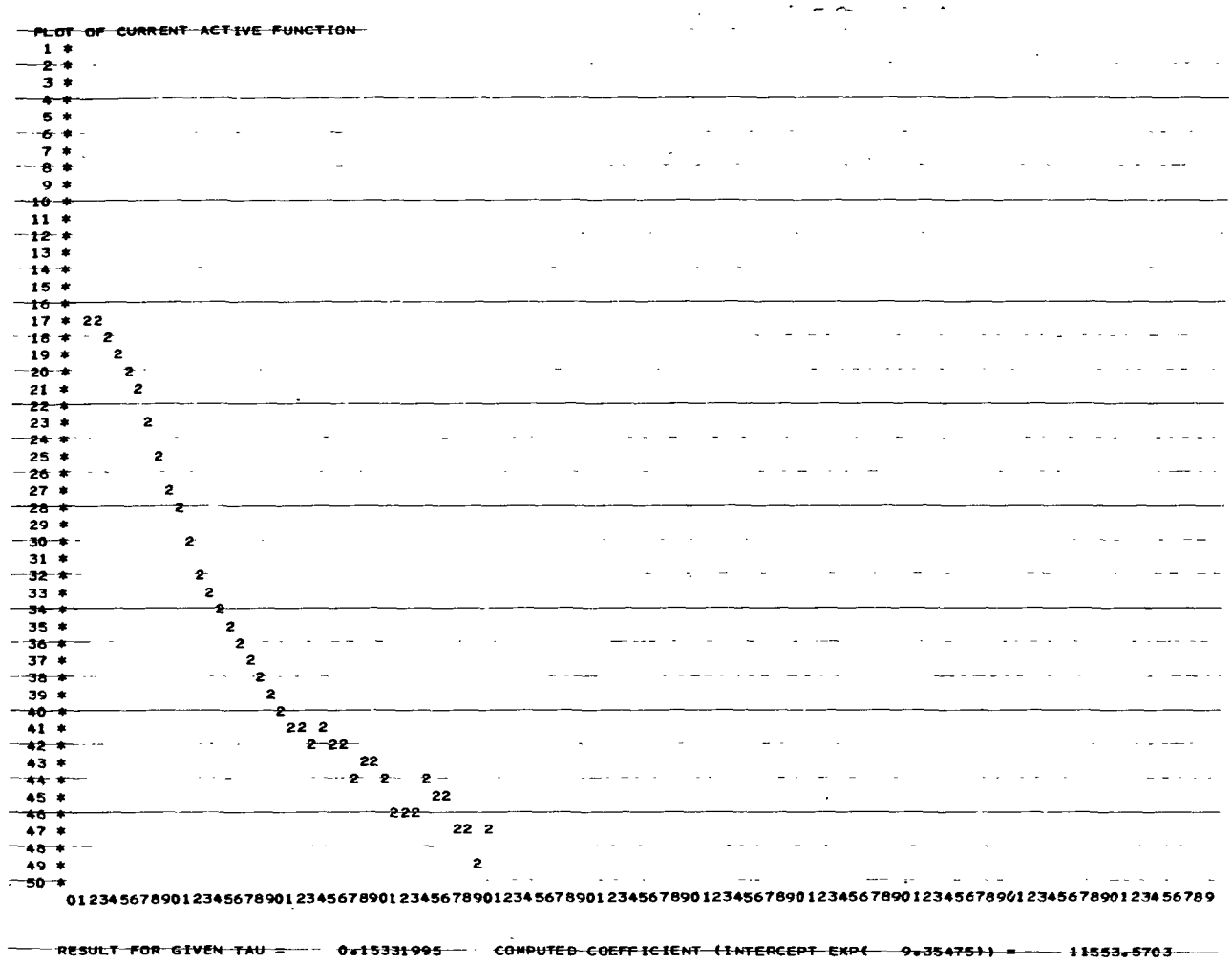
PLOT OF CURRENT ACTIVE FUNCTION
RESULT FOR GIVEN TAU = 0.15331995 COMPUTED COEFFICIENT (INTERCEPT EXP(9.35475)) = 11553.5703

```
 INPUT TAU=      0.96442997      START=  8      END= 18

 1)  98337.    2)  96474.    3)  88276.    4)  79091.    5)  65764.    6)  52192.    7)  39860.    8)  30573.
 9) -21586.   10)  15262.   11)  10638.   12)   7654.   13)   5151.   14)   4042.   15)   3560.   16)   2451.
17)   1567.   18)   1117.   19)    389.

PLOT OF CURRENT ACTIVE FUNCTION
 1 *
 2 *
 3 *
 4 *
 5 *
 6 *
 7 *
 8 *
 9 *
10 *
11 *
12 *
13 *
14 *
15 *
16 *
17 ●
18 * 33
19 *   33
20 *
21 *     3
22 *    3
23 *
24 *       3
25 *
26 ●        3
27 *
28 *
29 *         3
30 ●
31 *          3
32 *
33 *
34 *           3
35 *
36 *            3
37 *
38 *
39 ●             3
40 *
41 *              3
42 *               3
43 *
44 *
45 *                3
46 *
47 *
48 ●                 3
49 *
50 *                  3
    01234567890123456789012345678901234567890123456789012345678901234567890123456789012345678901234567890123456789

      LEAST SQUARES RESULT -      SLOPE= -0.96427786E 00      XINTER=      12.52630      AOLD=  0.11553570E 05
      LEAST SQUARES RESULT -      SLOPE= -0.11011246E 01      XINTER=      12.89714      AOLD=  0.12708918E 05
      LEAST SQUARES RESULT -      SLOPE= -0.96430689E 00      XINTER=      12.52630      AOLD=  0.11553566E 05
      LEAST SQUARES RESULT -      SLOPE= -0.97528434E 00      XINTER=      12.65496      AOLD=  0.11669090E 05
      LEAST SQUARES RESULT -      SLOPE= -0.96428692E 00      XINTER=      12.52624      AOLD=  0.11553563E 05
      LEAST SQUARES RESULT -      SLOPE= -0.96537668E 00      XINTER=      12.52912      AOLD=  0.11663109E 05
      LEAST SQUARES RESULT -      SLOPE= -0.96428692E 00      XINTER=      12.52624      AOLD=  0.11553559E 05
      LEAST SQUARES RESULT -      SLOPE= -0.96439409E 00      XINTER=      12.52656      AOLD=  0.11664703E 05
      LEAST SQUARES RESULT -      SLOPE= -0.96448123E 00      XINTER=      12.52679      AOLD=  0.11555848E 05
      LEAST SQUARES RESULT -      SLOPE= -0.96439409E 00      XINTER=      12.52656      AOLD=  0.11664699E 05
      LEAST SQUARES RESULT -      SLOPE= -0.96439588E 00      XINTER=      12.52662      AOLD=  0.11554809E 05
      LEAST SQUARES RESULT -      SLOPE= -0.96440679E 00      XINTER=      12.52653      AOLD=  0.11664918E 05
      LEAST SQUARES RESULT -      SLOPE= -0.96440864E 00      XINTER=      12.52656      AOLD=  0.11555027E 05
      LEAST SQUARES RESULT -      SLOPE= -0.96443039E 00      XINTER=      12.52662      AOLD=  0.11665137E 05
```

COMPUTED LINE - DATA Y(I)

I= 8	10.277	10.328	-0.051
I= 9	9.955	9.980	-0.025
I= 10	9.634	9.633	0.001
I= 11	9.312	9.272	0.040
I= 12	8.991	8.943	0.048
I= 13	8.669	8.547	0.122
I= 14	8.348	8.304	0.044
I= 15	8.026	8.177	-0.151
I= 16	7.705	7.804	-0.099
I= 17	7.384	7.357	0.027
I= 18	7.062	7.017	0.045

PLOT OF CURRENT ACTIVE FUNCTION

```
 1 *
 2 *
 3 *
 4 *
 5 *
 6 *
 7 *
 8 *
 9 *
10 *
11 *
12 *
13 *
14 *
15 *
16 *
17 *
18 *33
19 *   33
20 *
21 *     3
22 *      3
23 *
24 *       3
25 *
26 *        3
27 *
28 *
29 *          3
30 *
31 *           3
32 *
33 *
34 *            3
35 *
36 *             3
37 *
38 *
39 *               3
40 *
41 *                3
42 *                 3
43 *
44 *
45 *                   3
46 *
47 *
48 *                     3
49 *
50 *                      3
    0123456789012345678901234567890123456789012345678901234567890123456789012345678901234567890123456789012345678901234567890123456789
```

RESULT FOR GIVEN TAU = 0.96442997 COMPUTED COEFFICIENT (INTERCEPT EXP(12.52662)) = 275576.3125

FINAL CURVE Y = SUM OVER I OF A(I)*EXP(TAU(I)) WHERE

A(1) = 11038.74609375 TAU(1) = 0.01140280

A(2) = 11553.57031250 TAU(2) = 0.15331995

A(3) =275576.31250000 TAU(3) = 0.96442997

INDEX	COMPUTED	ORIGINAL	DIFFERENCE
1	331294.63	154053.00	-177241.63
2	254921.44	151572.00	-103349.44
3	199402.31	142786.00	-56616.31
4	159010.94	133039.00	-25971.94
5	129594.94	119177.00	-10417.94
6	108143.00	105095.00	-3048.00
7	92471.38	92276.00	-195.38
8	80996.38	82525.00	1528.63
9	72569.38	73094.00	524.63
10	66357.31	66347.00	-10.31
11	61755.91	61320.00	-435.91
12	58326.64	57950.00	-376.64
13	55751.43	55079.00	-672.43
14	53799.40	53618.00	-181.40
15	52302.98	52800.00	497.02
16	51140.45	51370.00	229.55
17	50223.37	50179.00	-44.37
18	49487.49	49435.00	-52.49
19	48886.03	48427.00	-459.03
20	48384.92	47701.00	-683.92
21	47959.32	47464.00	-495.32
22	47591.11	47331.00	-260.11
23	47266.96	46800.00	-466.96
24	46977.14	47377.00	399.86
25	46714.46	46818.00	103.54
26	46473.60	46775.00	301.40
27	46250.59	45831.00	-419.59
28	46042.45	46173.00	130.55
29	45846.93	46024.00	177.07
30	45662.31	45675.00	12.69
31	45487.27	44864.00	-623.27
32	45320.73	44857.00	-463.73
33	45161.89	45002.00	-159.89
34	45010.05	45437.00	426.95
35	44864.64	45016.00	151.36
36	44725.21	45040.00	314.79
37	44591.33	44580.00	-11.33
38	44462.65	44526.00	63.35
39	44338.86	44084.00	-254.86
40	44219.69	44330.00	110.31
41	44104.86	43917.00	-187.86
42	43994.16	43671.00	-323.16
43	43887.36	43739.00	-148.36
44	43784.27	43912.00	127.73
45	43684.68	43396.00	-288.68
46	43588.45	43672.00	83.55
47	43495.38	43098.00	-397.38
48	43405.34	43074.00	-331.34
49	43318.18	43184.00	-134.18
50	43233.75	43607.00	373.25
51	43151.92	43050.00	-101.92
52	43072.57	42996.00	-76.57
53	42995.58	42471.00	-524.58
54	42920.84	42796.00	-124.84
55	42848.25	42257.00	-591.25
56	42777.69	42473.00	-304.69
57	42709.09	42551.00	-158.09
58	42642.33	41749.00	-893.33
59	42577.34	41988.00	-589.34
60	42514.04	42730.00	215.96
61	42452.35	42639.00	186.65
62	42392.19	42455.00	62.81
63	42333.49	41957.00	-376.49
64	42276.20	42123.00	-153.20
65	42220.23	41914.00	-306.23
66	42165.53	41574.00	-591.53

INDEX	COMPUTED	ORIGINAL	DIFFERENCE
67	42112.05	41175.00	-937.05
68	42059.72	42149.00	89.28
69	42008.50	41670.00	-338.50
70	41958.34	41497.00	-461.34
71	41909.20	41944.00	34.80
72	41861.01	41250.00	-611.01
73	41813.75	40902.00	-911.75
74	41767.38	41359.00	-408.38
75	41721.84	41651.00	-70.84
76	41677.12	41479.00	-198.12
77	41633.16	41419.00	-214.16
78	41589.96	41665.00	75.04
79	41547.45	41196.00	-351.45
80	41505.63	41344.00	-161.63
81	41464.46	41699.00	234.54
82	41423.91	41981.00	557.09
83	41383.96	40905.00	-478.96
84	41344.58	40455.00	-889.58
85	41305.75	41097.00	-208.75
86	41267.46	40744.00	-523.46
87	41229.67	40449.00	-780.67
88	41192.37	41712.00	519.63
89	41155.53	41120.00	-35.53
90	41119.15	41055.00	-64.15
91	41083.20	40747.00	-336.20
92	41047.66	41164.00	116.34
93	41012.53	41085.00	72.47
94	40977.78	41228.00	250.22
95	40943.41	41036.00	92.59
96	40909.39	41852.00	942.61
97	40875.73	41470.00	594.27
98	40842.39	41078.00	235.61
99	40809.38	40935.00	125.62
100	40776.68	41060.00	283.32
101	40744.28	40734.00	-10.28
102	40712.18	40283.00	-429.18
103	40680.35	40213.00	-467.35
104	40648.79	40134.00	-514.79
105	40617.50	40420.00	-197.50
106	40586.47	40190.00	-396.47
107	40555.68	40237.00	-318.68
108	40525.14	39836.00	-689.14
109	40494.83	40558.00	63.17
110	40464.74	40429.00	-35.74
111	40434.88	40365.00	-69.88
112	40405.23	40462.00	56.77
113	40375.79	40542.00	166.21

CHI-SQUARE= 40375.78516 ABSOLUTE DIFFERENCE= 0.02934

"The aeronautical and space activities of the United States shall be conducted so as to contribute . . . to the expansion of human knowledge of phenomena in the atmosphere and space. The Administration shall provide for the widest practicable and appropriate dissemination of information concerning its activities and the results thereof."

— NATIONAL AERONAUTICS AND SPACE ACT OF 1958

NASA SCIENTIFIC AND TECHNICAL PUBLICATIONS

TECHNICAL REPORTS: Scientific and technical information considered important, complete, and a lasting contribution to existing knowledge.

TECHNICAL NOTES: Information less broad in scope but nevertheless of importance as a contribution to existing knowledge.

TECHNICAL MEMORANDUMS: Information receiving limited distribution because of preliminary data, security classification, or other reasons.

CONTRACTOR REPORTS: Scientific and technical information generated under a NASA contract or grant and considered an important contribution to existing knowledge.

TECHNICAL TRANSLATIONS: Information published in a foreign language considered to merit NASA distribution in English.

SPECIAL PUBLICATIONS: Information derived from or of value to NASA activities. Publications include conference proceedings, monographs, data compilations, handbooks, sourcebooks, and special bibliographies.

TECHNOLOGY UTILIZATION PUBLICATIONS: Information on technology used by NASA that may be of particular interest in commercial and other non-aerospace applications. Publications include Tech Briefs, Technology Utilization Reports and Technology Surveys.

Details on the availability of these publications may be obtained from:

SCIENTIFIC AND TECHNICAL INFORMATION OFFICE

NATIONAL AERONAUTICS AND SPACE ADMINISTRATION

Washington, D.C. 20546